

EUROPEAN ORGANISATION FOR NUCLEAR RESEARCH (CERN)



JHEP 09 (2018) 050
DOI: [10.1007/JHEP09\(2018\)050](https://doi.org/10.1007/JHEP09(2018)050)



CERN-EP-2018-034
11th October 2018

Search for supersymmetry in final states with charm jets and missing transverse momentum in 13 TeV $p p$ collisions with the ATLAS detector

The ATLAS Collaboration

A search for supersymmetric partners of top quarks decaying as $\tilde{t}_1 \rightarrow c\tilde{\chi}_1^0$ and supersymmetric partners of charm quarks decaying as $\tilde{c}_1 \rightarrow c\tilde{\chi}_1^0$, where $\tilde{\chi}_1^0$ is the lightest neutralino, is presented. The search uses 36.1 fb^{-1} $p p$ collision data at a centre-of-mass energy of 13 TeV collected by the ATLAS experiment at the Large Hadron Collider and is performed in final states with jets identified as containing charm hadrons. Assuming a 100% branching ratio to $c\tilde{\chi}_1^0$, top and charm squarks with masses up to 850 GeV are excluded at 95% confidence level for a massless lightest neutralino. For $m_{\tilde{t}_1, \tilde{c}_1} - m_{\tilde{\chi}_1^0} < 100 \text{ GeV}$, top and charm squark masses up to 500 GeV are excluded.

1 Introduction

Supersymmetry (SUSY) [1–6] provides an extension of the Standard Model (SM) which solves the hierarchy problem [7–10] by introducing partners of the known bosons and fermions. In R -parity-conserving supersymmetric models [11], supersymmetric partners are produced in pairs, and the lightest supersymmetric particle (LSP) is stable. The LSP could provide a viable candidate for dark matter [12, 13]. The scalar partners of right-handed and left-handed quarks, the \tilde{q}_R and \tilde{q}_L squarks, can mix to form two mass eigenstates, \tilde{q}_1 and \tilde{q}_2 , with \tilde{q}_1 defined to be the lighter state. The charginos and neutralinos are mixtures of the binos, winos and Higgsinos that are the supersymmetric partners of the $U(1)_Y$ and $SU(2)_L$ gauge bosons and the Higgs bosons, respectively. Their mass eigenstates are referred to as $\tilde{\chi}_i^\pm$ ($i = 1, 2$) and $\tilde{\chi}_j^0$ ($j = 1, 2, 3, 4$) in order of increasing masses. In the present work, the LSP is assumed to be the lightest neutralino $\tilde{\chi}_1^0$.

In supersymmetric models, naturalness [14, 15] arguments suggest that the mass of the lightest top squark, \tilde{t}_1 , should have mass of the same order of the top quark [16, 17]. The present analysis considers top-squark pair production with subsequent decays induced by flavour-violating effects into a charm quark and a LSP, $\tilde{t}_1 \rightarrow c\tilde{\chi}_1^0$, as indicated in the left panel of Figure 1. This results in final-state signatures characterised by the presence of two charm quarks and missing transverse momentum from the LSPs which escape the detector. The magnitude of flavour-violating effects inducing $\tilde{t}_1 \rightarrow c\tilde{\chi}_1^0$ decays is model dependent, and in certain cases the branching ratio of the $\tilde{t}_1 \rightarrow c\tilde{\chi}_1^0$ decay can exceed the branching ratios of the three- and four-body decays ($\tilde{t}_1 \rightarrow Wb\tilde{\chi}_1^0$ and $\tilde{t}_1 \rightarrow bf\bar{f}'\tilde{\chi}_1^0$, respectively, where f and f' are two fermions from the virtual W boson decay). This can occur due to significant mixing between the top squark and the charm squark, which may be induced by renormalisation group equations even if minimal flavour violation is assumed at a certain scale [18].

In generic supersymmetric models, squarks are not required to be mass degenerate, and in particular, charm squarks could be considerably lighter than other squark flavours [19]. This motivates searches for pair production of charm squarks, each of which decays as $\tilde{c}_1 \rightarrow c\tilde{\chi}_1^0$, as illustrated in the right panel of Figure 1. The experimental signature and the cross-section of such models are identical to those of top-squark production with the top squark decaying as $\tilde{t}_1 \rightarrow c\tilde{\chi}_1^0$ and, therefore, the two processes are treated on the same footing in this analysis. For both processes, a 100% branching ratio to $c\tilde{\chi}_1^0$ is assumed.

This paper presents a search for pair production of top and charm squarks decaying into a charm quark and the lightest neutralino, using 36.1 fb^{-1} of proton–proton (pp) collisions data at a centre-of-mass energy of $\sqrt{s} = 13\text{ TeV}$ collected by the ATLAS experiment at the Large Hadron Collider (LHC) in 2015 and 2016. A dedicated algorithm is used to identify jets containing charm hadrons (c -jets). The search improves on previous results [20, 21] from the ATLAS Collaboration using 20.3 fb^{-1} of 8 TeV data. A related search was recently reported by the CMS Collaboration [22].

2 ATLAS detector

The ATLAS experiment [23] at the LHC is a multi-purpose particle detector with a forward-backward symmetric cylindrical geometry and a near 4π coverage in solid angle.¹ It consists of an inner tracking de-

¹ ATLAS uses a right-handed coordinate system with its origin at the nominal interaction point (IP) in the centre of the detector and the z -axis along the beam pipe. The x -axis points from the IP to the centre of the LHC ring, and the y -axis points

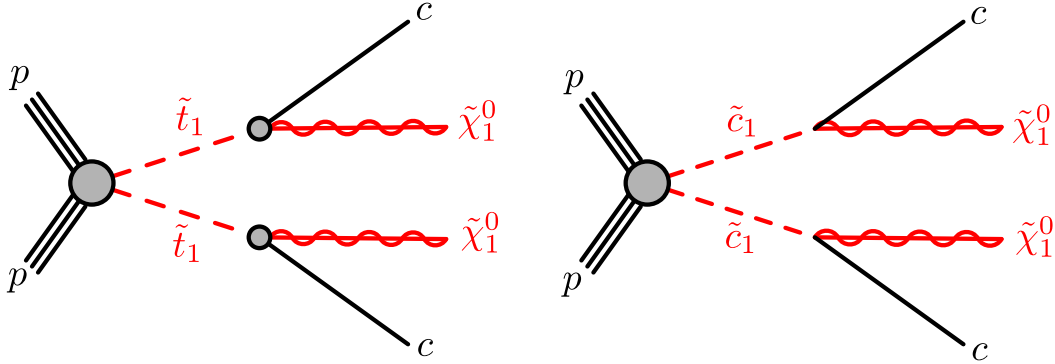


Figure 1: Production diagrams for the pair production of top and charm squarks with subsequent decay into charm quarks and two LSPs. The differentiation of particles and anti-particles is omitted in the diagrams but it is implicitly assumed. The direct squark production processes produce a top and charm squark–antisquark pair, respectively.

tector surrounded by a thin superconducting solenoid providing a 2 T axial magnetic field, electromagnetic and hadron calorimeters, and a muon spectrometer. The inner tracking detector covers the pseudorapidity range $|\eta| < 2.5$. It consists of silicon pixel, silicon microstrip, and transition-radiation tracking detectors. The newly installed innermost layer of pixel sensors [24] was operational for the first time during the 2015 data-taking, leading to an improvement of the flavour-tagging performance [25]. Lead/liquid-argon (LAr) sampling calorimeters provide electromagnetic (EM) energy measurements with high granularity. A hadron (steel/scintillator-tile) calorimeter covers the central pseudorapidity range ($|\eta| < 1.7$). The endcap and forward regions are instrumented with LAr calorimeters for both the EM and hadronic energy measurements up to $|\eta| = 4.9$. The muon spectrometer surrounds the calorimeters and is based on three large air-core toroidal superconducting magnets with eight coils each. The field integral of the toroids ranges between 2.0 and 6.0 Tm across most of the detector. The muon spectrometer includes a system of precision tracking chambers and fast detectors for triggering. A two-level trigger system [26] is used to select events. The first-level trigger is implemented in hardware and uses a subset of the detector information to reduce the accepted rate to at most 100 kHz. This is followed by a software-based trigger level that reduces the accepted event rate to about 1 kHz.

3 Data and simulated event samples

The data used in this analysis were collected by the ATLAS detector in pp collisions at the LHC with $\sqrt{s} = 13$ TeV and 25 ns proton bunch crossing interval over the 2015 and 2016 data-taking periods. The full dataset corresponds to an integrated luminosity of 36.1 fb^{-1} after the application of beam, detector, and data-quality requirements. The uncertainty in the combined 2015+2016 integrated luminosity is 2.1%. It is derived, following a methodology similar to that detailed in Ref. [27], from a calibration of the luminosity scale using x - y beam-separation scans performed in August 2015 and May 2016. On average,

upwards. Cylindrical coordinates (r, ϕ) are used in the transverse plane, ϕ being the azimuthal angle around the z -axis. The pseudorapidity is defined in terms of the polar angle θ as $\eta = -\ln \tan(\theta/2)$. Rapidity is defined as $y = 0.5 \ln[(E + p_z)/(E - p_z)]$, where E denotes the energy and p_z is the component of the momentum along the beam direction. Angular distance is measured in units of $\Delta R \equiv \sqrt{(\Delta y)^2 + (\Delta \phi)^2}$.

there are about 14 or 25 inelastic pp collisions (“pile-up”) in each bunch crossing in the 2015 and 2016 datasets, respectively.

In all search regions, events are required to pass a missing transverse momentum (E_T^{miss}) trigger with an online threshold of 70 GeV or 110 GeV for the 2015 and 2016 data periods, respectively. This trigger is fully efficient for events passing the preselection defined in Section 5.1. Events in control regions are selected using triggers requiring the presence of one electron or muon.

Monte Carlo (MC) simulated event samples are used to model the SUSY signal and to help in the estimation of SM background processes. The SUSY signal samples used in this analysis were generated using `MADGRAPH5_aMC@NLO` v2.2.3 [28] and interfaced to `PYTHIA` 8.186 [29] with the A14 set of tuned parameters [30] for the simulation of parton showering, hadronisation, and the description of the underlying event. The matrix element (ME) calculation was performed at tree level includes the emission of up to two additional partons. The ME to parton shower (PS) matching was done using the CKKW-L prescription [31], with a matching scale set to $m_{\tilde{t}_1, \tilde{c}_1}/4$. The mass of the top quark was fixed at 172.5 GeV. The NNPDF2.3LO [32] parton distribution function (PDF) set was used. Signal cross-sections were calculated at next-to-leading-order accuracy (NLO) in the strong coupling constant, adding the resummation of soft-gluon emission at next-to-leading-logarithm accuracy (NLO+NLL) [33–35]. The nominal cross-section and its uncertainty are based on predictions using different PDF sets and factorisation and renormalisation scales, as described in Ref. [36]. The same cross-section values were used for the pair production of top and charm squarks.

SM background samples were simulated using different MC event generator programs depending on the process. Events containing W or Z bosons with associated jets, and diboson events (WW , WZ and ZZ) were simulated using the `SHERPA` 2.2.1 [37] event generator. The ME calculation is performed using `COMIX` [38] and `OPENLOOPS` [39] for up to two partons at NLO and four partons at LO in $W/Z + \text{jets}$ events and up to one parton at NLO and three partons at LO in diboson events, and merged with the `SHERPA` parton shower [40] according to the ME+PS@NLO prescription [41]. The NNPDF3.0NNLO PDF set [42] was used in conjunction with dedicated parton shower tuning developed by the `SHERPA` authors. The $W/Z + \text{jets}$ events were normalised with NNLO QCD cross-sections [43]. For the generation of $t\bar{t}$ events, `POWHEG-BOX` v2 [44] was used with the CT10 PDF [45] set in the matrix element calculations. Electroweak t -channel, s -channel and Wt -channel single-top-quark events were generated with `POWHEG-BOX` v1. For s -channel and Wt -channel production, the CT10 PDF set was used, while for the t -channel production the four-flavour scheme was used for the NLO matrix element calculations together with the fixed four-flavour PDF set CT10f4. For $t\bar{t}$ and single-top-quark processes, top-quark spin correlations were preserved. The parton shower, hadronisation, and the underlying event were simulated using `PYTHIA` 6.428 [46] with the CTEQ6L1 PDF set and the corresponding Perugia 2012 set of tuned parameters [47]. The top-quark mass was set to 172.5 GeV. At least one leptonically decaying W boson was required in all generated $t\bar{t}$ and single-top-quark events. Fully hadronic decays do not produce sufficient E_T^{miss} to significantly contribute to the background.

The production of top-quark pairs in association with W , Z or Higgs bosons was modelled by samples generated at NLO using `MADGRAPH5_aMC@NLO` v2.2.3 and showered with `PYTHIA` 8.212. The $t\bar{t}WW$ process and the production of events with three or four top quarks were modelled at leading order (LO) using `MADGRAPH5_aMC@NLO` v2.2.3 interfaced to `PYTHIA` 8.212.

The `EVTGEN` 1.2.0 program [48] was used by all generators except `SHERPA` to describe the properties of b - and c -hadron decays.

Additional samples from different event generators and settings are used to estimate systematic uncertainties in the backgrounds, as described in Section 7.

All simulated events were overlaid with multiple pp collisions simulated with the soft QCD processes of PYTHIA 8.186 with the A2 tune settings and the MSTW2008LO PDF set [49], and reweighted to match the pile-up distribution observed in the data. The MC samples were processed through the ATLAS full detector simulation [50] based on GEANT4 [51] or a fast simulation [52] that uses a parameterisation for the calorimeter response and GEANT4 for the rest of the detector. All simulated events are reconstructed with the same algorithms as used for the data. In order to improve agreement between data and simulation, corrections are applied to the lepton trigger and identification efficiencies, momentum scale, energy resolution, and the efficiency of identifying jets containing charm hadrons [54–56].

4 Event Reconstruction

Interaction vertices from the proton–proton collisions are reconstructed from at least two tracks with transverse momentum $p_T > 400$ MeV, and are required to be consistent with the beam-spot envelope. The primary vertex is identified as the one with the largest sum of squares of the transverse momenta from associated tracks, $\sum p_{T,\text{track}}^2$ [53].

Reconstructed physics objects are labelled as *baseline* or *signal*, with the latter satisfying tighter identification and quality criteria. Baseline objects are used for the removal of overlaps between different reconstructed objects (“overlap removal”) and for lepton-veto purposes.

Electron baseline candidates are reconstructed from energy clusters in the electromagnetic calorimeter matched to inner detector tracks. A multivariate calibration is applied to correct the electron energy scale [54]. Electron candidates must have $|\eta| < 2.47$ and $p_T > 7$ GeV, and meet a set of “loose” quality criteria [55].

Muon baseline candidates are reconstructed from tracks in the muon spectrometer and the inner detector. Candidates for which the inner detector tracks are matched to an energy deposit in the calorimeter compatible with a minimum-ionizing particle are also considered. Muon candidates must have $|\eta| < 2.7$ and $p_T > 7$ GeV, and meet a set of “loose” quality criteria [56].

For signal lepton candidates used in the control region definitions, additional requirements are applied. Signal electrons are required to meet a set of “medium” quality criteria [55], a “loose” isolation requirement [55], and to have $p_T > 27$ GeV. Signal muons are required to pass a “loose” isolation requirement [56] and to have $p_T > 27$ GeV.

Jets are reconstructed from three-dimensional topological clusters [57] of calorimeter cells using the anti- k_t algorithm [58] with a radius parameter of $R = 0.4$ and a four-momentum recombination scheme. The jet energy is then corrected to the particle level by the application of a jet energy scale calibration derived from 13 TeV data and simulation [59]. To reduce pile-up effects, jets with $|\eta| < 2.4$ are tested for compatibility with the primary vertex and required to pass a set of “medium” requirements [60]. Baseline jets are required to have $|\eta| < 2.8$ and $p_T > 20$ GeV. These jets are used in the overlap removal procedure. Signal jets are required to also have $|\eta| < 2.5$ and $p_T > 30$ GeV.

Identifying c -jets is of crucial importance to this analysis. Two multivariate discriminants, MV2c100 and MV2cl100, are used to distinguish between c -jets and jets containing bottom hadrons (b -jets), and between c -jets and light-flavour jets (jets not containing a b - or a c -hadron), respectively. The discriminants are

based on the MV2 algorithm presented in Refs. [25, 61]. MV2c100 is trained with b -jets as signal and with background consisting exclusively of c -jets. MV2cl100 is trained with c -jets as signal and with background consisting exclusively of light-flavour jets. A “tight” working point was adopted in the analysis, resulting in a charm-tagging efficiency of about 18%, a b -jet rejection factor of 20, a light-flavour jet rejection factor of 200, and a hadronic τ jet rejection factor of 6, as evaluated in a sample of simulated $t\bar{t}$ events. The c -jet tagging rate is measured using a data sample rich in $t\bar{t}$ events, identifying c -jets from W boson decays. Correction factors dependent on the jet p_T are derived to match the tagging rate in the simulation to that measured in data. They are found to range from 0.83 to 0.88 in PYTHIA 8 MC samples. Similarly, correction factors for the mis-tag rate for b -jets are derived using dileptonic $t\bar{t}$ data events. They are found to range from 0.81 to 0.97 in PYTHIA 8 MC samples. Correction factors for the mis-tag rate for light-flavour jets are instead evaluated by comparing the MC simulation to an “adjusted” simulation where the track-based variables used in the flavour-tagging evaluation, e.g. the transverse impact parameter relative to the primary vertex, are scaled to match the data. The size of this correction is found to range between 1.3 and 1.9 across the considered jet p_T and η ranges in PYTHIA 8 MC samples.

To avoid object double counting, an overlap removal procedure is applied to resolve ambiguities among electrons, muons, and jets in the final state. Any muon candidate that is reconstructed with inner detector and calorimeter information only and which shares an inner detector track with an electron candidate is removed. Any electron candidate sharing an inner detector track with a remaining muon candidate is also removed. Jets within $\Delta R = 0.2$ of an electron are discarded. Jets with less than three tracks within $\Delta R = 0.2$ of a muon candidate are discarded. Any remaining electron candidate within $\Delta R = 0.4$ of a jet is discarded. Any remaining muon candidate within $\Delta R = 0.04 + 10/p_T^\mu(\text{GeV})$ of a jet is discarded.

The missing transverse momentum E_T^{miss} , whose magnitude is denoted by E_T^{miss} , is defined as the negative vector sum of the transverse momenta of electrons, jets and muons, to which is added a “soft term” that recovers the contributions from other low- p_T particles [62, 63]. The soft term is constructed from all tracks that are not associated with any of the preceding objects, and that are associated with the primary vertex.

5 Event Selection

All events used in this analysis are required to satisfy basic quality criteria in order to guarantee the good functionality of the detector during the data-taking and to increase the purity and quality of the data sample by rejecting non-collision events such as cosmic-ray and beam-halo events. To ensure that the event contains a pp interaction with large transverse momentum transfer, at least one vertex with a position consistent with the beam-spot position is required.

All events in signal regions are required to pass a preselection, presented in Section 5.1, that targets the c -jets + E_T^{miss} final state. Variables designed to reject SM background events are also defined in Section 5.1. Tighter selections are then applied to maximise the sensitivity to the signal models of interest, resulting in five signal regions, described in Section 5.2.

5.1 Preselection

Stop and scharm pair production followed by $\tilde{t}_1 \rightarrow c\tilde{\chi}_1^0$ and $\tilde{c}_1 \rightarrow c\tilde{\chi}_1^0$ decays have the same final state characterised by E_T^{miss} and at least two c -jets. No prompt leptons are expected, and therefore events

with at least one baseline electron or muon candidate, as defined in Section 4, are vetoed in order to reduce contamination from SM background processes with at most a signal rejection of only a few percent. In order to ensure full efficiency for the E_T^{miss} trigger used in the data selection, a requirement on $E_T^{\text{miss}} > 250 \text{ GeV}$ is applied. At least two jets are required, and the jet leading in p_T (leading jet) is required to satisfy $p_T^{j_1} > 250 \text{ GeV}$. In addition, at least one jet is required to be charm-tagged. A requirement on the minimum angle between the E_T^{miss} and each signal jet, $\Delta\phi_{\min}(\text{jet}, E_T^{\text{miss}}) > 0.4$, is imposed in order to reduce the multijet background arising from mismeasured E_T^{miss} .

5.2 Signal Regions

The signal characteristics depend strongly on the mass difference between the top or charm squark and the lightest neutralino, $\Delta m = m_{\tilde{t}_1, \tilde{c}_1} - m_{\tilde{\chi}_1^0}$. A large mass difference ($\Delta m > 300 \text{ GeV}$) leads to high- p_T jets and high E_T^{miss} . For smaller mass differences, the E_T^{miss} is substantially reduced. To target such signal scenarios, an additional initial-state radiation (ISR) jet is required to boost the system, leading to larger values of E_T^{miss} . Specific signal region selections (SRs) are optimised to target different signal topologies. Five signal regions (SR1–SR5) are defined in total, targeting scenarios with increasingly large mass splittings Δm . All signal region selections require a missing transverse momentum of at least 500 GeV .

Requiring the presence of one or more charm-tagged jets results in an enhancement of events with hadronically decaying τ -leptons, as they have a high probability of being mis-tagged. The minimum transverse mass m_T^c of charm-tagged jets and E_T^{miss} is defined as

$$m_T^c = \min_{c\text{-jets}} \sqrt{2 \cdot E_T^{\text{miss}} p_T^c \cdot (1 - \cos \Delta\phi(E_T^{\text{miss}}, p_T^c))},$$

where $\Delta\phi(E_T^{\text{miss}}, p_T^c)$ is the azimuthal angle between the charm-tagged jet and the missing transverse momentum. The m_T^c variable shows a large rejection power against events with hadronically decaying τ -leptons. The requirement of $m_T^c > 120 \text{ GeV}$ in all SRs reduces this contribution to less than 5% of the total background events. The m_T^c variable also provides discrimination against other backgrounds, such as Z +jet production with invisibly decaying Z bosons.

An overview of the selection requirements in all signal regions is given in Table 1.

Signal region **SR1** targets compressed mass scenarios with Δm smaller than $\sim 50 \text{ GeV}$. In such scenarios, the c -jets are expected to have p_T below the 30 GeV threshold for signal jets, and may not always be reconstructed. For even smaller values of Δm , neither c -jet is expected to be reconstructed. Another analysis, the “monojet” analysis described in Ref. [64], is sensitive to this type of signal. Signal region **SR2** targets compressed mass scenarios with Δm larger than 50 GeV but smaller than $\sim 100 \text{ GeV}$. Both c -jets are expected to be reconstructed and at least three jets are required. Signal regions **SR3** and **SR4** target scenarios with intermediate values of Δm , $100\text{--}450 \text{ GeV}$. Requirements on the charm-tagged jet transverse momentum and on m_T^c are tightened, and more stringent thresholds on the second and third jets’ transverse momenta are applied. An upper bound is imposed on the value of m_T^c in signal regions **SR1–SR3** as this is found to increase the sensitivity of the analysis. In signal regions **SR1–SR4**, the leading jet is primarily expected to arise from initial-state radiation, and is therefore required to fail the charm-tagging requirement. Finally, signal region **SR5** targets scenarios with values of Δm greater than around 450 GeV , such that the leading two jets are usually the c -jets from the decay of the \tilde{t}_1 or

\tilde{c}_1 . Therefore, the leading jet is no longer required to fail the charm-tagging requirement. In addition, requirements on the jet transverse momenta and m_T^c are further tightened relative to **SR1–SR4**.

According to the selected benchmark model, about 20 signal events pass the selection criteria for the corresponding SR of interest. A full overview is reported in Table 7.

	SR1	SR2	SR3	SR4	SR5
Trigger	E_T^{miss} triggers				
Leptons	0 e AND 0 μ				
E_T^{miss} [GeV]	> 500				
$\Delta\phi_{\min}(\text{jet}, E_T^{\text{miss}})$ [rad]	> 0.4				
$N_{c\text{-jets}}$	≥ 1				
N_{jets}	≥ 2	≥ 3	≥ 3	≥ 3	≥ 3
Leading jet c -tag veto	yes	yes	yes	yes	no
$p_T^{j_1}$ [GeV]	> 250	> 250	> 250	> 250	> 300
$p_T^{j_2}$ [GeV]	–	–	> 100	> 140	> 200
$p_T^{j_3}$ [GeV]	–	–	> 80	> 120	> 150
$p_T^{c_1}$ [GeV]	< 100	> 60	> 80	> 100	> 150
m_T^c [GeV]	$\in (120, 250)$	$\in (120, 250)$	$\in (175, 400)$	> 200	> 400

Table 1: Overview of the signal region selection criteria. N_{jets} and $N_{c\text{-jets}}$ indicate the total number of jets and c -jets, respectively; $p_T^{j_1}$, $p_T^{j_2}$ and $p_T^{j_3}$ indicate the transverse momentum of the leading, sub-leading and sub-sub-leading jet; and $p_T^{c_1}$ is the transverse momentum of the c -jet with the highest p_T .

6 Background estimation

The main background contribution in this analysis arises from Z +jets production with the Z boson decaying into neutrinos. Across all the SRs this process contributes up to 50–60% of the total background expectation. Other significant background contributions arise from W +jets production in association with a heavy-flavour jet where the W boson decays into a τ -lepton and a neutrino ($\sim 10\%$ of the total background expectations in the SRs), followed by diboson and $t\bar{t}$ production ($\sim 10\%$ and 5–10% of the total SR expectations, respectively). Minor backgrounds including $Z \rightarrow \tau\tau$, single-top and $t\bar{t}$ production in association with additional vector bosons, which account for less than 5% of the total background, are grouped together and hereafter referred to as the “Other” contribution. The contribution of the multijet background is evaluated using dedicated data-driven techniques, but is found to be negligible in all regions and therefore not further considered. Contributions from diboson production and other small backgrounds are determined from simulation only.

The Z +jets, W +jets and top-quark background yields in the SRs are estimated using simulated samples normalised to data in dedicated control regions (CRs). Three CRs are constructed separately for each SR. They are designed to enhance the contribution of a particular background component, as described in Section 6.1, and are required to be disjoint from the SRs while still retaining similar kinematic and flavour-composition properties.

6.1 Control region definitions

To ensure that the control regions are statistically independent of the signal regions, the lepton veto applied in the preselection (Section 5.1) is modified such that each control region requires at least one signal electron or muon. In order to ensure a similar background composition between signal and control regions, identical requirements are placed on the jet multiplicity and flavour tagging in control regions and corresponding signal regions. Requirements on E_T^{miss} and jet momenta are lowered in the control regions relative to the signal regions, to ensure that the control region samples have enough events. In addition to these common criteria, specific selections to target Z -jets, W -jets and top-quark production backgrounds are imposed as described in Sections 6.1.1 and 6.1.2. The potential contamination from signal in each CR is found to be negligible for all signal hypotheses that have not yet been excluded.

6.1.1 Z control regions

The Z -jets events that pass the SR requirements are mostly from $Z(\rightarrow \nu\nu)$ production in association with a charm quark, followed by $Z(\rightarrow \nu\nu)$ production in association with light-flavour jets, some of which have been mis-tagged as c -jets. Control regions enriched in Z -jets events are defined by requiring two same-flavour (SF), opposite-sign (OS) leptons (electrons or muons) with an invariant mass $m_{\ell\ell}$ close to the Z boson mass ($76 \text{ GeV} < m_{\ell\ell} < 106 \text{ GeV}$). The lepton momenta are then vectorially added to the E_T^{miss} to mimic the expected missing transverse momentum spectrum of $Z(\rightarrow \nu\nu)$ -jets events. Other quantities depending on E_T^{miss} are also recomputed accordingly. In the following, all variables corrected in this manner are indicated with the superscript ‘‘corr’’. A missing transverse momentum requirement $E_T^{\text{miss}} < 75 \text{ GeV}$ is also applied in the Z control regions to reduce the contribution of the $t\bar{t}$ background. The full set of criteria is summarised in Table 2. MC studies show that the jet flavour composition in all the Z control regions is in excellent agreement with the composition in the signal regions.

6.1.2 W and top-quark control regions

The W -jets and top-quark background events passing the SR requirements are mostly events with hadronically decaying τ -leptons, where the charm-tagged jet is an ISR jet containing a charm hadron, or a mistagged light-flavour jet. Most of the events with a hadronically decaying τ -lepton mis-tagged as a c -jet are instead rejected by the m_T^c requirement applied in the SRs. Samples enriched in both the W -jets and top-quark processes are obtained by selecting events with exactly one signal lepton (electron or muon) and with W boson transverse mass $m_T = \sqrt{2 \cdot E_T^{\text{miss}} p_T^{\text{lep}} \cdot (1 - \cos \Delta\phi(E_T^{\text{miss}}, p_T^{\text{lep}}))} > 60 \text{ GeV}$.

From simulation it is determined that in the SRs on average 40% of the τ -lepton’s momentum is carried by visible decay products, while the remaining 60% is carried by neutrinos. Therefore, in the CRs, to mimic the τ -lepton’s decay behaviour as closely as possible, single-lepton events are selected and the lepton is replaced with a jet whose p_T is 40% of the lepton p_T , to mimic the visible part of the τ -lepton decay. The remaining 60% of the lepton momentum is added to the E_T^{miss} calculation, to mimic the neutrino contribution. Jets obtained using this procedure are further considered in the analysis only if they pass the signal jet p_T and η requirements described in Section 4. All variables computed from either jets or E_T^{miss} are recomputed accordingly and indicated with the superscript ‘‘corr’’.

	Z CR1	Z CR2	Z CR3	Z CR4	Z CR5
Trigger		E_T^{miss} OR single lepton			
Leptons		2 SF OS e OR μ			
$m_{\ell\ell}$ [GeV]		$\in (76, 106)$			
$\Delta\phi_{\min}(\text{jet}, E_T^{\text{miss,corr}})$ [rad]		> 0.4			
$N_{c\text{-jets}}$		≥ 1			
E_T^{miss} [GeV]		< 75			
$E_T^{\text{miss,corr}}$ [GeV]		> 250			
$p_T^{j_1}$ [GeV]		> 250			
N_{jets}	≥ 2	≥ 3	≥ 3	≥ 3	≥ 3
Leading jet c -tag veto	yes	yes	yes	yes	no
$p_T^{j_2}$ [GeV]	–	–	> 100	> 100	> 100
$p_T^{j_3}$ [GeV]	–	–	> 80	> 100	–
$p_T^{c_1}$ [GeV]	< 100	> 60	> 80	> 100	> 100
$m_T^{c,\text{corr}}$ [GeV]	$\in (120, 250)$	$\in (120, 250)$	$\in (175, 400)$	> 200	> 400

Table 2: Overview of the Z control region selection criteria. N_{jets} and $N_{c\text{-jets}}$ indicate the total number of jets and c -jets, respectively; $p_T^{j_1}$, $p_T^{j_2}$ and $p_T^{j_3}$ indicate the transverse momentum of the leading, sub-leading and sub-sub-leading jet; and $p_T^{c_1}$ is the transverse momentum of the c -jet with the highest p_T . Variables with the superscript “corr” refer to variables corrected as described in the text.

As in the Z CRs, the requirements on E_T^{miss} and jet momenta are relaxed relative to the corresponding signal regions to obtain enough events for the background estimation, while all other criteria are kept the same.

In order to define separate CRs for W +jets and the top-quark processes, two kinematic variables are introduced.

$m_{t,W}^{\text{had}}$: this variable is only defined in events with at least three jets. First, the jet pair with the invariant mass m_{jj} closest to the W boson mass is selected. Then a third jet is selected such that the invariant mass m_{jjj} of all three jets is closest to the top-quark mass. In addition, at least one of these jets is required to be charm-tagged.

m_{jj}^W : the jet pair with m_{jj} closest to the W boson mass is selected. Here, all pairs of jets where neither jet is charm-tagged are considered first, and the pair with m_{jj} closest to the W boson mass is chosen. If no pairs of jets where neither jet is charm-tagged exist, then pairs containing at least one charm-tagged jet are considered and the pair with m_{jj} closest to the W boson mass is chosen.

When computing $m_{t,W}^{\text{had}}$ and m_{jj}^W , jets obtained from the replacement of leptons as described above are not considered. The two variables have a strong discrimination power between top-quark and W +jets processes. The requirement of $50 \text{ GeV} < m_{t,W}^{\text{had}} < 220 \text{ GeV}$ results in a 62–71% pure top-quark sample, depending on the region. The W CRs are defined by inverting the $m_{t,W}^{\text{had}}$ selection and requiring in addition $m_{jj}^W > 175 \text{ GeV}$. This results in a 55–78% purity for the W +jets process, depending on the region. An overview of the full selection list for the W CRs and the top-quark CRs (referred to as “Top CRs”) are reported in Table 3. MC studies show that the jet flavour composition in all the W control regions is in excellent agreement with that in the signal regions, except for W CR4, where a difference up to 33% is

observed between SR and CR. An additional systematic uncertainty is derived to account for this difference as described in Section 7.

	W/Top CR1	W/Top CR2	W/Top CR3	W/Top CR4	W/Top CR5
Trigger			E_T^{miss} OR single lepton		
Lepton			1 e OR 1 μ		
p_T^{lep} [GeV]			> 27		
$\Delta\phi_{\min}(\text{jet}, E_T^{\text{miss}})$ [rad]		$\Delta\phi_{\min}(\text{jet}, E_T^{\text{miss}}) > 0.4$ OR $\Delta\phi_{\min}(\text{jet}, E_T^{\text{miss,corr}}) > 0.4$			
m_T [GeV]			> 60		
$E_T^{\text{miss,corr}}$ [GeV]			> 250		
$p_T^{j_1, \text{corr}}$ [GeV]			> 250		
$N_{c\text{-jets}}$			≥ 1		
$N_{\text{jets}}^{\text{corr}}$	≥ 2	≥ 3	≥ 3	≥ 3	≥ 3
Leading jet c -tag veto	yes	yes	yes	yes	no
$p_T^{j_2, \text{corr}}$ [GeV]	–	–	> 100	> 100	> 100
$p_T^{j_3, \text{corr}}$ [GeV]	–	–	> 80	> 100	–
$p_T^{c_1}$ [GeV]	< 100	> 60	> 80	> 100	> 100
$m_T^{c, \text{corr}}$ [GeV]	$\in (120, 250)$	$\in (120, 250)$	$\in (175, 400)$	> 200	> 400
$m_{t,W}^{\text{had}}$ [GeV]	For $W: < 50$ OR > 220 For Top: $\in (50, 220)$				
m_{jj}^W [GeV]	For $W: > 175$ For Top: no requirement				

Table 3: Overview of the W and Top control region selection criteria. N_{jets} and $N_{c\text{-jets}}$ indicate the total number of jets and c -jets, respectively; $p_T^{j_1}$, $p_T^{j_2}$ and $p_T^{j_3}$ indicate the transverse momentum of the leading, sub-leading and sub-sub-leading jet; and $p_T^{c_1}$ is the transverse momentum of the c -jet with the highest p_T and p_T^{lep} is the lepton p_T . Variables with the superscript “corr” refer to variables corrected as described in the text.

6.2 Background-only fit

For each signal region, the normalisations of the W +jets, Z +jets and top-quark backgrounds are determined through a binned likelihood fit performed simultaneously to the observed number of events in the associated control regions. The likelihood is constructed as a product of Poissonian probability density functions describing the observed data counts in the control regions and Gaussian constraint terms for the systematic uncertainties described in Section 7. Poisson distributions are also included in the likelihood to describe the MC simulation’s statistical uncertainties. The fit is performed using the HistFitter package [65] with the assumption that no signal is present and it is referred to as the “background-only” fit. Correlations in background yield predictions across different regions due to common systematic uncertainties are accounted for in the fit.

The background normalisation factors (μ factors) obtained in the fit are summarised in Table 4, including all the detector-related systematic uncertainties as described in Section 7.

Fit parameter	SR1	SR2	SR3	SR4	SR5
μ_W	$1.13^{+0.38}_{-0.28}$	$1.20^{+0.44}_{-0.39}$	$1.70^{+0.39}_{-0.33}$	$1.49^{+0.31}_{-0.26}$	$1.28^{+0.30}_{-0.24}$
μ_Z	$1.36^{+0.17}_{-0.15}$	$1.34^{+0.26}_{-0.22}$	$1.22^{+0.27}_{-0.23}$	$1.29^{+0.26}_{-0.22}$	$1.30^{+0.28}_{-0.23}$
μ_{Top}	$1.15^{+0.38}_{-0.28}$	$1.28^{+0.55}_{-0.47}$	$0.86^{+0.31}_{-0.35}$	$0.79^{+0.35}_{-0.29}$	$1.02^{+0.46}_{-0.32}$

Table 4: Normalisation factors after the background-only fit. The central values with the detector-related systematic uncertainties, corresponding to one standard deviation, are reported.

Figure 2 shows examples of comparisons between data and the SM prediction for the $E_T^{\text{miss,corr}}$ and m_T^c distributions, for some of the Z CRs, W CRs and Top CRs. The backgrounds are scaled by the normalisation factors extracted from the background-only fit. Good agreement between data and the prediction is observed in the shapes of all distributions.

6.3 Validation regions

After the background-only fit is performed, the validity of the extrapolation of the background estimate outside the control regions is tested in dedicated validation regions (VRs). Validation regions are not used to constrain the background normalisation in the fit. They are required to have kinematic properties and flavour-tagging compositions similar to those in the signal regions, while keeping the potential contamination from signal as low as possible. This is achieved by retaining most of the selection criteria used in the signal region and inverting or restricting the requirements on E_T^{miss} , m_T^c , and the jet momenta to limit the potential signal contribution. All validation region selections require $m_{jj}^W > 125 \text{ GeV}$ and $m_T^c > 120 \text{ GeV}$. Depending on the signal region, two or three VRs (referred to as A, B and C) are defined to separately validate the modelling of kinematic variables used in the signal region definitions: E_T^{miss} , $p_T^{j_1}$ and $p_T^{j_2}$. A full list of all the selection criteria used to define the validation regions is reported in Table 5. The signal contamination in the validation regions was examined for all considered signals that have not yet been excluded, and was found to be at most 25%.

Figure 3 shows a comparison between the number of events predicted by the background-only fit and the data, for all validation regions. The pulls, estimated as the difference between the observed number of events and the predicted background yields divided by the total uncertainty, are also shown. No evidence of significant background mismodelling is observed in the VRs.

	VR1	VR2	VR3	VR4	VR5
Trigger			E_T^{miss} triggers		
Leptons			0 e AND 0 μ		
E_T^{miss} [GeV]			> 500		
$\Delta\phi_{\text{min}}(\text{jet}, E_T^{\text{miss}})$ [rad]			> 0.4		
$N_{c\text{-jets}}$			≥ 1		
m_{jj}^W [GeV]			> 125		
N_{jets}	≥ 2	≥ 3	≥ 3	≥ 3	≥ 3
Leading jet c -tag veto	yes	yes	yes	yes	no
$p_T^{j_1}$ [GeV]	> 250	> 250	> 250	> 250	> 300
$p_T^{c_1}$ [GeV]	< 100	> 60	> 80	> 100	> 200
m_T^c [GeV]	> 250	$\in (300, 450)$	$\in (300, 400)$	$\in (300, 500)$	> 400
A	E_T^{miss} [GeV]	< 350	< 350	< 350	< 350
	$p_T^{j_2}$ [GeV]	–	< 175	< 200	< 200
B	$p_T^{j_1}$ [GeV]	< 350	< 350	< 350	–
	$p_T^{j_2}$ [GeV]	–	< 175	< 200	< 175
C	E_T^{miss} [GeV]	–	< 350	< 350	–
	$p_T^{j_1}$ [GeV]	–	< 350	< 350	–

Table 5: Overview of the validation region selection criteria. N_{jets} and $N_{c\text{-jets}}$ indicate the total number of jets and c -jets, respectively; $p_T^{j_1}$ and $p_T^{j_2}$ indicate the transverse momentum of the leading and sub-leading jet; and $p_T^{c_1}$ is the transverse momentum of the c -jet with the highest p_T .

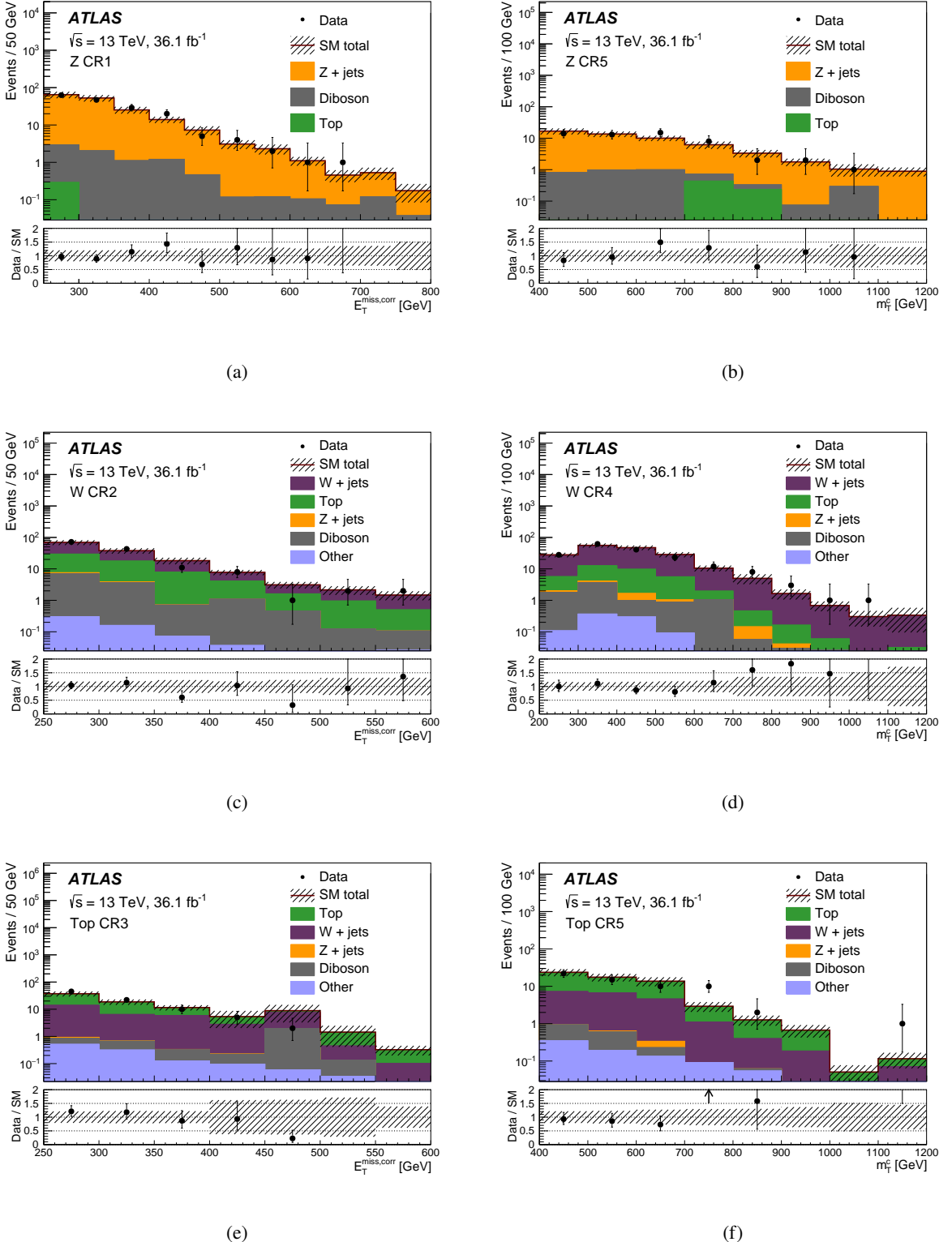


Figure 2: Examples of comparisons between data and expectation after the background-only fit for the $E_T^{\text{miss,corr}}$ distribution (a) Z CR1, (c) W CR2 and (e) Top CR3, and for the m_T^c distribution (b) Z CR5, (d) W CR4 and (f) Top CR5 . The contributions from all SM backgrounds are shown as a histogram stack. The shaded band indicates the detector-related systematic uncertainties and the statistical uncertainties of the MC samples. The error bars on the data points indicate the data's statistical uncertainty. The lower panel shows the ratio of the data to the SM prediction after the background-only fit.

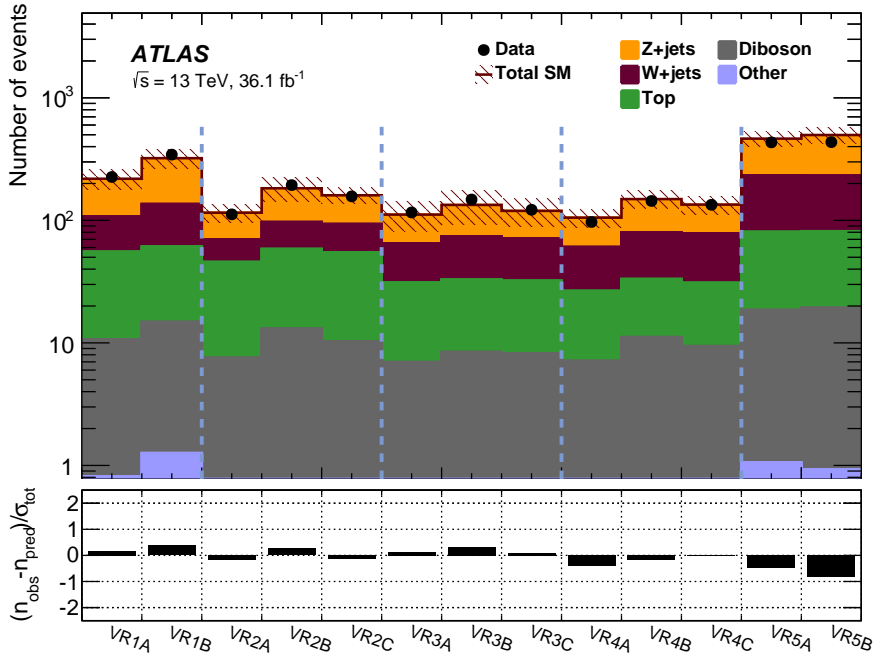


Figure 3: Comparison of the numbers of data events and predicted SM yields in each validation region. The normalisation of the backgrounds is obtained from the fit to the CRs. The shaded band indicates the total background uncertainty. The lower panel shows the pulls, estimated as the difference between the observed number of events (n_{obs}) and the predicted background yields (n_{pred}) divided by the total uncertainty (σ_{tot}).

7 Systematic Uncertainties

Various sources of systematic uncertainty are considered in this analysis. Uncertainties are treated as correlated across different regions where appropriate. Uncertainties corresponding to the number of events in the control regions used to constrain background normalisations are also considered.

The dominant experimental systematic effects on the estimated background rates are due to the uncertainties in the c -tagging efficiency and the jet energy scale (JES) [59]. The flavour-tagging uncertainties are estimated by varying the η -, p_T - and flavour-dependent scale factors applied to each jet in the simulation within a range that reflects the systematic uncertainty in the measured tagging efficiency and mis-tag rates in 13 TeV data. This uncertainty in the scale factors is in the range 15–40%, 3–12%, and 11–18% for the light-flavour jet, b -jet and c -jet scale factors, respectively. The uncertainties on the estimated background rates due to the uncertainties in the c -tagging efficiency and the JES are found to be 7–9% and 5–8%, respectively, across the different signal regions. The uncertainties associated with lepton reconstruction and energy measurements, as well as the jet energy resolution [66], are also considered but have a negligible impact on the final results. Lepton and jet-related uncertainties are propagated to the E_T^{miss} calculation, and additional uncertainties are included in the energy scale and resolution of the soft term [67].

Theoretical and modelling uncertainties of the top-quark-pair background are computed as the difference between the prediction from nominal samples and those from alternative samples differing in parameter

settings or in the choice of generator. Hadronisation and PS uncertainties are estimated using samples generated using PowHEG-Box v2 and showered by HERWIG++ v2.7.1 [68] with the UEEE5 [69] underlying-event tune. Uncertainties related to initial- and final-state radiation modelling, PS tune and choice of the h_{damp} parameter value in PowHEG-Box v2 are estimated using alternative settings of the event generators. Finally, an alternative sample produced using the SHERPA 2.2.1 generator with settings as those defined for V +jets samples, is used to estimate the event generator uncertainties.

Theoretical uncertainties in the modelling of V +jets production are assessed by considering alternative samples with varied merging (CKKW-L), resummation, renormalisation, and factorisation scales, as well as PDF variations from the NNPDF3.0NNLO replicas. The uncertainties in the background estimates in the SRs arising from renormalisation scale and PDF variations are 6–11% and 7–15%, respectively. In all SRs, they are among the dominant systematic uncertainties.

To account for differences in the heavy-flavour composition between the W CR4 and SR4, an additional normalisation uncertainty of 54% [70] is assigned in these regions to the heavy-flavour component of W +jets. The effect of this uncertainty on the background estimate is found to be small, around 1%.

Uncertainties in the diboson background are evaluated by considering different resummation, normalisation, and factorisation scales using alternative samples. An additional 15% uncertainty is assigned to its normalisation, accounting for the specific choice of the EWK parameters. The single-top-quark background forms less than 2% of the total background in all signal regions; a 100% uncertainty is assigned to its normalisation, with no impact on the search sensitivity.

The dominant relative uncertainties affecting the background estimates in each signal region are summarised in Table 6. The uncertainties on the μ factors are also included.

Source \ Region	SR1 [%]	SR2 [%]	SR3 [%]	SR4 [%]	SR5 [%]
μ_Z	6.7	9.3	12	11	13
μ_W	4.5	5.6	4.8	4.4	3.9
μ_{Top}	2.9	7.7	2.2	2.0	2.1
JES	7.9	5.0	6.8	5.2	5.6
c -tagging	6.7	8.9	9.3	8.1	7.0
W/Z +jets scale variations	11	5.8	7.6	6.5	5.2
W/Z +jets resummation scale	7.8	3.7	2.5	5.6	4.7
W/Z +jets PDF	7.7	7.1	14	15	9.1
Total	18	15	19	18	16

Table 6: Summary of the dominant experimental and theoretical uncertainties for each signal region. Uncertainties are quoted as percentages of the total SM background predictions. The individual uncertainties can be correlated, and do not necessarily add in quadrature to the total background uncertainty.

For the SUSY signal processes, both the experimental and theoretical uncertainties in the expected signal yield are considered. Experimental uncertainties are found to be between 11% and 24% across the $\tilde{t}_1, \tilde{c}_1 - \tilde{\chi}_1^0$ mass plane. In all SRs, they are largely dominated by the uncertainty in the c -tagging efficiency. They vary between 10% and 20% for squark masses in the range between 300 GeV and 1000 GeV. Additional uncertainties in the acceptance and efficiency of the SUSY signal MC samples are considered, due to the

variation of the QCD coupling constant α_S , the renormalisation and factorisation scales, the CKKW scale used to match the parton shower and matrix element descriptions, and the parton shower tunes. The total magnitude of these uncertainties ranges up to about 13%, depending on the signal region and sparticle masses considered.

Theoretical uncertainties in the NLO+NLL cross-section are calculated for each SUSY signal scenario and are dominated by the uncertainties in the renormalisation and factorisation scales, followed by the uncertainty in the PDF. These uncertainties are not treated using a nuisance parameter in any of the fits considered, since their impact is quantified separately.

8 Results

The observed event yields for each signal region are shown in Table 7 together with the estimated background contributions after the fit. The total uncertainty in the estimated background ranges from 15% to 20%, depending on the signal region, and is dominated by the uncertainty in the $Z+jets$ background. No significant excess above the SM prediction obtained after the fit is seen in any of the regions. The smallest observed p -value, which expresses the probability that the background fluctuates to the data or above, is 0.41 in region SR2. The largest deficit is observed in SR3, where 23 events are observed while 31 ± 6 events are predicted. Figure 4 shows a comparison of the observed and predicted yields in all SRs, together with the pull in each region.

Comparisons of the data to the SM predictions are shown in Figure 5 for the E_T^{miss} distribution in each SR. The expected distribution from a representative signal point is overlaid on each plot. Good agreement in the shapes of the data and predicted distributions is observed in all cases and again no significant excess above the SM prediction is observed.

In the absence of a signal, expected and observed 95% confidence level (CL) limits (S_{exp}^{95} and S_{obs}^{95} , respectively) are set on the number of possible events from sources beyond the Standard Model (BSM) in each signal region using the CL_s prescription [71, 72]. Limits on the visible cross-section σ_{vis} of a BSM signal, defined as the product of the production cross-section σ , the acceptance A and the selection efficiency ϵ , are also computed as $\sigma_{\text{vis}} = S_{\text{obs}}^{95} / \int \mathcal{L} dt$, where $\int \mathcal{L} dt$ is the integrated luminosity. The results are shown in the lower part of Table 7.

The profile-likelihood-ratio test statistic is used to set limits on the top-squark and charm-squark pair production signal models considered in this paper. If the observed CL_s value for a particular signal model is smaller than 0.05, the model is excluded at the 95% CL. The results are presented in the $\tilde{t}_1, \tilde{c}_1-\tilde{\chi}_1^0$ mass plane in Figure 6. At each point in the mass plane, the signal region with the smallest expected value of CL_s is used to set the limit. Changes in the trend of the exclusion contour are observable around $m(\tilde{t}_1, \tilde{c}_1, \tilde{\chi}_1^0) = (480, 400)$ GeV and $m(\tilde{t}_1, \tilde{c}_1, \tilde{\chi}_1^0) = (500, 300)$ GeV. They are due to the transitions between SR2 and SR3, and between SR3 and SR4, respectively. The grey region has been excluded by ATLAS searches with an energetic jet and large missing transverse momentum described in Ref. [64]. This region is characterised by events with soft c -jets, for which the efficiency of the signal regions of the present analysis is very low. For larger values of Δm , the search in Ref. [64] loses sensitivity due to a veto on jet activity beyond four jets, required in the signal regions of the search. For signal models characterised by $\Delta m < 200$ GeV the same results are also presented in the $m_{\tilde{t}_1, \tilde{c}_1}-\Delta m$ plane as shown in Figure 7.

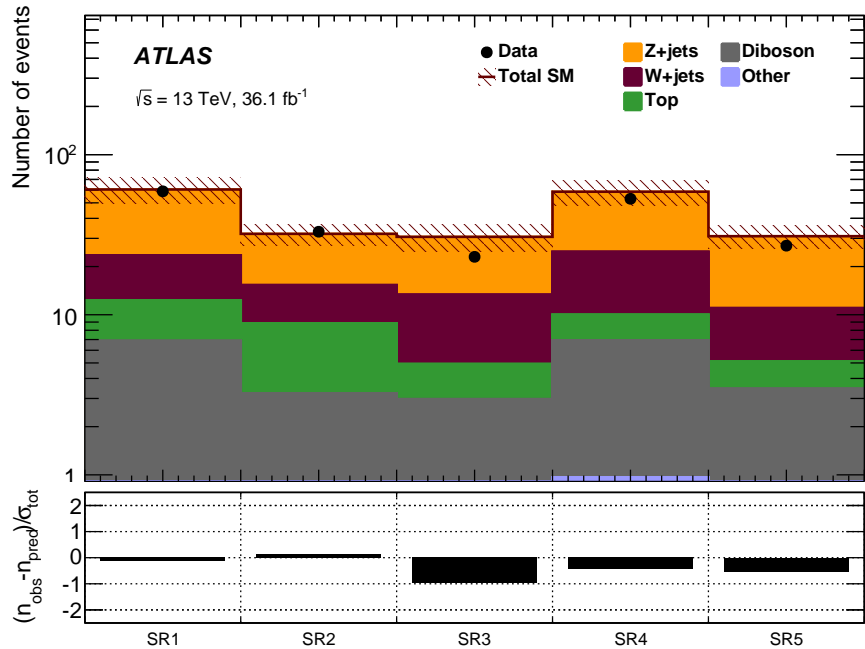


Figure 4: Comparison of the numbers of data events and predicted SM yields in each signal region. The normalisation of the backgrounds is obtained from the fit to the CRs. The shaded band indicates the total background uncertainty. The lower panel shows the pulls, estimated as the difference between the observed number of events (n_{obs}) and the predicted background yields (n_{pred}) divided by the total uncertainty (σ_{tot}).

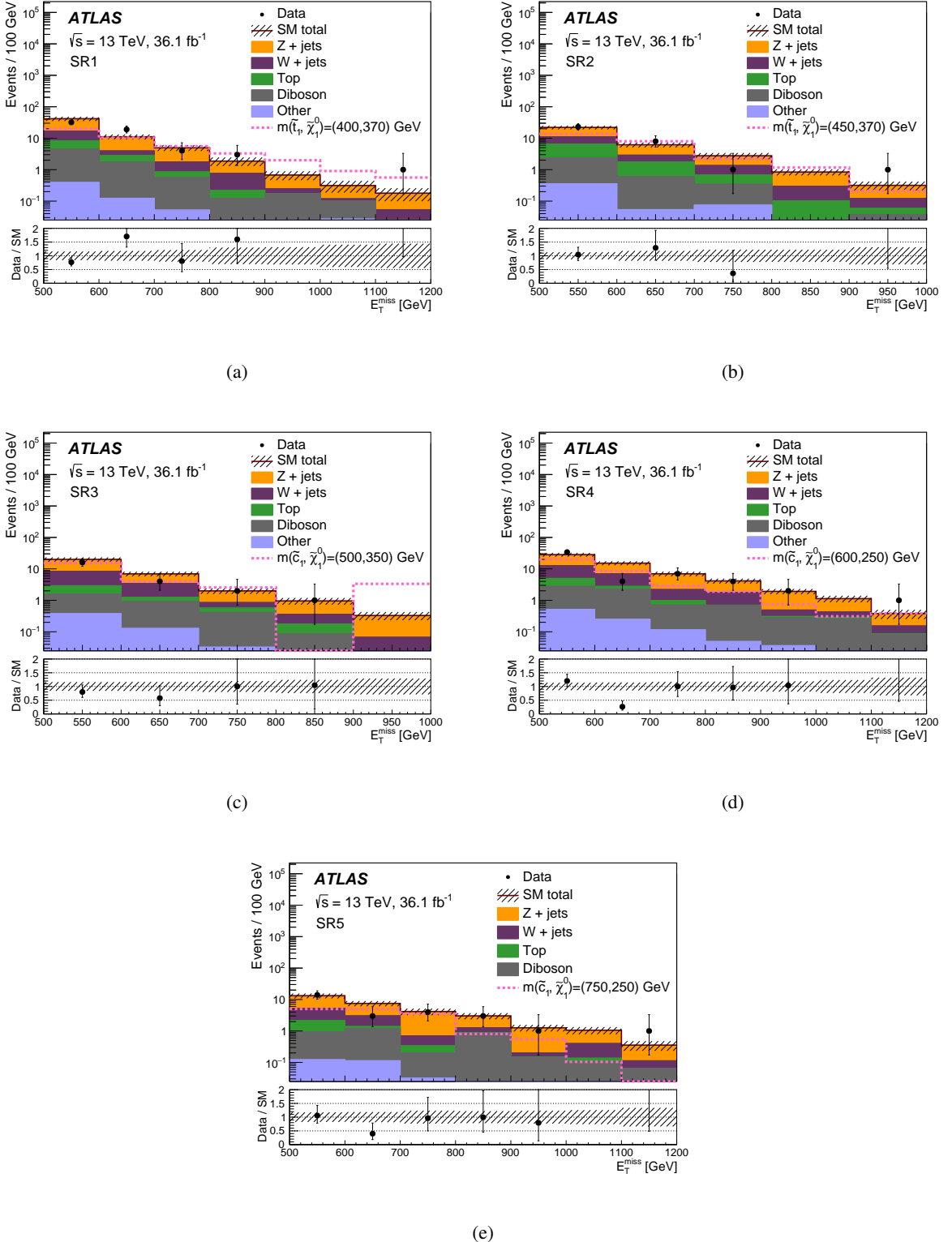


Figure 5: Comparison between data and expectation after the background-only fit for the E_T^{miss} distribution (a) in SR1, (b) in SR2, (c) in SR3, (d) in SR4, and (e) in SR5. The shaded band indicates the detector-related systematic uncertainties and the statistical uncertainties of the MC samples, while the error bars on the data points indicate the data's statistical uncertainty. The final bin in each histogram includes the overflow. The lower panel shows the ratio of the data to the SM prediction after the background-only fit. In each plot, the distribution is also shown for a representative signal point.

Yields	SR1	SR2	SR3	SR4	SR5
Observed	59	33	23	53	27
Total SM	61 ± 11	32 ± 5	31 ± 6	59 ± 11	31 ± 5
Z+jets	37.1 ± 7.8	16.7 ± 3.2	17 ± 5	34 ± 8	20 ± 4
W+jets	11.2 ± 5.1	6.5 ± 2.3	8.4 ± 2.0	15 ± 4	5.9 ± 1.5
Top	5.4 ± 2.0	5.6 ± 2.6	2.0 ± 2.0	3.1 ± 1.8	1.7 ± 0.7
Diboson	6.3 ± 2.1	2.7 ± 1.7	2.4 ± 0.7	5.9 ± 2.3	3.2 ± 1.6
Other	0.6 ± 0.1	0.5 ± 0.1	0.5 ± 0.1	1.0 ± 0.1	0.3 ± 0.1
Signal benchmarks					
$(m_{\tilde{t}_1}, m_{\tilde{\chi}_1^0}) = (450, 425)$ GeV	22.7 ± 4.0	9.1 ± 2.6	1.6 ± 1.0	1.84 ± 0.71	0.45 ± 0.27
$(m_{\tilde{t}_1}, m_{\tilde{\chi}_1^0}) = (500, 420)$ GeV	18.3 ± 3.4	19.7 ± 4.9	15.2 ± 4.1	8.0 ± 2.2	1.26 ± 0.64
$(m_{\tilde{t}_1}, m_{\tilde{\chi}_1^0}) = (500, 350)$ GeV	5.4 ± 2.0	11.6 ± 3.3	26.1 ± 6.7	18.7 ± 5.4	3.0 ± 1.1
$(m_{\tilde{t}_1}, m_{\tilde{\chi}_1^0}) = (600, 350)$ GeV	1.91 ± 0.87	3.2 ± 1.3	10.5 ± 3.0	24.0 ± 5.9	7.0 ± 2.2
$(m_{\tilde{t}_1}, m_{\tilde{\chi}_1^0}) = (900, 1)$ GeV	0.67 ± 0.19	0.61 ± 0.21	1.61 ± 0.50	11.7 ± 2.0	10.2 ± 1.8
$\langle \sigma_{\text{vis}} \rangle_{\text{obs}}^{95}$ [fb]	0.67	0.46	0.33	0.59	0.40
S_{obs}^{95}	24.2	16.6	11.9	21.3	14.3
S_{exp}^{95}	$24.4^{+13.2}_{-7.6}$	$16.0^{+5.6}_{-4.4}$	$15.0^{+5.2}_{-3.1}$	$24.9^{+9.6}_{-7.1}$	$15.3^{+6.8}_{-2.2}$
$p(s = 0)$	0.5	0.41	0.5	0.5	0.5

Table 7: Observed and expected yields for all the signal regions considered in the analysis. The uncertainties include experimental, theoretical, and Monte Carlo statistical uncertainties. Benchmark signal models yields are also given for each SR. The lower part of the table reports the 95% CL upper limits on the visible cross-section, $\langle \sigma_{\text{vis}} \rangle_{\text{obs}}^{95}$, on the number of signal events, S_{obs}^{95} , and on the number of signal events given the expected number (and $\pm 1\sigma$ excursions of the expectation) of background events, S_{exp}^{95} . The discovery p -value, $p(s = 0)$, where s is the number of signal events, is also reported. The value of 0.5 is assigned in the case of a downward data fluctuation where the number of observed events is less than the expected number of events.

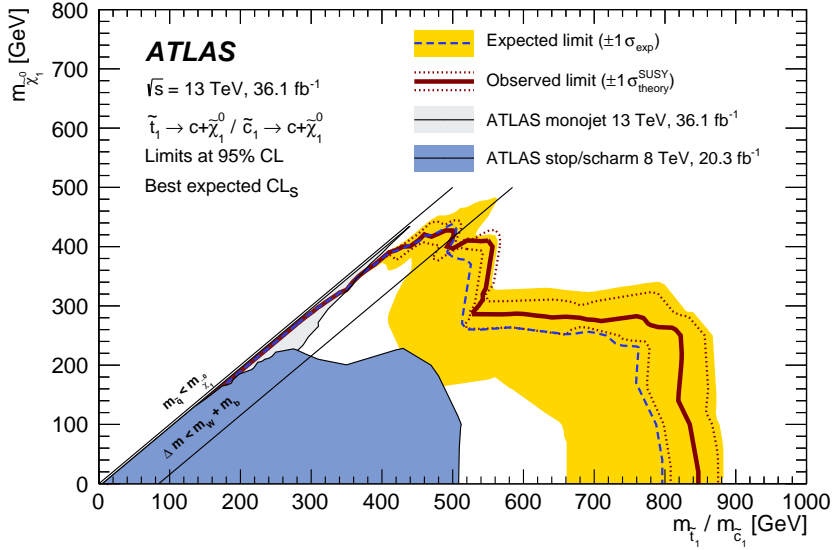


Figure 6: Observed and expected exclusion contours at 95% CL, as well as $\pm 1\sigma$ variation of the expected limit, in the $\tilde{t}_1, \tilde{c}_1-\tilde{\chi}_1^0$ mass plane. The SR with the best expected sensitivity is adopted for each point of the parameter space. The solid band around the expected limit (dashed line) shows the impact of the experimental and SM background theoretical uncertainties. The dotted lines show the impact on the observed limit of the variation of the nominal signal cross-section by $\pm 1\sigma$ of its theoretical uncertainties. The observed limit from the monojet search at $\sqrt{s} = 13$ TeV [64] and from the Run-1 analysis [20, 21] at $\sqrt{s} = 8$ TeV are also overlaid. Δm denotes $m_{\tilde{t}_1, \tilde{c}_1} - m_{\tilde{\chi}_1^0}$.

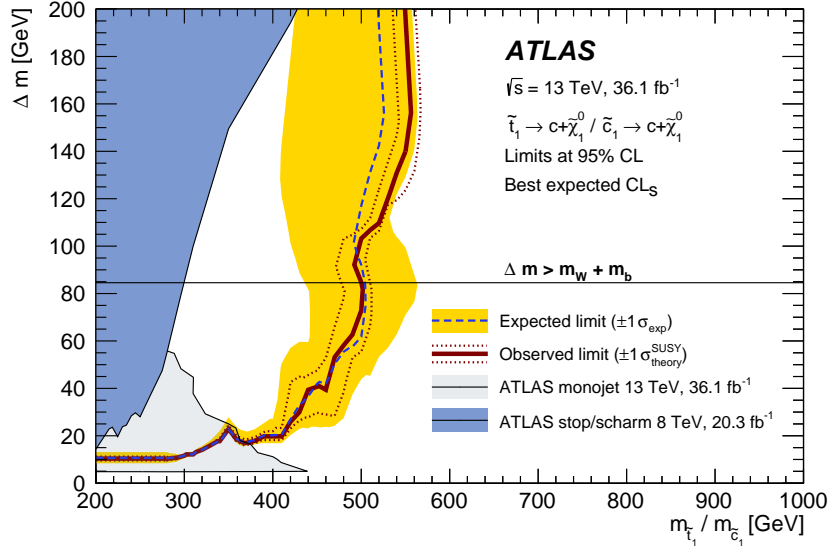


Figure 7: Observed and expected exclusion contours at 95% CL, as well as $\pm 1\sigma$ variation of the expected limit, in the $m_{\tilde{t}_1, \tilde{c}_1}-\Delta m$ plane, where Δm denotes $m_{\tilde{t}_1, \tilde{c}_1} - m_{\tilde{\chi}_1^0}$. The SR with the best expected sensitivity is adopted for each point of the parameter space. The solid band around the expected limit (dashed line) shows the impact of the experimental and SM background theoretical uncertainties. The dotted lines show the impact on the observed limit of the variation of the nominal signal cross-section by $\pm 1\sigma$ of its theoretical uncertainties. The observed limit from the monojet search at $\sqrt{s} = 13$ TeV [64] and from the Run-1 analysis [20, 21] at $\sqrt{s} = 8$ TeV are also overlaid.

9 Conclusion

This paper reports a search for direct top-squark and charm-squark pair production in final states with charm-tagged jets and missing transverse momentum, based on a 36.1 fb^{-1} dataset of $\sqrt{s} = 13\text{ TeV}$ proton–proton collisions recorded by the ATLAS experiment at the LHC in 2015 and 2016. No significant excess above the expected Standard Model background is found and model-independent exclusion limits at 95% CL are set on the visible cross-section. Assuming a 100% branching ratio to $c\tilde{\chi}_1^0$, top and charm squarks with masses up to 850 GeV are excluded at 95% CL for a massless lightest neutralino. For $m_{\tilde{t}_1, \tilde{c}_1} - m_{\tilde{\chi}_1^0} < 100\text{ GeV}$, top and charm squarks with masses up to 500 GeV are excluded.

Acknowledgements

We thank CERN for the very successful operation of the LHC, as well as the support staff from our institutions without whom ATLAS could not be operated efficiently.

We acknowledge the support of ANPCyT, Argentina; YerPhI, Armenia; ARC, Australia; BMWFW and FWF, Austria; ANAS, Azerbaijan; SSTC, Belarus; CNPq and FAPESP, Brazil; NSERC, NRC and CFI, Canada; CERN; CONICYT, Chile; CAS, MOST and NSFC, China; COLCIENCIAS, Colombia; MSMT CR, MPO CR and VSC CR, Czech Republic; DNRF and DNSRC, Denmark; IN2P3-CNRS, CEA-DRF/IRFU, France; SRNSFG, Georgia; BMBF, HGF, and MPG, Germany; GSRT, Greece; RGC, Hong Kong SAR, China; ISF, I-CORE and Benoziyo Center, Israel; INFN, Italy; MEXT and JSPS, Japan; CNRST, Morocco; NWO, Netherlands; RCN, Norway; MNiSW and NCN, Poland; FCT, Portugal; MNE/IFA, Romania; MES of Russia and NRC KI, Russian Federation; JINR; MESTD, Serbia; MSSR, Slovakia; ARRS and MIZŠ, Slovenia; DST/NRF, South Africa; MINECO, Spain; SRC and Wallenberg Foundation, Sweden; SERI, SNSF and Cantons of Bern and Geneva, Switzerland; MOST, Taiwan; TAEK, Turkey; STFC, United Kingdom; DOE and NSF, United States of America. In addition, individual groups and members have received support from BCKDF, the Canada Council, CANARIE, CRC, Compute Canada, FQRNT, and the Ontario Innovation Trust, Canada; EPLANET, ERC, ERDF, FP7, Horizon 2020 and Marie Skłodowska-Curie Actions, European Union; Investissements d’Avenir Labex and Idex, ANR, Région Auvergne and Fondation Partager le Savoir, France; DFG and AvH Foundation, Germany; Herakleitos, Thales and Aristeia programmes co-financed by EU-ESF and the Greek NSRF; BSF, GIF and Minerva, Israel; BRF, Norway; CERCA Programme Generalitat de Catalunya, Generalitat Valenciana, Spain; the Royal Society and Leverhulme Trust, United Kingdom.

The crucial computing support from all WLCG partners is acknowledged gratefully, in particular from CERN, the ATLAS Tier-1 facilities at TRIUMF (Canada), NDGF (Denmark, Norway, Sweden), CC-IN2P3 (France), KIT/GridKA (Germany), INFN-CNAF (Italy), NL-T1 (Netherlands), PIC (Spain), ASGC (Taiwan), RAL (UK) and BNL (USA), the Tier-2 facilities worldwide and large non-WLCG resource providers. Major contributors of computing resources are listed in Ref. [73].

References

- [1] Yu. A. Golfand and E. P. Likhtman, *Extension of the algebra of Poincaré group generators and violation of P invariance*, JETP Lett. **13** (1971) 323, [Pisma Zh. Eksp. Teor. Fiz. **13** (1971) 452].
- [2] D. V. Volkov and V. P. Akulov, *Is the neutrino a Goldstone particle?*, Phys. Lett. B **46** (1973) 109.
- [3] J. Wess and B. Zumino, *Supergauge transformations in four-dimensions*, Nucl. Phys. B **70** (1974) 39.
- [4] J. Wess and B. Zumino, *Supergauge invariant extension of quantum electrodynamics*, Nucl. Phys. B **78** (1974) 1.
- [5] S. Ferrara and B. Zumino, *Supergauge invariant Yang-Mills theories*, Nucl. Phys. B **79** (1974) 413.
- [6] A. Salam and J. A. Strathdee, *Super-symmetry and non-Abelian gauges*, Phys. Lett. B **51** (1974) 353.
- [7] N. Sakai, *Naturalness in supersymmetric GUTs*, Z. Phys. C **11** (1981) 153.
- [8] S. Dimopoulos, S. Raby and F. Wilczek, *Supersymmetry and the scale of unification*, Phys. Rev. D **24** (1981) 1681.
- [9] L. E. Ibanez and G. G. Ross, *Low-energy predictions in supersymmetric grand unified theories*, Phys. Lett. B **105** (1981) 439.
- [10] S. Dimopoulos and H. Georgi, *Softly broken supersymmetry and $SU(5)$* , Nucl. Phys. B **193** (1981) 150.
- [11] G. R. Farrar and P. Fayet, *Phenomenology of the production, decay, and detection of new hadronic states associated with supersymmetry*, Phys. Lett. B **76** (1978) 575.
- [12] H. Goldberg, *Constraint on the photino mass from cosmology*, Phys. Rev. Lett. **50** (1983) 1419, [Erratum: Phys. Rev. Lett. **103** (2009) 099905].
- [13] J. R. Ellis, J. S. Hagelin, D. V. Nanopoulos, K. A. Olive and M. Srednicki, *Supersymmetric relics from the Big Bang*, Nucl. Phys. B **238** (1984) 453.
- [14] R. Barbieri and G. F. Giudice, *Upper bounds on supersymmetric particle masses*, Nucl. Phys. B **306** (1988) 63.
- [15] B. de Carlos and J. A. Casas, *One loop analysis of the electroweak breaking in supersymmetric models and the fine tuning problem*, Phys. Lett. B **309** (1993) 320, arXiv: [9303291](#).
- [16] K. Inoue, A. Kakuto, H. Komatsu and S. Takeshita, *Aspects of grand unified models with softly broken supersymmetry*, Prog. Theor. Phys. **68** (1982) 927, [Erratum: Prog. Theor. Phys. **70**, 330 (1983)].
- [17] J. R. Ellis and S. Rudaz, *Search for supersymmetry in toponium decays*, Phys. Lett. B **128** (1983) 248.
- [18] R. Gröber, M. Mühlleitner, E. Popenda and A. Wlotzka, *Light stop decays into $W b \tilde{\chi}_1^0$ near the kinematic threshold*, Phys. Lett. B **747** (2015) 144, arXiv: [1502.05935](#).
- [19] R. Mahbubani, M. Papucci, G. Perez, J. T. Ruderman and A. Weiler, *Light nondegenerate squarks at the LHC*, Phys. Rev. Lett. **110** (2013) 151804, arXiv: [1212.3328](#).

- [20] ATLAS Collaboration, *Search for pair-produced third-generation squarks decaying via charm quarks or in compressed supersymmetric scenarios in pp collisions at $\sqrt{s} = 8$ TeV with the ATLAS detector*, *Phys. Rev. D* **90** (2014) 052008, arXiv: [1407.0608](#).
- [21] ATLAS Collaboration, *Search for scalar charm quark pair production in pp collisions at $\sqrt{s} = 8$ TeV with the ATLAS detector*, *Phys. Rev. Lett.* **114** (2015) 161801, arXiv: [1501.01325](#).
- [22] CMS Collaboration, *Search for the pair production of third-generation squarks with two-body decays to a bottom or charm quark and a neutralino in proton–proton collisions at $\sqrt{s} = 13$ TeV*, *Phys. Lett. B* **778** (2018) 263, arXiv: [1707.07274](#).
- [23] ATLAS Collaboration, *The ATLAS Experiment at the CERN Large Hadron Collider*, *JINST* **3** (2008) S08003.
- [24] ATLAS Collaboration, *ATLAS insertable b-layer technical design report*, ATLAS-TDR-19, 2010, URL: <https://cds.cern.ch/record/1291633>,
ATLAS insertable b-layer technical design report addendum, ATLAS-TDR-19-ADD-1, 2012, URL: <https://cds.cern.ch/record/1451888>.
- [25] ATLAS Collaboration, *Optimisation of the ATLAS b-tagging performance for the 2016 LHC Run*, ATL-PHYS-PUB-2016-012, 2016, URL: <https://cds.cern.ch/record/2160731>.
- [26] ATLAS Collaboration, *Performance of the ATLAS trigger system in 2015*, *Eur. Phys. J. C* **77** (2017) 317, arXiv: [1611.09661](#).
- [27] ATLAS Collaboration, *Luminosity determination in pp collisions at $\sqrt{s} = 8$ TeV using the ATLAS detector at the LHC*, *Eur. Phys. J. C* **76** (2016) 653, arXiv: [1608.03953 \[hep-ex\]](#).
- [28] J. Alwall et al., *The automated computation of tree-level and next-to-leading order differential cross sections, and their matching to parton shower simulations*, *JHEP* **07** (2014) 079, arXiv: [1405.0301](#).
- [29] T. Sjostrand, S. Mrenna and P. Z. Skands, *A brief introduction to PYTHIA 8.1*, *Comput. Phys. Commun.* **178** (2008) 852, arXiv: [0710.3820](#).
- [30] ATLAS Collaboration, *Summary of ATLAS Pythia 8 tunes*, ATL-PHYS-PUB-2012-003, 2012, URL: <https://cds.cern.ch/record/1474107>.
- [31] L. Lönnblad and S. Prestel, *Merging multi-leg NLO matrix elements with parton showers*, *JHEP* **03** (2013) 166, arXiv: [1211.7278](#).
- [32] R. D. Ball et al., *Parton distributions with LHC data*, *Nucl. Phys. B* **867** (2013) 244, arXiv: [1207.1303](#).
- [33] W. Beenakker, M. Kramer, T. Plehn, M. Spira and P. M. Zerwas, *Stop production at hadron colliders*, *Nucl. Phys. B* **515** (1998) 3, arXiv: [9710451](#).
- [34] W. Beenakker et al., *Supersymmetric top and bottom squark production at hadron colliders*, *JHEP* **08** (2010) 098, arXiv: [1006.4771](#).
- [35] W. Beenakker et al., *Squark and gluino hadroproduction*, *Int. J. Mod. Phys. A* **26** (2011) 2637, arXiv: [1105.1110](#).
- [36] C. Borschensky et al., *Squark and gluino production cross sections in pp collisions at $\sqrt{s} = 13, 14, 33$ and 100 TeV*, *Eur. Phys. J. C* **74** (2014) 3174, arXiv: [1407.5066](#).

- [37] T. Gleisberg et al., *Event generation with SHERPA 1.1*, *JHEP* **02** (2009) 007, arXiv: [0811.4622](#).
- [38] T. Gleisberg and S. Höche, *Comix, a new matrix element generator*, *JHEP* **12** (2008) 039, arXiv: [0808.3674](#).
- [39] F. Cascioli, P. Maierhofer and S. Pozzorini, *Scattering amplitudes with OpenLoops*, *Phys. Rev. Lett.* **108** (2012) 111601, arXiv: [1111.5206](#).
- [40] S. Schumann and F. Krauss, *A Parton shower algorithm based on Catani-Seymour dipole factorisation*, *JHEP* **03** (2008) 038, arXiv: [0709.1027](#).
- [41] S. Höche, F. Krauss, M. Schönher and F. Siegert, *QCD matrix elements + parton showers: the NLO case*, *JHEP* **04** (2013) 027, arXiv: [1207.5030](#).
- [42] NNPDF Collaboration: R. D. Ball et al., *Parton distributions for the LHC Run II*, *JHEP* **04** (2015) 040, arXiv: [1410.8849](#).
- [43] R. Gavin, Y. Li, F. Petriello and S. Quackenbush, *FEWZ 2.0: a code for hadronic Z production at next-to-next-to-leading order*, *Comput. Phys. Commun.* **182** (2011) 2388, arXiv: [1011.3540](#).
- [44] S. Alioli, P. Nason, C. Oleari and E. Re, *A general framework for implementing NLO calculations in shower Monte Carlo programs: the POWHEG BOX*, *JHEP* **06** (2010) 043, arXiv: [1002.2581](#).
- [45] H.-L. Lai et al., *New parton distributions for collider physics*, *Phys. Rev. D* **82** (2010) 074024, arXiv: [1007.2241](#).
- [46] T. Sjöstrand, S. Mrenna and P. Z. Skands, *PYTHIA 6.4 physics and manual*, *JHEP* **05** (2006) 026, arXiv: [0603175](#).
- [47] P. Z. Skands, *Tuning Monte Carlo generators: the Perugia tunes*, *Phys. Rev. D* **82** (2010) 074018, arXiv: [1005.3457](#).
- [48] D. J. Lange, *The EvtGen particle decay simulation package*, *Nucl. Instrum. Meth. A* **462** (2001) 152.
- [49] A. D. Martin, W. J. Stirling, R. S. Thorne and G. Watt, *Parton distributions for the LHC*, *Eur. Phys. J. C* **63** (2009) 189, arXiv: [0901.0002](#).
- [50] ATLAS Collaboration, *The ATLAS Simulation Infrastructure*, *Eur. Phys. J. C* **70** (2010) 823, arXiv: [1005.4568 \[physics.ins-det\]](#).
- [51] S. Agostinelli et al., *GEANT4: a simulation toolkit*, *Nucl. Instrum. Meth. A* **506** (2003) 250.
- [52] ATLAS Collaboration, *The simulation principle and performance of the ATLAS fast calorimeter simulation FastCaloSim*, ATL-PHYS-PUB-2010-013, 2010, URL: <https://cds.cern.ch/record/1300517>.
- [53] ATLAS Collaboration, *Vertex Reconstruction Performance of the ATLAS Detector at $\sqrt{s} = 13 \text{ TeV}$* , ATL-PHYS-PUB-2015-026, 2015, URL: <https://cds.cern.ch/record/2037717>.
- [54] ATLAS Collaboration, *Electron and photon energy calibration with the ATLAS detector using LHC Run 1 data*, *Eur. Phys. J. C* **74** (2014) 3071, arXiv: [1407.5063 \[hep-ex\]](#).
- [55] ATLAS Collaboration, *Electron efficiency measurements with the ATLAS detector using the 2015 LHC proton–proton collision data*, ATLAS-CONF-2016-024, 2016, URL: <https://cds.cern.ch/record/2157687>.

- [56] ATLAS Collaboration, *Muon reconstruction performance of the ATLAS detector in proton–proton collision data at $\sqrt{s} = 13$ TeV*, *Eur. Phys. J. C* **76** (2016) 292, arXiv: [1603.05598 \[hep-ex\]](#).
- [57] ATLAS Collaboration, *Topological cell clustering in the ATLAS calorimeters and its performance in LHC Run 1*, *Eur. Phys. J. C* **77** (2017) 490, arXiv: [1603.02934 \[hep-ex\]](#).
- [58] M. Cacciari, G. P. Salam and G. Soyez, *The anti- k_t jet clustering algorithm*, *JHEP* **04** (2008) 063, arXiv: [0802.1189](#).
- [59] ATLAS Collaboration, *Jet energy scale measurements and their systematic uncertainties in proton–proton collisions at $\sqrt{s} = 13$ TeV with the ATLAS detector*, *Phys. Rev. D* **96** (2017) 072002, arXiv: [1703.09665 \[hep-ex\]](#).
- [60] ATLAS Collaboration, *Performance of pile-up mitigation techniques for jets in pp collisions at $\sqrt{s} = 8$ TeV using the ATLAS detector*, *Eur. Phys. J. C* **76** (2016) 581, arXiv: [1510.03823 \[hep-ex\]](#).
- [61] ATLAS Collaboration, *Commissioning of the ATLAS b-tagging algorithms using $t\bar{t}$ events in early Run 2 data*, ATL-PHYS-PUB-2015-039, 2015, URL: <https://cds.cern.ch/record/2047871>.
- [62] ATLAS Collaboration, *Performance of algorithms that reconstruct missing transverse momentum in $\sqrt{s} = 8$ TeV proton-proton collisions in the ATLAS detector*, *Eur. Phys. J. C* **77** (2017) 241, arXiv: [1609.09324](#).
- [63] ATLAS Collaboration, *Performance of missing transverse momentum reconstruction with the ATLAS detector using proton-proton collisions at $\sqrt{s} = 13$ TeV*, (2018), arXiv: [1802.08168](#).
- [64] ATLAS Collaboration, *Search for dark matter and other new phenomena in events with an energetic jet and large missing transverse momentum using the ATLAS detector*, *JHEP* **01** (2018) 126, arXiv: [1711.03301](#).
- [65] M. Baak et al., *HistFitter software framework for statistical data analysis*, *Eur. Phys. J. C* **75** (2015) 153, arXiv: [1410.1280](#).
- [66] ATLAS Collaboration, *Jet energy resolution in proton–proton collisions at $\sqrt{s} = 7$ TeV recorded in 2010 with the ATLAS detector*, *Eur. Phys. J. C* **73** (2013) 2306, arXiv: [1210.6210 \[hep-ex\]](#).
- [67] ATLAS Collaboration, *Expected performance of missing transverse momentum reconstruction for the ATLAS detector at $\sqrt{s} = 13$ TeV*, ATL-PHYS-PUB-2015-023, 2015, URL: <https://cds.cern.ch/record/2037700>.
- [68] M. Bähr et al., *Herwig++ physics and manual*, *Eur. Phys. J. C* **58** (2008) 639, arXiv: [0803.0883](#).
- [69] S. Gieseke, C. Rohr and A. Siodmok, *Colour reconnections in Herwig++*, *Eur. Phys. J. C* **72** (2012) 2225, arXiv: [1206.0041](#).
- [70] ATLAS Collaboration, *Measurement of the cross section for the production of a W boson in association with b-jets in pp collisions at $\sqrt{s} = 7$ TeV with the ATLAS detector*, *Phys. Lett. B* **707** (2012) 418, arXiv: [1109.1470 \[hep-ex\]](#).
- [71] T. Junk, *Confidence level computation for combining searches with small statistics*, *Nucl. Instrum. Meth. A* **434** (1999) 435, arXiv: [9902006](#).
- [72] A. L. Read, *Presentation of search results: the CL_S technique*, *J. Phys. G* **28** (2002) 2693.
- [73] ATLAS Collaboration, *ATLAS Computing Acknowledgements*, ATL-GEN-PUB-2016-002, URL: <https://cds.cern.ch/record/2202407>.

The ATLAS Collaboration

M. Aaboud^{34d}, G. Aad⁹⁹, B. Abbott¹²⁵, O. Abdinov^{13,*}, B. Abeloos¹²⁹, S.H. Abidi¹⁶⁵, O.S. AbouZeid¹⁴³, N.L. Abraham¹⁵³, H. Abramowicz¹⁵⁹, H. Abreu¹⁵⁸, Y. Abulaiti⁶, B.S. Acharya^{64a,64b,p}, S. Adachi¹⁶¹, L. Adamczyk^{81a}, J. Adelman¹¹⁹, M. Adersberger¹¹², T. Adye¹⁴¹, A.A. Affolder¹⁴³, Y. Afik¹⁵⁸, C. Agheorghiesei^{27c}, J.A. Aguilar-Saavedra^{137f,137a}, F. Ahmadov^{77,ai}, G. Aielli^{71a,71b}, S. Akatsuka⁸³, T.P.A. Åkesson⁹⁴, E. Akilli⁵², A.V. Akimov¹⁰⁸, G.L. Alberghi^{23b,23a}, J. Albert¹⁷⁴, P. Albicocco⁴⁹, M.J. Alconada Verzini⁸⁶, S. Alderweireldt¹¹⁷, M. Aleksa³⁵, I.N. Aleksandrov⁷⁷, C. Alexa^{27b}, G. Alexander¹⁵⁹, T. Alexopoulos¹⁰, M. Alhoob¹²⁵, B. Ali¹³⁹, G. Alimonti^{66a}, J. Alison³⁶, S.P. Alkire¹⁴⁵, C. Allaire¹²⁹, B.M.M. Allbrooke¹⁵³, B.W. Allen¹²⁸, P.P. Allport²¹, A. Aloisio^{67a,67b}, A. Alonso³⁹, F. Alonso⁸⁶, C. Alpigiani¹⁴⁵, A.A. Alshehri⁵⁵, M.I. Alstaty⁹⁹, B. Alvarez Gonzalez³⁵, D. Álvarez Piqueras¹⁷², M.G. Alvaggi^{67a,67b}, B.T. Amadio¹⁸, Y. Amaral Coutinho^{78b}, L. Ambroz¹³², C. Amelung²⁶, D. Amidei¹⁰³, S.P. Amor Dos Santos^{137a,137c}, S. Amoroso³⁵, C.S. Amrouche⁵², C. Anastopoulos¹⁴⁶, L.S. Ancu⁵², N. Andari²¹, T. Andeen¹¹, C.F. Anders^{59b}, J.K. Anders²⁰, K.J. Anderson³⁶, A. Andreazza^{66a,66b}, V. Andrei^{59a}, S. Angelidakis³⁷, I. Angelozzi¹¹⁸, A. Angerami³⁸, A.V. Anisenkov^{120b,120a}, A. Annovi^{69a}, C. Antel^{59a}, M.T. Anthony¹⁴⁶, M. Antonelli⁴⁹, D.J.A. Antrim¹⁶⁹, F. Anulli^{70a}, M. Aoki⁷⁹, L. Aperio Bella³⁵, G. Arabidze¹⁰⁴, Y. Arai⁷⁹, J.P. Araque^{137a}, V. Araujo Ferraz^{78b}, R. Araujo Pereira^{78b}, A.T.H. Arce⁴⁷, R.E. Ardell⁹¹, F.A. Arduh⁸⁶, J-F. Arguin¹⁰⁷, S. Argyropoulos⁷⁵, A.J. Armbruster³⁵, L.J. Armitage⁹⁰, O. Arnaez¹⁶⁵, H. Arnold¹¹⁸, M. Arratia³¹, O. Arslan²⁴, A. Artamonov^{109,*}, G. Artoni¹³², S. Artz⁹⁷, S. Asai¹⁶¹, N. Asbah⁴⁴, A. Ashkenazi¹⁵⁹, E.M. Asimakopoulou¹⁷⁰, L. Asquith¹⁵³, K. Assamagan²⁹, R. Astalos^{28a}, R.J. Atkin^{32a}, M. Atkinson¹⁷¹, N.B. Atlay¹⁴⁸, K. Augsten¹³⁹, G. Avolio³⁵, R. Avramidou^{58a}, B. Axen¹⁸, M.K. Ayoub^{15a}, G. Azuelos^{107,ax}, A.E. Baas^{59a}, M.J. Baca²¹, H. Bachacou¹⁴², K. Bachas^{65a,65b}, M. Backes¹³², P. Bagnaia^{70a,70b}, M. Bahmani⁸², H. Bahrasemani¹⁴⁹, A.J. Bailey¹⁷², J.T. Baines¹⁴¹, M. Bajic³⁹, O.K. Baker¹⁸¹, P.J. Bakker¹¹⁸, D. Bakshi Gupta⁹³, E.M. Baldin^{120b,120a}, P. Balek¹⁷⁸, F. Balli¹⁴², W.K. Balunas¹³⁴, E. Banas⁸², A. Bandyopadhyay²⁴, S. Banerjee^{179,l}, A.A.E. Bannoura¹⁸⁰, L. Barak¹⁵⁹, W.M. Barbe³⁷, E.L. Barberio¹⁰², D. Barberis^{53b,53a}, M. Barbero⁹⁹, T. Barillari¹¹³, M-S. Barisits³⁵, J. Barkeloo¹²⁸, T. Barklow¹⁵⁰, N. Barlow³¹, R. Barnea¹⁵⁸, S.L. Barnes^{58c}, B.M. Barnett¹⁴¹, R.M. Barnett¹⁸, Z. Barnovska-Blenessy^{58a}, A. Baroncelli^{72a}, G. Barone²⁶, A.J. Barr¹³², L. Barranco Navarro¹⁷², F. Barreiro⁹⁶, J. Barreiro Guimarães da Costa^{15a}, R. Bartoldus¹⁵⁰, A.E. Barton⁸⁷, P. Bartos^{28a}, A. Basalaev¹³⁵, A. Bassalat¹²⁹, R.L. Bates⁵⁵, S.J. Batista¹⁶⁵, S. Batlamous^{34e}, J.R. Batley³¹, M. Battaglia¹⁴³, M. Bauce^{70a,70b}, F. Bauer¹⁴², K.T. Bauer¹⁶⁹, H.S. Bawa^{150,n}, J.B. Beacham¹²³, M.D. Beattie⁸⁷, T. Beau¹³³, P.H. Beauchemin¹⁶⁸, P. Bechtle²⁴, H.C. Beck⁵¹, H.P. Beck^{20,t}, K. Becker⁵⁰, M. Becker⁹⁷, C. Becot¹²², A. Beddall^{12d}, A.J. Beddall^{12a}, V.A. Bednyakov⁷⁷, M. Bedognetti¹¹⁸, C.P. Bee¹⁵², T.A. Beermann³⁵, M. Begalli^{78b}, M. Begel²⁹, A. Behera¹⁵², J.K. Behr⁴⁴, A.S. Bell⁹², G. Bella¹⁵⁹, L. Bellagamba^{23b}, A. Bellerive³³, M. Bellomo¹⁵⁸, K. Belotskiy¹¹⁰, N.L. Belyaev¹¹⁰, O. Benary^{159,*}, D. Benchekroun^{34a}, M. Bender¹¹², N. Benekos¹⁰, Y. Benhammou¹⁵⁹, E. Benhar Noccioli¹⁸¹, J. Benitez⁷⁵, D.P. Benjamin⁴⁷, M. Benoit⁵², J.R. Bensinger²⁶, S. Bentvelsen¹¹⁸, L. Beresford¹³², M. Beretta⁴⁹, D. Berge⁴⁴, E. Bergeaas Kuutmann¹⁷⁰, N. Berger⁵, L.J. Bergsten²⁶, J. Beringer¹⁸, S. Berlendis⁵⁶, N.R. Bernard¹⁰⁰, G. Bernardi¹³³, C. Bernius¹⁵⁰, F.U. Bernlochner²⁴, T. Berry⁹¹, P. Berta⁹⁷, C. Bertella^{15a}, G. Bertoli^{43a,43b}, I.A. Bertram⁸⁷, C. Bertsche⁴⁴, G.J. Besjes³⁹, O. Bessidskaia Bylund^{43a,43b}, M. Bessner⁴⁴, N. Besson¹⁴², A. Bethani⁹⁸, S. Bethke¹¹³, A. Betti²⁴, A.J. Bevan⁹⁰, J. Beyer¹¹³, R.M. Bianchi¹³⁶, O. Biebel¹¹², D. Biedermann¹⁹, R. Bielski⁹⁸, K. Bierwagen⁹⁷, N.V. Biesuz^{69a,69b}, M. Biglietti^{72a}, T.R.V. Billoud¹⁰⁷, M. Bindi⁵¹, A. Bingul^{12d}, C. Bini^{70a,70b}, S. Biondi^{23b,23a}, T. Bisanz⁵¹, C. Bittrich⁴⁶, D.M. Bjergaard⁴⁷, J.E. Black¹⁵⁰, K.M. Black²⁵, R.E. Blair⁶, T. Blazek^{28a}, I. Bloch⁴⁴, C. Blocker²⁶, A. Blue⁵⁵, U. Blumenschein⁹⁰,

Dr. Blunier^{144a}, G.J. Bobbink¹¹⁸, V.S. Bobrovnikov^{120b,120a}, S.S. Bocchetta⁹⁴, A. Bocci⁴⁷, C. Bock¹¹², D. Boerner¹⁸⁰, D. Bogavac¹¹², A.G. Bogdanchikov^{120b,120a}, C. Bohm^{43a}, V. Boisvert⁹¹, P. Bokan¹⁷⁰, T. Bold^{81a}, A.S. Boldyrev¹¹¹, A.E. Bolz^{59b}, M. Bomben¹³³, M. Bona⁹⁰, J.S. Bonilla¹²⁸, M. Boonekamp¹⁴², A. Borisov¹²¹, G. Borissov⁸⁷, J. Bortfeldt³⁵, D. Bortoletto¹³², V. Bortolotto^{71a,61b,61c,71b}, D. Boscherini^{23b}, M. Bosman¹⁴, J.D. Bossio Sola³⁰, J. Boudreau¹³⁶, E.V. Bouhova-Thacker⁸⁷, D. Boumediene³⁷, C. Bourdarios¹²⁹, S.K. Boutle⁵⁵, A. Boveia¹²³, J. Boyd³⁵, I.R. Boyko⁷⁷, A.J. Bozson⁹¹, J. Bracinik²¹, N. Brahimi⁹⁹, A. Brandt⁸, G. Brandt¹⁸⁰, O. Brandt^{59a}, F. Braren⁴⁴, U. Bratzler¹⁶², B. Brau¹⁰⁰, J.E. Brau¹²⁸, W.D. Breaden Madden⁵⁵, K. Brendlinger⁴⁴, A.J. Brennan¹⁰², L. Brenner⁴⁴, R. Brenner¹⁷⁰, S. Bressler¹⁷⁸, B. Brickwedde⁹⁷, D.L. Briglin²¹, T.M. Bristow⁴⁸, D. Britton⁵⁵, D. Britzger^{59b}, I. Brock²⁴, R. Brock¹⁰⁴, G. Brooijmans³⁸, T. Brooks⁹¹, W.K. Brooks^{144b}, E. Brost¹¹⁹, J.H. Broughton²¹, P.A. Bruckman de Renstrom⁸², D. Bruncko^{28b}, A. Bruni^{23b}, G. Bruni^{23b}, L.S. Bruni¹¹⁸, S. Bruno^{71a,71b}, B.H. Brunt³¹, M. Bruschi^{23b}, N. Bruscino¹³⁶, P. Bryant³⁶, L. Bryngemark⁴⁴, T. Buanes¹⁷, Q. Buat³⁵, P. Buchholz¹⁴⁸, A.G. Buckley⁵⁵, I.A. Budagov⁷⁷, M.K. Bugge¹³¹, F. Bührer⁵⁰, O. Bulekov¹¹⁰, D. Bullock⁸, T.J. Burch¹¹⁹, S. Burdin⁸⁸, C.D. Burgard¹¹⁸, A.M. Burger⁵, B. Burghgrave¹¹⁹, K. Burka⁸², S. Burke¹⁴¹, I. Burmeister⁴⁵, J.T.P. Burr¹³², D. Büscher⁵⁰, V. Büscher⁹⁷, E. Buschmann⁵¹, P. Bussey⁵⁵, J.M. Butler²⁵, C.M. Buttar⁵⁵, J.M. Butterworth⁹², P. Butti³⁵, W. Buttinger³⁵, A. Buzatu¹⁵⁵, A.R. Buzykaev^{120b,120a}, G. Cabras^{23b,23a}, S. Cabrera Urbán¹⁷², D. Caforio¹³⁹, H. Cai¹⁷¹, V.M.M. Cairo², O. Cakir^{4a}, N. Calace⁵², P. Calafiura¹⁸, A. Calandri⁹⁹, G. Calderini¹³³, P. Calfayan⁶³, G. Callea^{40b,40a}, L.P. Caloba^{78b}, S. Calvente Lopez⁹⁶, D. Calvet³⁷, S. Calvet³⁷, T.P. Calvet¹⁵², M. Calvetti^{69a,69b}, R. Camacho Toro³⁶, S. Camarda³⁵, P. Camarri^{71a,71b}, D. Cameron¹³¹, R. Caminal Armadans¹⁰⁰, C. Camincher⁵⁶, S. Campana³⁵, M. Campanelli⁹², A. Camplani^{66a,66b}, A. Campoverde¹⁴⁸, V. Canale^{67a,67b}, M. Cano Bret^{58c}, J. Cantero¹²⁶, T. Cao¹⁵⁹, Y. Cao¹⁷¹, M.D.M. Capeans Garrido³⁵, I. Caprini^{27b}, M. Caprini^{27b}, M. Capua^{40b,40a}, R.M. Carbone³⁸, R. Cardarelli^{71a}, F.C. Cardillo⁵⁰, I. Carli¹⁴⁰, T. Carli³⁵, G. Carlino^{67a}, B.T. Carlson¹³⁶, L. Carminati^{66a,66b}, R.M.D. Carney^{43a,43b}, S. Caron¹¹⁷, E. Carquin^{144b}, S. Carrá^{66a,66b}, G.D. Carrillo-Montoya³⁵, D. Casadei^{32b}, M.P. Casado^{14,h}, A.F. Casha¹⁶⁵, M. Casolino¹⁴, D.W. Casper¹⁶⁹, R. Castelijn¹¹⁸, V. Castillo Gimenez¹⁷², N.F. Castro^{137a,137e}, A. Catinaccio³⁵, J.R. Catmore¹³¹, A. Cattai³⁵, J. Caudron²⁴, V. Cavaliere²⁹, E. Cavallaro¹⁴, D. Cavalli^{66a}, M. Cavalli-Sforza¹⁴, V. Cavasinni^{69a,69b}, E. Celebi^{12b}, F. Ceradini^{72a,72b}, L. Cerdá Alberich¹⁷², A.S. Cerqueira^{78a}, A. Cerri¹⁵³, L. Cerrito^{71a,71b}, F. Cerutti¹⁸, A. Cervelli^{23b,23a}, S.A. Cetin^{12b}, A. Chafaq^{34a}, D. Chakraborty¹¹⁹, S.K. Chan⁵⁷, W.S. Chan¹¹⁸, Y.L. Chan^{61a}, P. Chang¹⁷¹, J.D. Chapman³¹, D.G. Charlton²¹, C.C. Chau³³, C.A. Chavez Barajas¹⁵³, S. Che¹²³, A. Chegwidden¹⁰⁴, S. Chekanov⁶, S.V. Chekulaev^{166a}, G.A. Chelkov^{77,aw}, M.A. Chelstowska³⁵, C. Chen^{58a}, C.H. Chen⁷⁶, H. Chen²⁹, J. Chen^{58a}, J. Chen³⁸, S. Chen¹³⁴, S.J. Chen^{15c}, X. Chen^{15b,av}, Y. Chen⁸⁰, Y-H. Chen⁴⁴, H.C. Cheng¹⁰³, H.J. Cheng^{15d}, A. Cheplakov⁷⁷, E. Cheremushkina¹²¹, R. Cherkaoui El Moursli^{34e}, E. Cheu⁷, K. Cheung⁶², L. Chevalier¹⁴², V. Chiarella⁴⁹, G. Chiarelli^{69a}, G. Chiodini^{65a}, A.S. Chisholm³⁵, A. Chitan^{27b}, I. Chiu¹⁶¹, Y.H. Chiu¹⁷⁴, M.V. Chizhov⁷⁷, K. Choi⁶³, A.R. Chomont¹²⁹, S. Chouridou¹⁶⁰, Y.S. Chow¹¹⁸, V. Christodoulou⁹², M.C. Chu^{61a}, J. Chudoba¹³⁸, A.J. Chuinard¹⁰¹, J.J. Chwastowski⁸², L. Chytka¹²⁷, D. Cinca⁴⁵, V. Cindro⁸⁹, I.A. Cioară²⁴, A. Ciocio¹⁸, F. Cirotto^{67a,67b}, Z.H. Citron¹⁷⁸, M. Citterio^{66a}, A. Clark⁵², M.R. Clark³⁸, P.J. Clark⁴⁸, R.N. Clarke¹⁸, C. Clement^{43a,43b}, Y. Coadou⁹⁹, M. Cobal^{64a,64c}, A. Coccaro^{53b,53a}, J. Cochran⁷⁶, L. Colasurdo¹¹⁷, B. Cole³⁸, A.P. Colijn¹¹⁸, J. Collot⁵⁶, P. Conde Muñoz^{137a,137b}, E. Coniavitis⁵⁰, S.H. Connell^{32b}, I.A. Connelly⁹⁸, S. Constantinescu^{27b}, F. Conventi^{67a,ay}, A.M. Cooper-Sarkar¹³², F. Cormier¹⁷³, K.J.R. Cormier¹⁶⁵, M. Corradi^{70a,70b}, E.E. Corrigan⁹⁴, F. Corriveau^{101,ag}, A. Cortes-Gonzalez³⁵, M.J. Costa¹⁷², D. Costanzo¹⁴⁶, G. Cottin³¹, G. Cowan⁹¹, B.E. Cox⁹⁸, J. Crane⁹⁸, K. Cranmer¹²², S.J. Crawley⁵⁵, R.A. Creager¹³⁴, G. Cree³³, S. Crépé-Renaudin⁵⁶, F. Crescioli¹³³, M. Cristinziani²⁴, V. Croft¹²², G. Crosetti^{40b,40a}, A. Cueto⁹⁶, T. Cuhadar Donszelmann¹⁴⁶, A.R. Cukierman¹⁵⁰, M. Curatolo⁴⁹, J. Cúth⁹⁷, S. Czekierda⁸²,

P. Czodrowski³⁵, M.J. Da Cunha Sargedas De Sousa^{58b}, C. Da Via⁹⁸, W. Dabrowski^{81a}, T. Dado^{28a,aa},
 S. Dahbi^{34e}, T. Dai¹⁰³, O. Dale¹⁷, F. Dallaire¹⁰⁷, C. Dallapiccola¹⁰⁰, M. Dam³⁹, G. D'amen^{23b,23a},
 J.R. Dandoy¹³⁴, M.F. Daneri³⁰, N.P. Dang^{179,l}, N.D Dann⁹⁸, M. Danninger¹⁷³, V. Dao³⁵, G. Darbo^{53b},
 S. Darmora⁸, O. Dartsi⁵, A. Dattagupta¹²⁸, T. Daubney⁴⁴, S. D'Auria⁵⁵, W. Davey²⁴, C. David⁴⁴,
 T. Davidek¹⁴⁰, D.R. Davis⁴⁷, E. Dawe¹⁰², I. Dawson¹⁴⁶, K. De⁸, R. De Asmundis^{67a}, A. De Benedetti¹²⁵,
 S. De Castro^{23b,23a}, S. De Cecco¹³³, N. De Groot¹¹⁷, P. de Jong¹¹⁸, H. De la Torre¹⁰⁴, F. De Lorenzi⁷⁶,
 A. De Maria^{51,v}, D. De Pedis^{70a}, A. De Salvo^{70a}, U. De Sanctis^{71a,71b}, A. De Santo¹⁵³,
 K. De Vasconcelos Corga⁹⁹, J.B. De Vivie De Regie¹²⁹, C. Debenedetti¹⁴³, D.V. Dedovich⁷⁷,
 N. Dehghanian³, M. Del Gaudio^{40b,40a}, J. Del Peso⁹⁶, D. Delgove¹²⁹, F. Deliot¹⁴², C.M. Delitzsch⁷,
 M. Della Pietra^{67a,67b}, D. Della Volpe⁵², A. Dell'Acqua³⁵, L. Dell'Asta²⁵, M. Delmastro⁵, C. Delporte¹²⁹,
 P.A. Delsart⁵⁶, D.A. DeMarco¹⁶⁵, S. Demers¹⁸¹, M. Demichev⁷⁷, S.P. Denisov¹²¹, D. Denysiuk¹¹⁸,
 L. D'Eramo¹³³, D. Derendarz⁸², J.E. Derkaoui^{34d}, F. Derue¹³³, P. Dervan⁸⁸, K. Desch²⁴, C. Deterre⁴⁴,
 K. Dette¹⁶⁵, M.R. Devesa³⁰, P.O. Deviveiros³⁵, A. Dewhurst¹⁴¹, S. Dhaliwal²⁶, F.A. Di Bello⁵²,
 A. Di Ciaccio^{71a,71b}, L. Di Ciaccio⁵, W.K. Di Clemente¹³⁴, C. Di Donato^{67a,67b}, A. Di Girolamo³⁵,
 B. Di Micco^{72a,72b}, R. Di Nardo³⁵, K.F. Di Petrillo⁵⁷, A. Di Simone⁵⁰, R. Di Sipio¹⁶⁵, D. Di Valentino³³,
 C. Diaconu⁹⁹, M. Diamond¹⁶⁵, F.A. Dias³⁹, T. Dias Do Vale^{137a}, M.A. Diaz^{144a}, J. Dickinson¹⁸,
 E.B. Diehl¹⁰³, J. Dietrich¹⁹, S. Díez Cornell⁴⁴, A. Dimitrievska¹⁸, J. Dingfelder²⁴, F. Dittus³⁵,
 F. Djama⁹⁹, T. Djobava^{157b}, J.I. Djuvsland^{59a}, M.A.B. Do Vale^{78c}, M. Dobre^{27b}, D. Dodsworth²⁶,
 C. Doglioni⁹⁴, J. Dolejsi¹⁴⁰, Z. Dolezal¹⁴⁰, M. Donadelli^{78d}, J. Donini³⁷, M. D'Onofrio⁸⁸, J. Dopke¹⁴¹,
 A. Doria^{67a}, M.T. Dova⁸⁶, A.T. Doyle⁵⁵, E. Drechsler⁵¹, E. Dreyer¹⁴⁹, T. Dreyer⁵¹, M. Dris¹⁰, Y. Du^{58b},
 J. Duarte-Campderros¹⁵⁹, F. Dubinin¹⁰⁸, A. Dubreuil⁵², E. Duchovni¹⁷⁸, G. Duckeck¹¹²,
 A. Ducourthial¹³³, O.A. Ducu^{107,z}, D. Duda¹¹⁸, A. Dudarev³⁵, A.C. Dudder⁹⁷, E.M. Duffield¹⁸,
 L. Duflot¹²⁹, M. Dührssen³⁵, C. Dülsen¹⁸⁰, M. Dumancic¹⁷⁸, A.E. Dumitriu^{27b,f}, A.K. Duncan⁵⁵,
 M. Dunford^{59a}, A. Duperrin⁹⁹, H. Duran Yildiz^{4a}, M. Düren⁵⁴, A. Durglishvili^{157b}, D. Duschinger⁴⁶,
 B. Dutta⁴⁴, D. Duvnjak¹, M. Dyndal⁴⁴, B.S. Dziedzic⁸², C. Eckardt⁴⁴, K.M. Ecker¹¹³, R.C. Edgar¹⁰³,
 T. Eifert³⁵, G. Eigen¹⁷, K. Einsweiler¹⁸, T. Ekelof¹⁷⁰, M. El Kacimi^{34c}, R. El Kosseifi⁹⁹, V. Ellajosyula⁹⁹,
 M. Ellert¹⁷⁰, F. Ellinghaus¹⁸⁰, A.A. Elliot¹⁷⁴, N. Ellis³⁵, J. Elmsheuser²⁹, M. Elsing³⁵, D. Emeliyanov¹⁴¹,
 Y. Enari¹⁶¹, J.S. Ennis¹⁷⁶, M.B. Epland⁴⁷, J. Erdmann⁴⁵, A. Ereditato²⁰, S. Errede¹⁷¹, M. Escalier¹²⁹,
 C. Escobar¹⁷², B. Esposito⁴⁹, O. Estrada Pastor¹⁷², A.I. Etienne¹⁴², E. Etzion¹⁵⁹, H. Evans⁶³,
 A. Ezhilov¹³⁵, M. Ezzi^{34e}, F. Fabbri^{23b,23a}, L. Fabbri^{23b,23a}, V. Fabiani¹¹⁷, G. Facini⁹²,
 R.M. Fakhrutdinov¹²¹, S. Falciano^{70a}, P.J. Falke⁵, S. Falke⁵, J. Faltova¹⁴⁰, Y. Fang^{15a}, M. Fanti^{66a,66b},
 A. Farbin⁸, A. Farilla^{72a}, E.M. Farina^{68a,68b}, T. Farooque¹⁰⁴, S. Farrell¹⁸, S.M. Farrington¹⁷⁶,
 P. Farthouat³⁵, F. Fassi^{34e}, P. Fassnacht³⁵, D. Fassouliotis⁹, M. Faucci Giannelli⁴⁸, A. Favareto^{53b,53a},
 W.J. Fawcett⁵², L. Fayard¹²⁹, O.L. Fedin^{135,r}, W. Fedorko¹⁷³, M. Feickert⁴¹, S. Feigl¹³¹, L. Feligioni⁹⁹,
 C. Feng^{58b}, E.J. Feng³⁵, M. Feng⁴⁷, M.J. Fenton⁵⁵, A.B. Fenyuk¹²¹, L. Feremenga⁸, J. Ferrando⁴⁴,
 A. Ferrari¹⁷⁰, P. Ferrari¹¹⁸, R. Ferrari^{68a}, D.E. Ferreira de Lima^{59b}, A. Ferrer¹⁷², D. Ferrere⁵²,
 C. Ferretti¹⁰³, F. Fiedler⁹⁷, A. Filipčič⁸⁹, F. Filthaut¹¹⁷, M. Fincke-Keeler¹⁷⁴, K.D. Finelli²⁵,
 M.C.N. Fiolhais^{137a,137c,b}, L. Fiorini¹⁷², C. Fischer¹⁴, J. Fischer¹⁸⁰, W.C. Fisher¹⁰⁴, N. Flaschel⁴⁴,
 I. Fleck¹⁴⁸, P. Fleischmann¹⁰³, R.R.M. Fletcher¹³⁴, T. Flick¹⁸⁰, B.M. Flierl¹¹², L.M. Flores¹³⁴,
 L.R. Flores Castillo^{61a}, N. Fomin¹⁷, G.T. Forcolin⁹⁸, A. Formica¹⁴², F.A. Förster¹⁴, A.C. Forti⁹⁸,
 A.G. Foster²¹, D. Fournier¹²⁹, H. Fox⁸⁷, S. Fracchia¹⁴⁶, P. Francavilla^{69a,69b}, M. Franchini^{23b,23a},
 S. Franchino^{59a}, D. Francis³⁵, L. Franconi¹³¹, M. Franklin⁵⁷, M. Frate¹⁶⁹, M. Fraternali^{68a,68b},
 D. Freeborn⁹², S.M. Fressard-Batraneanu³⁵, B. Freund¹⁰⁷, W.S. Freund^{78b}, D. Froidevaux³⁵,
 J.A. Frost¹³², C. Fukunaga¹⁶², T. Fusayasu¹¹⁴, J. Fuster¹⁷², O. Gabizon¹⁵⁸, A. Gabrielli^{23b,23a},
 A. Gabrielli¹⁸, G.P. Gach^{81a}, S. Gadatsch⁵², S. Gadomski⁵², P. Gadow¹¹³, G. Gagliardi^{53b,53a},
 L.G. Gagnon¹⁰⁷, C. Galea^{27b}, B. Galhardo^{137a,137c}, E.J. Gallas¹³², B.J. Gallop¹⁴¹, P. Gallus¹³⁹,
 G. Galster³⁹, R. Gamboa Goni⁹⁰, K.K. Gan¹²³, S. Ganguly¹⁷⁸, Y. Gao⁸⁸, Y.S. Gao^{150,n}, C. García¹⁷²,

J.E. García Navarro¹⁷², J.A. García Pascual^{15a}, M. Garcia-Sciveres¹⁸, R.W. Gardner³⁶, N. Garelli¹⁵⁰, V. Garonne¹³¹, K. Gasnikova⁴⁴, A. Gaudiello^{53b,53a}, G. Gaudio^{68a}, I.L. Gavrilenko¹⁰⁸, A. Gavrilyuk¹⁰⁹, C. Gay¹⁷³, G. Gaycken²⁴, E.N. Gazis¹⁰, C.N.P. Gee¹⁴¹, J. Geisen⁵¹, M. Geisen⁹⁷, M.P. Geisler^{59a}, K. Gellerstedt^{43a,43b}, C. Gemme^{53b}, M.H. Genest⁵⁶, C. Geng¹⁰³, S. Gentile^{70a,70b}, C. Gentsos¹⁶⁰, S. George⁹¹, D. Gerbaudo¹⁴, G. Gessner⁴⁵, S. Ghasemi¹⁴⁸, M. Ghneimat²⁴, B. Giacobbe^{23b}, S. Giagu^{70a,70b}, N. Giangiacomi^{23b,23a}, P. Giannetti^{69a}, S.M. Gibson⁹¹, M. Gignac¹⁴³, D. Gillberg³³, G. Gilles¹⁸⁰, D.M. Gingrich^{3,ax}, M.P. Giordani^{64a,64c}, F.M. Giorgi^{23b}, P.F. Giraud¹⁴², P. Giromini⁵⁷, G. Giugliarelli^{64a,64c}, D. Giugni^{66a}, F. Giuli¹³², M. Giulini^{59b}, S. Gkaitatzis¹⁶⁰, I. Gkialas^{9,k}, E.L. Gkougkousis¹⁴, P. Gkountoumis¹⁰, L.K. Gladilin¹¹¹, C. Glasman⁹⁶, J. Glatzer¹⁴, P.C.F. Glaysher⁴⁴, A. Glazov⁴⁴, M. Goblirsch-Kolb²⁶, J. Godlewski⁸², S. Goldfarb¹⁰², T. Golling⁵², D. Golubkov¹²¹, A. Gomes^{137a,137b,137d}, R. Goncalves Gama^{78a}, R. Gonçalo^{137a}, G. Gonella⁵⁰, L. Gonella²¹, A. Gongadze⁷⁷, F. Gonnella²¹, J.L. Gonski⁵⁷, S. González de la Hoz¹⁷², S. Gonzalez-Sevilla⁵², L. Goossens³⁵, P.A. Gorbounov¹⁰⁹, H.A. Gordon²⁹, B. Gorini³⁵, E. Gorini^{65a,65b}, A. Gorišek⁸⁹, A.T. Goshaw⁴⁷, C. Gössling⁴⁵, M.I. Gostkin⁷⁷, C.A. Gottardo²⁴, C.R. Goudet¹²⁹, D. Goujdami^{34c}, A.G. Goussiou¹⁴⁵, N. Govender^{32b,d}, C. Goy⁵, E. Gozani¹⁵⁸, I. Grabowska-Bold^{81a}, P.O.J. Gradin¹⁷⁰, E.C. Graham⁸⁸, J. Gramling¹⁶⁹, E. Gramstad¹³¹, S. Grancagnolo¹⁹, V. Gratchev¹³⁵, P.M. Gravila^{27f}, C. Gray⁵⁵, H.M. Gray¹⁸, Z.D. Greenwood^{93,al}, C. Grefe²⁴, K. Gregersen⁹², I.M. Gregor⁴⁴, P. Grenier¹⁵⁰, K. Grevtsov⁴⁴, J. Griffiths⁸, A.A. Grillo¹⁴³, K. Grimm^{150,c}, S. Grinstein^{14,ab}, Ph. Gris³⁷, J.-F. Grivaz¹²⁹, S. Groh⁹⁷, E. Gross¹⁷⁸, J. Grosse-Knetter⁵¹, G.C. Grossi⁹³, Z.J. Grout⁹², A. Grummer¹¹⁶, L. Guan¹⁰³, W. Guan¹⁷⁹, J. Guenther³⁵, A. Guerguichon¹²⁹, F. Guescini^{166a}, D. Guest¹⁶⁹, O. Gueta¹⁵⁹, R. Gugel⁵⁰, B. Gui¹²³, T. Guillemin⁵, S. Guindon³⁵, U. Gul⁵⁵, C. Gumpert³⁵, J. Guo^{58c}, W. Guo¹⁰³, Y. Guo^{58a,u}, Z. Guo⁹⁹, R. Gupta⁴¹, S. Gurbuz^{12c}, G. Gustavino¹²⁵, B.J. Gutelman¹⁵⁸, P. Gutierrez¹²⁵, N.G. Gutierrez Ortiz⁹², C. Gutschow⁹², C. Guyot¹⁴², M.P. Guzik^{81a}, C. Gwenlan¹³², C.B. Gwilliam⁸⁸, A. Haas¹²², C. Haber¹⁸, H.K. Hadavand⁸, N. Haddad^{34e}, A. Hadef⁹⁹, S. Hageböck²⁴, M. Hagihara¹⁶⁷, H. Hakobyan^{182,*}, M. Haleem¹⁷⁵, J. Haley¹²⁶, G. Halladjian¹⁰⁴, G.D. Hallewell⁹⁹, K. Hamacher¹⁸⁰, P. Hamal¹²⁷, K. Hamano¹⁷⁴, A. Hamilton^{32a}, G.N. Hamity¹⁴⁶, K. Han^{58a,ak}, L. Han^{58a}, S. Han^{15d}, K. Hanagaki^{79,x}, M. Hance¹⁴³, D.M. Handl¹¹², B. Haney¹³⁴, R. Hankache¹³³, P. Hanke^{59a}, E. Hansen⁹⁴, J.B. Hansen³⁹, J.D. Hansen³⁹, M.C. Hansen²⁴, P.H. Hansen³⁹, K. Hara¹⁶⁷, A.S. Hard¹⁷⁹, T. Harenberg¹⁸⁰, S. Harkusha¹⁰⁵, P.F. Harrison¹⁷⁶, N.M. Hartmann¹¹², Y. Hasegawa¹⁴⁷, A. Hasib⁴⁸, S. Hassani¹⁴², S. Haug²⁰, R. Hauser¹⁰⁴, L. Hauswald⁴⁶, L.B. Havener³⁸, M. Havranek¹³⁹, C.M. Hawkes²¹, R.J. Hawkings³⁵, D. Hayden¹⁰⁴, C. Hayes¹⁵², C.P. Hays¹³², J.M. Hays⁹⁰, H.S. Hayward⁸⁸, S.J. Haywood¹⁴¹, M.P. Heath⁴⁸, V. Hedberg⁹⁴, L. Heelan⁸, S. Heer²⁴, K.K. Heidegger⁵⁰, S. Heim⁴⁴, T. Heim¹⁸, B. Heinemann^{44,as}, J.J. Heinrich¹¹², L. Heinrich¹²², C. Heinz⁵⁴, J. Hejbal¹³⁸, L. Helary³⁵, A. Held¹⁷³, S. Hellesund¹³¹, S. Hellman^{43a,43b}, C. Helsens³⁵, R.C.W. Henderson⁸⁷, Y. Heng¹⁷⁹, S. Henkelmann¹⁷³, A.M. Henriques Correia³⁵, G.H. Herbert¹⁹, H. Herde²⁶, V. Herget¹⁷⁵, Y. Hernández Jiménez^{32c}, H. Herr⁹⁷, G. Herten⁵⁰, R. Hertenberger¹¹², L. Hervas³⁵, T.C. Herwig¹³⁴, G.G. Hesketh⁹², N.P. Hessey^{166a}, J.W. Hetherly⁴¹, S. Higashino⁷⁹, E. Higón-Rodríguez¹⁷², K. Hildebrand³⁶, E. Hill¹⁷⁴, J.C. Hill³¹, K.H. Hiller⁴⁴, S.J. Hillier²¹, M. Hils⁴⁶, I. Hinchliffe¹⁸, M. Hirose¹³⁰, D. Hirschbuehl¹⁸⁰, B. Hiti⁸⁹, O. Hladík¹³⁸, D.R. Hlaluku^{32c}, X. Hoad⁴⁸, J. Hobbs¹⁵², N. Hod^{166a}, M.C. Hodgkinson¹⁴⁶, A. Hoecker³⁵, M.R. Hoeferkamp¹¹⁶, F. Hoenig¹¹², D. Hohn²⁴, D. Hohov¹²⁹, T.R. Holmes³⁶, M. Holzbock¹¹², M. Homann⁴⁵, S. Honda¹⁶⁷, T. Honda⁷⁹, T.M. Hong¹³⁶, B.H. Hooberman¹⁷¹, W.H. Hopkins¹²⁸, Y. Horii¹¹⁵, P. Horn⁴⁶, A.J. Horton¹⁴⁹, L.A. Horyn³⁶, J.-Y. Hostachy⁵⁶, A. Hostiuc¹⁴⁵, S. Hou¹⁵⁵, A. Hoummada^{34a}, J. Howarth⁹⁸, J. Hoya⁸⁶, M. Hrabovsky¹²⁷, J. Hrdinka³⁵, I. Hristova¹⁹, J. Hrivnac¹²⁹, A. Hrynevich¹⁰⁶, T. Hrynev'ova⁵, P.J. Hsu⁶², S.-C. Hsu¹⁴⁵, Q. Hu²⁹, S. Hu^{58c}, Y. Huang^{15a}, Z. Hubacek¹³⁹, F. Hubaut⁹⁹, M. Huebner²⁴, F. Huegging²⁴, T.B. Huffman¹³², E.W. Hughes³⁸, M. Huhtinen³⁵, R.F.H. Hunter³³, P. Huo¹⁵², A.M. Hupe³³, N. Huseynov^{77,ai}, J. Huston¹⁰⁴, J. Huth⁵⁷, R. Hyneman¹⁰³, G. Iacobucci⁵², G. Iakovidis²⁹,

I. Ibragimov¹⁴⁸, L. Iconomidou-Fayard¹²⁹, Z. Idrissi^{34e}, P. Iengo³⁵, R. Ignazzi³⁹, O. Igonkina^{118,ae},
 R. Iguchi¹⁶¹, T. Iizawa¹⁷⁷, Y. Ikegami⁷⁹, M. Ikeno⁷⁹, D. Iliadis¹⁶⁰, N. Ilic¹⁵⁰, F. Iltzsche⁴⁶,
 G. Introzzi^{68a,68b}, M. Iodice^{72a}, K. Iordanidou³⁸, V. Ippolito^{70a,70b}, M.F. Isacson¹⁷⁰, N. Ishijima¹³⁰,
 M. Ishino¹⁶¹, M. Ishitsuka¹⁶³, C. Issever¹³², S. Isti^{12c,aq}, F. Ito¹⁶⁷, J.M. Iturbe Ponce^{61a}, R. Iuppa^{73a,73b},
 A. Ivina¹⁷⁸, H. Iwasaki⁷⁹, J.M. Izen⁴², V. Izzo^{67a}, S. Jabbar³, P. Jacka¹³⁸, P. Jackson¹, R.M. Jacobs²⁴,
 V. Jain², G. Jäkel¹⁸⁰, K.B. Jakobi⁹⁷, K. Jakobs⁵⁰, S. Jakobsen⁷⁴, T. Jakoubek¹³⁸, D.O. Jamin¹²⁶,
 D.K. Jana⁹³, R. Jansky⁵², J. Janssen²⁴, M. Janus⁵¹, P.A. Janus^{81a}, G. Jarlskog⁹⁴, N. Javadov^{77,ai},
 T. Javůrek⁵⁰, M. Javurkova⁵⁰, F. Jeanneau¹⁴², L. Jeanty¹⁸, J. Jejelava^{157a,aj}, A. Jelinskas¹⁷⁶, P. Jenni^{50,e},
 J. Jeong⁴⁴, C. Jeske¹⁷⁶, S. Jézéquel⁵, H. Ji¹⁷⁹, J. Jia¹⁵², H. Jiang⁷⁶, Y. Jiang^{58a}, Z. Jiang^{150,s}, S. Jiggins⁵⁰,
 F.A. Jimenez Morales³⁷, J. Jimenez Pena¹⁷², S. Jin^{15c}, A. Jinaru^{27b}, O. Jinnouchi¹⁶³, H. Jivan^{32c},
 P. Johansson¹⁴⁶, K.A. Johns⁷, C.A. Johnson⁶³, W.J. Johnson¹⁴⁵, K. Jon-And^{43a,43b}, R.W.L. Jones⁸⁷,
 S.D. Jones¹⁵³, S. Jones⁷, T.J. Jones⁸⁸, J. Jongmanns^{59a}, P.M. Jorge^{137a,137b}, J. Jovicevic^{166a}, X. Ju¹⁷⁹,
 J.J. Junggeburth¹¹³, A. Juste Rozas^{14,ab}, A. Kaczmarska⁸², M. Kado¹²⁹, H. Kagan¹²³, M. Kagan¹⁵⁰,
 T. Kaji¹⁷⁷, E. Kajomovitz¹⁵⁸, C.W. Kalderon⁹⁴, A. Kaluza⁹⁷, S. Kama⁴¹, A. Kamenshchikov¹²¹,
 L. Kanjur⁸⁹, Y. Kano¹⁶¹, V.A. Kantserov¹¹⁰, J. Kanzaki⁷⁹, B. Kaplan¹²², L.S. Kaplan¹⁷⁹, D. Kar^{32c},
 M.J. Kareem^{166b}, E. Karentzos¹⁰, S.N. Karpov⁷⁷, Z.M. Karpova⁷⁷, V. Kartvelishvili⁸⁷,
 A.N. Karyukhin¹²¹, K. Kasahara¹⁶⁷, L. Kashif¹⁷⁹, R.D. Kass¹²³, A. Kastanas¹⁵¹, Y. Kataoka¹⁶¹,
 C. Kato¹⁶¹, A. Katre⁵², J. Katzy⁴⁴, K. Kawade⁸⁰, K. Kawagoe⁸⁵, T. Kawamoto¹⁶¹, G. Kawamura⁵¹,
 E.F. Kay⁸⁸, V.F. Kazanin^{120b,120a}, R. Keeler¹⁷⁴, R. Kehoe⁴¹, J.S. Keller³³, E. Kellermann⁹⁴,
 J.J. Kempster²¹, J. Kendrick²¹, O. Kepka¹³⁸, S. Kersten¹⁸⁰, B.P. Kerševan⁸⁹, R.A. Keyes¹⁰¹,
 M. Khader¹⁷¹, F. Khalil-Zada¹³, A. Khanov¹²⁶, A.G. Kharlamov^{120b,120a}, T. Kharlamova^{120b,120a},
 A. Khodinov¹⁶⁴, T.J. Khoo⁵², V. Khovanskiy^{109,*}, E. Khramov⁷⁷, J. Khubua^{157b}, S. Kido⁸⁰, M. Kiehn⁵²,
 C.R. Kilby⁹¹, H.Y. Kim⁸, S.H. Kim¹⁶⁷, Y.K. Kim³⁶, N. Kimura^{64a,64c}, O.M. Kind¹⁹, B.T. King⁸⁸,
 D. Kirchmeier⁴⁶, J. Kirk¹⁴¹, A.E. Kiryunin¹¹³, T. Kishimoto¹⁶¹, D. Kisielewska^{81a}, V. Kitali⁴⁴,
 O. Kiverny⁵, E. Kladiva^{28b,*}, T. Klapdor-Kleingrothaus⁵⁰, M.H. Klein¹⁰³, M. Klein⁸⁸, U. Klein⁸⁸,
 K. Kleinknecht⁹⁷, P. Klimek¹¹⁹, A. Klimentov²⁹, R. Klingenberg^{45,*}, T. Klingl²⁴, T. Klioutchnikova³⁵,
 F.F. Klitzner¹¹², P. Kluit¹¹⁸, S. Kluth¹¹³, E. Knerner⁷⁴, E.B.F.G. Knoops⁹⁹, A. Knue⁵⁰,
 A. Kobayashi¹⁶¹, D. Kobayashi⁸⁵, T. Kobayashi¹⁶¹, M. Kobel⁴⁶, M. Kocian¹⁵⁰, P. Kodys¹⁴⁰, T. Koffas³³,
 E. Koffeman¹¹⁸, N.M. Köhler¹¹³, T. Koi¹⁵⁰, M. Kolb^{59b}, I. Koletsou⁵, T. Kondo⁷⁹, N. Kondrashova^{58c},
 K. Köneke⁵⁰, A.C. König¹¹⁷, T. Kono^{79,ar}, R. Konoplich^{122,an}, N. Konstantinidis⁹², B. Konya⁹⁴,
 R. Kopeliansky⁶³, S. Koperny^{81a}, K. Korcyl⁸², K. Kordas¹⁶⁰, A. Korn⁹², I. Korolkov¹⁴,
 E.V. Korolkova¹⁴⁶, O. Kortner¹¹³, S. Kortner¹¹³, T. Kosek¹⁴⁰, V.V. Kostyukhin²⁴, A. Kotwal⁴⁷,
 A. Koulouris¹⁰, A. Kourkoumeli-Charalampidi^{68a,68b}, C. Kourkoumelis⁹, E. Kourlitis¹⁴⁶,
 V. Kouskoura²⁹, A.B. Kowalewska⁸², R. Kowalewski¹⁷⁴, T.Z. Kowalski^{81a}, C. Kozakai¹⁶¹,
 W. Kozanecki¹⁴², A.S. Kozhin¹²¹, V.A. Kramarenko¹¹¹, G. Kramberger⁸⁹, D. Krasnopevtsev¹¹⁰,
 M.W. Krasny¹³³, A. Krasznahorkay³⁵, D. Krauss¹¹³, J.A. Kremer^{81a}, J. Kretzschmar⁸⁸, K. Kreutzfeldt⁵⁴,
 P. Krieger¹⁶⁵, K. Krizka¹⁸, K. Kroeninger⁴⁵, H. Kroha¹¹³, J. Kroll¹³⁸, J. Kroll¹³⁴, J. Kroseberg²⁴,
 J. Krstic¹⁶, U. Kruchonak⁷⁷, H. Krüger²⁴, N. Krumnack⁷⁶, M.C. Kruse⁴⁷, T. Kubota¹⁰², S. Kuday^{4b},
 J.T. Kuechler¹⁸⁰, S. Kuehn³⁵, A. Kugel^{59a}, F. Kuger¹⁷⁵, T. Kuhl⁴⁴, V. Kukhtin⁷⁷, R. Kukla⁹⁹,
 Y. Kulchitsky¹⁰⁵, S. Kuleshov^{144b}, Y.P. Kulinich¹⁷¹, M. Kuna⁵⁶, T. Kunigo⁸³, A. Kupco¹³⁸, T. Kupfer⁴⁵,
 O. Kuprash¹⁵⁹, H. Kurashige⁸⁰, L.L. Kurchaninov^{166a}, Y.A. Kurochkin¹⁰⁵, M.G. Kurth^{15d},
 E.S. Kuwertz¹⁷⁴, M. Kuze¹⁶³, J. Kvita¹²⁷, T. Kwan¹⁷⁴, A. La Rosa¹¹³, J.L. La Rosa Navarro^{78d},
 L. La Rotonda^{40b,40a}, F. La Ruffa^{40b,40a}, C. Lacasta¹⁷², F. Lacava^{70a,70b}, J. Lacey⁴⁴, D.P.J. Lack⁹⁸,
 H. Lacker¹⁹, D. Lacour¹³³, E. Ladygin⁷⁷, R. Lafaye⁵, B. Laforge¹³³, S. Lai⁵¹, S. Lammers⁶³, W. Lampl⁷,
 E. Lançon²⁹, U. Landgraf⁵⁰, M.P.J. Landon⁹⁰, M.C. Lanfermann⁵², V.S. Lang⁴⁴, J.C. Lange¹⁴,
 R.J. Langenberg³⁵, A.J. Lankford¹⁶⁹, F. Lanni²⁹, K. Lantzsch²⁴, A. Lanza^{68a}, A. Lapertosa^{53b,53a},
 S. Laplace¹³³, J.F. Laporte¹⁴², T. Lari^{66a}, F. Lasagni Manghi^{23b,23a}, M. Lassnig³⁵, T.S. Lau^{61a},

A. Laudrain¹²⁹, A.T. Law¹⁴³, P. Laycock⁸⁸, M. Lazzaroni^{66a,66b}, B. Le¹⁰², O. Le Dortz¹³³,
 E. Le Guirriec⁹⁹, E.P. Le Quilleuc¹⁴², M. LeBlanc⁷, T. LeCompte⁶, F. Ledroit-Guillon⁵⁶, C.A. Lee²⁹,
 G.R. Lee^{144a}, L. Lee⁵⁷, S.C. Lee¹⁵⁵, B. Lefebvre¹⁰¹, M. Lefebvre¹⁷⁴, F. Legger¹¹², C. Leggett¹⁸,
 G. Lehmann Miotto³⁵, W.A. Leight⁴⁴, A. Leisos^{160,y}, M.A.L. Leite^{78d}, R. Leitner¹⁴⁰, D. Lellouch¹⁷⁸,
 B. Lemmer⁵¹, K.J.C. Leney⁹², T. Lenz²⁴, B. Lenzi³⁵, R. Leone⁷, S. Leone^{69a}, C. Leonidopoulos⁴⁸,
 G. Lerner¹⁵³, C. Leroy¹⁰⁷, R. Les¹⁶⁵, A.A.J. Lesage¹⁴², C.G. Lester³¹, M. Levchenko¹³⁵, J. Levêque⁵,
 D. Levin¹⁰³, L.J. Levinson¹⁷⁸, M. Levy²¹, D. Lewis⁹⁰, B. Li^{58a,u}, C-Q. Li^{58a,am}, H. Li^{58b}, L. Li^{58c},
 Q. Li^{15d}, Q.Y. Li^{58a}, S. Li^{58d,58c}, X. Li^{58c}, Y. Li¹⁴⁸, Z. Liang^{15a}, B. Liberti^{71a}, A. Liblong¹⁶⁵, K. Lie^{61c},
 S. Liem¹¹⁸, A. Limosani¹⁵⁴, C.Y. Lin³¹, K. Lin¹⁰⁴, S.C. Lin¹⁵⁶, T.H. Lin⁹⁷, R.A. Linck⁶³,
 B.E. Lindquist¹⁵², A.L. Lioni⁵², E. Lipeles¹³⁴, A. Lipniacka¹⁷, M. Lisovyi^{59b}, T.M. Liss^{171,au},
 A. Lister¹⁷³, A.M. Litke¹⁴³, J.D. Little⁸, B. Liu⁷⁶, B.L. Liu⁶, H.B. Liu²⁹, H. Liu¹⁰³, J.B. Liu^{58a},
 J.K.K. Liu¹³², K. Liu¹³³, M. Liu^{58a}, P. Liu¹⁸, Y.L. Liu^{58a}, Y.W. Liu^{58a}, M. Livan^{68a,68b}, A. Lleres⁵⁶,
 J. Llorente Merino^{15a}, S.L. Lloyd⁹⁰, C.Y. Lo^{61b}, F. Lo Sterzo⁴¹, E.M. Lobodzinska⁴⁴, P. Loch⁷,
 F.K. Loebinger⁹⁸, K.M. Loew²⁶, T. Lohse¹⁹, K. Lohwasser¹⁴⁶, M. Lokajicek¹³⁸, B.A. Long²⁵,
 J.D. Long¹⁷¹, R.E. Long⁸⁷, L. Longo^{65a,65b}, K.A.Looper¹²³, J.A. Lopez^{144b}, I. Lopez Paz¹⁴,
 A. Lopez Solis¹³³, J. Lorenz¹¹², N. Lorenzo Martinez⁵, M. Losada²², P.J. Lösel¹¹², A. Lösle⁵⁰, X. Lou⁴⁴,
 X. Lou^{15a}, A. Lounis¹²⁹, J. Love⁶, P.A. Love⁸⁷, J.J. Lozano Bahilo¹⁷², H. Lu^{61a}, N. Lu¹⁰³, Y.J. Lu⁶²,
 H.J. Lubatti¹⁴⁵, C. Luci^{70a,70b}, A. Lucotte⁵⁶, C. Luedtke⁵⁰, F. Luehring⁶³, I. Luise¹³³, W. Lukas⁷⁴,
 L. Luminari^{70a}, B. Lund-Jensen¹⁵¹, M.S. Lutz¹⁰⁰, P.M. Luzi¹³³, D. Lynn²⁹, R. Lysak¹³⁸, E. Lytken⁹⁴,
 F. Lyu^{15a}, V. Lyubushkin⁷⁷, H. Ma²⁹, L.L. Ma^{58b}, Y. Ma^{58b}, G. Maccarrone⁴⁹, A. Macchiolo¹¹³,
 C.M. Macdonald¹⁴⁶, J. Machado Miguens^{134,137b}, D. Madaffari¹⁷², R. Madar³⁷, W.F. Mader⁴⁶,
 A. Madsen⁴⁴, N. Madysa⁴⁶, J. Maeda⁸⁰, S. Maeland¹⁷, T. Maeno²⁹, A.S. Maevskiy¹¹¹, V. Magerl⁵⁰,
 C. Maidantchik^{78b}, T. Maier¹¹², A. Maio^{137a,137b,137d}, O. Majersky^{28a}, S. Majewski¹²⁸, Y. Makida⁷⁹,
 N. Makovec¹²⁹, B. Malaescu¹³³, Pa. Malecki⁸², V.P. Maleev¹³⁵, F. Malek⁵⁶, U. Mallik⁷⁵, D. Malon⁶,
 C. Malone³¹, S. Maltezos¹⁰, S. Malyukov³⁵, J. Mamuzic¹⁷², G. Mancini⁴⁹, I. Mandic⁸⁹, J. Maneira^{137a},
 L. Manhaes de Andrade Filho^{78a}, J. Manjarres Ramos⁴⁶, K.H. Mankinen⁹⁴, A. Mann¹¹², A. Manousos⁷⁴,
 B. Mansouli¹⁴², J.D. Mansour^{15a}, R. Mantefel¹⁰¹, M. Mantoani⁵¹, S. Manzoni^{66a,66b}, G. Marcea³⁰,
 L. March⁵², L. Marchese¹³², G. Marchiori¹³³, M. Marcisovsky¹³⁸, C.A. Marin Tobon³⁵,
 M. Marjanovic³⁷, D.E. Marley¹⁰³, F. Marroquim^{78b}, Z. Marshall¹⁸, M.U.F Martensson¹⁷⁰,
 S. Marti-Garcia¹⁷², C.B. Martin¹²³, T.A. Martin¹⁷⁶, V.J. Martin⁴⁸, B. Martin dit Latour¹⁷,
 M. Martinez^{14,ab}, V.I. Martinez Outschoorn¹⁰⁰, S. Martin-Haugh¹⁴¹, V.S. Martoiu^{27b}, A.C. Martyniuk⁹²,
 A. Marzin³⁵, L. Masetti⁹⁷, T. Mashimo¹⁶¹, R. Mashinistov¹⁰⁸, J. Masik⁹⁸, A.L. Maslennikov^{120b,120a},
 L.H. Mason¹⁰², L. Massa^{71a,71b}, P. Mastrandrea⁵, A. Mastroberardino^{40b,40a}, T. Masubuchi¹⁶¹,
 P. Mättig¹⁸⁰, J. Maurer^{27b}, B. Maček⁸⁹, S.J. Maxfield⁸⁸, D.A. Maximov^{120b,120a}, R. Mazini¹⁵⁵,
 I. Maznas¹⁶⁰, S.M. Mazza¹⁴³, N.C. Mc Fadden¹¹⁶, G. Mc Goldrick¹⁶⁵, S.P. Mc Kee¹⁰³, A. McCarn¹⁰³,
 T.G. McCarthy¹¹³, L.I. McClymont⁹², E.F. McDonald¹⁰², J.A. McFayden³⁵, G. Mchedlidze⁵¹,
 M.A. McKay⁴¹, K.D. McLean¹⁷⁴, S.J. McMahon¹⁴¹, P.C. McNamara¹⁰², C.J. McNicol¹⁷⁶,
 R.A. McPherson^{174,ag}, J.E. Mdhluli^{32c}, Z.A. Meadows¹⁰⁰, S. Meehan¹⁴⁵, T.M. Megy⁵⁰, S. Mehlhase¹¹²,
 A. Mehta⁸⁸, T. Meideck⁵⁶, B. Meirose⁴², D. Melini^{172,i}, B.R. Mellado Garcia^{32c}, J.D. Mellenthin⁵¹,
 M. Melo^{28a}, F. Meloni²⁰, A. Melzer²⁴, S.B. Menary⁹⁸, L. Meng⁸⁸, X.T. Meng¹⁰³, A. Mengarelli^{23b,23a},
 S. Menke¹¹³, E. Meoni^{40b,40a}, S. Mergelmeyer¹⁹, C. Merlassino²⁰, P. Mermod⁵², L. Merola^{67a,67b},
 C. Meroni^{66a}, F.S. Merritt³⁶, A. Messina^{70a,70b}, J. Metcalfe⁶, A.S. Mete¹⁶⁹, C. Meyer¹³⁴, J. Meyer¹⁵⁸,
 J-P. Meyer¹⁴², H. Meyer Zu Theenhausen^{59a}, F. Miano¹⁵³, R.P. Middleton¹⁴¹, L. Mijović⁴⁸,
 G. Mikenberg¹⁷⁸, M. Mikestikova¹³⁸, M. Mikuž⁸⁹, M. Milesi¹⁰², A. Milic¹⁶⁵, D.A. Millar⁹⁰,
 D.W. Miller³⁶, A. Milov¹⁷⁸, D.A. Milstead^{43a,43b}, A.A. Minaenko¹²¹, I.A. Minashvili^{157b}, A.I. Mincer¹²²,
 B. Mindur^{81a}, M. Mineev⁷⁷, Y. Minegishi¹⁶¹, Y. Ming¹⁷⁹, L.M. Mir¹⁴, A. Mirto^{65a,65b}, K.P. Mistry¹³⁴,
 T. Mitani¹⁷⁷, J. Mitrevski¹¹², V.A. Mitsou¹⁷², A. Miucci²⁰, P.S. Miyagawa¹⁴⁶, A. Mizukami⁷⁹,

J.U. Mjörnmark⁹⁴, T. Mkrtchyan¹⁸², M. Mlynarikova¹⁴⁰, T. Moa^{43a,43b}, K. Mochizuki¹⁰⁷, P. Mogg⁵⁰, S. Mohapatra³⁸, S. Molander^{43a,43b}, R. Moles-Valls²⁴, M.C. Mondragon¹⁰⁴, K. Mönig⁴⁴, J. Monk³⁹, E. Monnier⁹⁹, A. Montalbano¹⁴⁹, J. Montejo Berlingen³⁵, F. Monticelli⁸⁶, S. Monzani^{66a}, R.W. Moore³, N. Morange¹²⁹, D. Moreno²², M. Moreno Llácer³⁵, P. Morettini^{53b}, M. Morgenstern¹¹⁸, S. Morgenstern³⁵, D. Mori¹⁴⁹, T. Mori¹⁶¹, M. Morii⁵⁷, M. Morinaga¹⁷⁷, V. Morisbak¹³¹, A.K. Morley³⁵, G. Mornacchi³⁵, J.D. Morris⁹⁰, L. Morvaj¹⁵², P. Moschovakos¹⁰, M. Mosidze^{157b}, H.J. Moss¹⁴⁶, J. Moss^{150,o}, K. Motohashi¹⁶³, R. Mount¹⁵⁰, E. Mountricha²⁹, E.J.W. Moyse¹⁰⁰, S. Muanza⁹⁹, F. Mueller¹¹³, J. Mueller¹³⁶, R.S.P. Mueller¹¹², D. Muenstermann⁸⁷, P. Mullen⁵⁵, G.A. Mullier²⁰, F.J. Munoz Sanchez⁹⁸, P. Murin^{28b}, W.J. Murray^{176,141}, A. Murrone^{66a,66b}, M. Muškinja⁸⁹, C. Mwewa^{32a}, A.G. Myagkov^{121,ao}, J. Myers¹²⁸, M. Myska¹³⁹, B.P. Nachman¹⁸, O. Nackenhorst⁴⁵, K. Nagai¹³², R. Nagai^{79,ar}, K. Nagano⁷⁹, Y. Nagasaka⁶⁰, K. Nagata¹⁶⁷, M. Nagel⁵⁰, E. Nagy⁹⁹, A.M. Nairz³⁵, Y. Nakahama¹¹⁵, K. Nakamura⁷⁹, T. Nakamura¹⁶¹, I. Nakano¹²⁴, F. Napolitano^{59a}, R.F. Naranjo Garcia⁴⁴, R. Narayan¹¹, D.I. Narrias Villar^{59a}, I. Naryshkin¹³⁵, T. Naumann⁴⁴, G. Navarro²², R. Nayyar⁷, H.A. Neal^{103,*}, P.Y. Nechaeva¹⁰⁸, T.J. Neep¹⁴², A. Negri^{68a,68b}, M. Negrini^{23b}, S. Nektarijevic¹¹⁷, C. Nellist⁵¹, M.E. Nelson¹³², S. Nemecek¹³⁸, P. Nemethy¹²², M. Nessi^{35,g}, M.S. Neubauer¹⁷¹, M. Neumann¹⁸⁰, P.R. Newman²¹, T.Y. Ng^{61c}, Y.S. Ng¹⁹, H.D.N. Nguyen⁹⁹, T. Nguyen Manh¹⁰⁷, E. Nibigira³⁷, R.B. Nickerson¹³², R. Nicolaïdou¹⁴², J. Nielsen¹⁴³, N. Nikiforou¹¹, V. Nikolaenko^{121,ao}, I. Nikolic-Audit¹³³, K. Nikolopoulos²¹, P. Nilsson²⁹, Y. Ninomiya⁷⁹, A. Nisati^{70a}, N. Nishu^{58c}, R. Nisius¹¹³, I. Nitsche⁴⁵, T. Nitta¹⁷⁷, T. Nobe¹⁶¹, Y. Noguchi⁸³, M. Nomachi¹³⁰, I. Nomidis³³, M.A. Nomura²⁹, T. Nooney⁹⁰, M. Nordberg³⁵, N. Norjoharuddeen¹³², T. Novak⁸⁹, O. Novgorodova⁴⁶, R. Novotny¹³⁹, M. Nozaki⁷⁹, L. Nozka¹²⁷, K. Ntekas¹⁶⁹, E. Nurse⁹², F. Nuti¹⁰², F.G. Oakham^{33,ax}, H. Oberlack¹¹³, T. Obermann²⁴, J. Ocariz¹³³, A. Ochi⁸⁰, I. Ochoa³⁸, J.P. Ochoa-Ricoux^{144a}, K. O'Connor²⁶, S. Oda⁸⁵, S. Odaka⁷⁹, A. Oh⁹⁸, S.H. Oh⁴⁷, C.C. Ohm¹⁵¹, H. Ohman¹⁷⁰, H. Oide^{53b,53a}, H. Okawa¹⁶⁷, Y. Okazaki⁸³, Y. Okumura¹⁶¹, T. Okuyama⁷⁹, A. Olariu^{27b}, L.F. Oleiro Seabra^{137a}, S.A. Olivares Pino^{144a}, D. Oliveira Damazio²⁹, J.L. Oliver¹, M.J.R. Olsson³⁶, A. Olszewski⁸², J. Olszowska⁸², D.C. O'Neil¹⁴⁹, A. Onofre^{137a,137e}, K. Onogi¹¹⁵, P.U.E. Onyisi¹¹, H. Oppen¹³¹, M.J. Oreglia³⁶, Y. Oren¹⁵⁹, D. Orestano^{72a,72b}, E.C. Orgill⁹⁸, N. Orlando^{61b}, A.A. O'Rourke⁴⁴, R.S. Orr¹⁶⁵, B. Osculati^{53b,53a,*}, V. O'Shea⁵⁵, R. Ospanov^{58a}, G. Otero y Garzon³⁰, H. Otono⁸⁵, M. Ouchrif^{34d}, F. Ould-Saada¹³¹, A. Ouraou¹⁴², K.P. Oussoren¹¹⁸, Q. Ouyang^{15a}, M. Owen⁵⁵, R.E. Owen²¹, V.E. Ozcan^{12c}, N. Ozturk⁸, K. Pachal¹⁴⁹, A. Pacheco Pages¹⁴, L. Pacheco Rodriguez¹⁴², C. Padilla Aranda¹⁴, S. Pagan Griso¹⁸, M. Paganini¹⁸¹, G. Palacino⁶³, S. Palazzo^{40b,40a}, S. Palestini³⁵, M. Palka^{81b}, D. Pallin³⁷, I. Panagoulias¹⁰, C.E. Pandini⁵², J.G. Panduro Vazquez⁹¹, P. Pani³⁵, L. Paolozzi⁵², T.D. Papadopoulou¹⁰, K. Papageorgiou^{9,k}, A. Paramonov⁶, D. Paredes Hernandez^{61b}, B. Parida^{58c}, A.J. Parker⁸⁷, K.A. Parker⁴⁴, M.A. Parker³¹, F. Parodi^{53b,53a}, J.A. Parsons³⁸, U. Parzefall⁵⁰, V.R. Pascuzzi¹⁶⁵, J.M.P. Pasner¹⁴³, E. Pasqualucci^{70a}, S. Passaggio^{53b}, F. Pastore⁹¹, P. Pasuwan^{43a,43b}, S. Pataraia⁹⁷, J.R. Pater⁹⁸, A. Pathak^{179,1}, T. Pauly³⁵, B. Pearson¹¹³, S. Pedraza Lopez¹⁷², R. Pedro^{137a,137b}, S.V. Peleganchuk^{120b,120a}, O. Penc¹³⁸, C. Peng^{15d}, H. Peng^{58a}, J. Penwell⁶³, B.S. Peralva^{78a}, M.M. Perego¹⁴², A.P. Pereira Peixoto^{137a}, D.V. Perepelitsa²⁹, F. Peri¹⁹, L. Perini^{66a,66b}, H. Pernegger³⁵, S. Perrella^{67a,67b}, V.D. Peshekhonov^{77,*}, K. Peters⁴⁴, R.F.Y. Peters⁹⁸, B.A. Petersen³⁵, T.C. Petersen³⁹, E. Petit⁵⁶, A. Petridis¹, C. Petridou¹⁶⁰, P. Petroff¹²⁹, E. Petrolo^{70a}, M. Petrov¹³², F. Petrucci^{72a,72b}, N.E. Pettersson¹⁰⁰, A. Peyaud¹⁴², R. Pezoa^{144b}, T. Pham¹⁰², F.H. Phillips¹⁰⁴, P.W. Phillips¹⁴¹, G. Piacquadio¹⁵², E. Pianori¹⁷⁶, A. Picazio¹⁰⁰, M.A. Pickering¹³², R. Piegai³⁰, J.E. Pilcher³⁶, A.D. Pilkington⁹⁸, M. Pinamonti^{71a,71b}, J.L. Pinfold³, M. Pitt¹⁷⁸, M.-A. Pleier²⁹, V. Pleskot¹⁴⁰, E. Plotnikova⁷⁷, D. Pluth⁷⁶, P. Podberezko^{120b,120a}, R. Poettgen⁹⁴, R. Poggi^{68a,68b}, L. Poggioli¹²⁹, I. Pogrebnyak¹⁰⁴, D. Pohl²⁴, I. Pokharel⁵¹, G. Polesello^{68a}, A. Poley⁴⁴, A. Policicchio^{40b,40a}, R. Polifka³⁵, A. Polini^{23b}, C.S. Pollard⁴⁴, V. Polychronakos²⁹, D. Ponomarenko¹¹⁰, L. Pontecorvo^{70a}, G.A. Popenciu^{27d}, D.M. Portillo Quintero¹³³, S. Pospisil¹³⁹, K. Potamianos⁴⁴,

I.N. Potrap⁷⁷, C.J. Potter³¹, H. Potti¹¹, T. Poulsen⁹⁴, J. Poveda³⁵, M.E. Pozo Astigarraga³⁵,
 P. Pralavorio⁹⁹, S. Prell⁷⁶, D. Price⁹⁸, M. Primavera^{65a}, S. Prince¹⁰¹, N. Proklova¹¹⁰, K. Prokofiev^{61c},
 F. Prokoshin^{144b}, S. Protopopescu²⁹, J. Proudfoot⁶, M. Przybycien^{81a}, A. Puri¹⁷¹, P. Puzo¹²⁹, J. Qian¹⁰³,
 Y. Qin⁹⁸, A. Quadt⁵¹, M. Queitsch-Maitland⁴⁴, A. Qureshi¹, S.K. Radhakrishnan¹⁵², P. Rados¹⁰²,
 F. Ragusa^{66a,66b}, G. Rahal⁹⁵, J.A. Raine⁹⁸, S. Rajagopalan²⁹, T. Rashid¹²⁹, S. Raspopov⁵,
 M.G. Ratti^{66a,66b}, D.M. Rauch⁴⁴, F. Rauscher¹¹², S. Rave⁹⁷, B. Ravina¹⁴⁶, I. Ravinovich¹⁷⁸,
 J.H. Rawling⁹⁸, M. Raymond³⁵, A.L. Read¹³¹, N.P. Readioff⁵⁶, M. Reale^{65a,65b}, D.M. Rebuzzi^{68a,68b},
 A. Redelbach¹⁷⁵, G. Redlinger²⁹, R. Reece¹⁴³, R.G. Reed^{32c}, K. Reeves⁴², L. Rehnisch¹⁹, J. Reichert¹³⁴,
 A. Reiss⁹⁷, C. Rembser³⁵, H. Ren^{15d}, M. Rescigno^{70a}, S. Resconi^{66a}, E.D. Ressegue¹³⁴, S. Rettie¹⁷³,
 E. Reynolds²¹, O.L. Rezanova^{120b,120a}, P. Reznicek¹⁴⁰, R. Richter¹¹³, S. Richter⁹², E. Richter-Was^{81b},
 O. Ricken²⁴, M. Ridel¹³³, P. Rieck¹¹³, C.J. Riegel¹⁸⁰, O. Rifki⁴⁴, M. Rijssenbeek¹⁵², A. Rimoldi^{68a,68b},
 M. Rimoldi²⁰, L. Rinaldi^{23b}, G. Ripellino¹⁵¹, B. Ristic³⁵, E. Ritsch³⁵, I. Riu¹⁴, J.C. Rivera Vergara^{144a},
 F. Rizatdinova¹²⁶, E. Rizvi⁹⁰, C. Rizzi¹⁴, R.T. Roberts⁹⁸, S.H. Robertson^{101,ag},
 A. Robichaud-Veronneau¹⁰¹, D. Robinson³¹, J.E.M. Robinson⁴⁴, A. Robson⁵⁵, E. Rocco⁹⁷,
 C. Roda^{69a,69b}, Y. Rodina^{99,ac}, S. Rodriguez Bosca¹⁷², A. Rodriguez Perez¹⁴, D. Rodriguez Rodriguez¹⁷²,
 A.M. Rodríguez Vera^{166b}, S. Roe³⁵, C.S. Rogan⁵⁷, O. Røhne¹³¹, R. Röhrig¹¹³, C.P.A. Roland⁶³,
 J. Roloff⁵⁷, A. Romanouk¹¹⁰, M. Romano^{23b,23a}, E. Romero Adam¹⁷², N. Rompotis⁸⁸, M. Ronzani¹²²,
 L. Roos¹³³, S. Rosati^{70a}, K. Rosbach⁵⁰, P. Rose¹⁴³, N-A. Rosien⁵¹, E. Rossi^{67a,67b}, L.P. Rossi^{53b},
 L. Rossini^{66a,66b}, J.H.N. Rosten³¹, R. Rosten¹⁴⁵, M. Rotaru^{27b}, J. Rothberg¹⁴⁵, D. Rousseau¹²⁹,
 D. Roy^{32c}, A. Rozanov⁹⁹, Y. Rozen¹⁵⁸, X. Ruan^{32c}, F. Rubbo¹⁵⁰, F. Rühr⁵⁰, A. Ruiz-Martinez³³,
 Z. Rurikova⁵⁰, N.A. Rusakovich⁷⁷, H.L. Russell¹⁰¹, J.P. Rutherford⁷, N. Ruthmann³⁵,
 E.M. Rüttinger^{44,m}, Y.F. Ryabov¹³⁵, M. Rybar¹⁷¹, G. Rybkin¹²⁹, S. Ryu⁶, A. Ryzhov¹²¹, G.F. Rzehorž⁵¹,
 P. Sabatini⁵¹, G. Sabato¹¹⁸, S. Sacerdoti¹²⁹, H.F-W. Sadrozinski¹⁴³, R. Sadykov⁷⁷, F. Safai Tehrani^{70a},
 P. Saha¹¹⁹, M. Sahinsoy^{59a}, M. Saimpert⁴⁴, M. Saito¹⁶¹, T. Saito¹⁶¹, H. Sakamoto¹⁶¹, A. Sakharov^{122,an},
 D. Salamani⁵², G. Salamanna^{72a,72b}, J.E. Salazar Loyola^{144b}, D. Salek¹¹⁸, P.H. Sales De Bruin¹⁷⁰,
 D. Salihagic¹¹³, A. Salnikov¹⁵⁰, J. Salt¹⁷², D. Salvatore^{40b,40a}, F. Salvatore¹⁵³, A. Salvucci^{61a,61b,61c},
 A. Salzburger³⁵, D. Sammel⁵⁰, D. Sampsonidis¹⁶⁰, D. Sampsonidou¹⁶⁰, J. Sánchez¹⁷²,
 A. Sanchez Pineda^{64a,64c}, H. Sandaker¹³¹, C.O. Sander⁴⁴, M. Sandhoff¹⁸⁰, C. Sandoval²²,
 D.P.C. Sankey¹⁴¹, M. Sannino^{53b,53a}, Y. Sano¹¹⁵, A. Sansoni⁴⁹, C. Santoni³⁷, H. Santos^{137a},
 I. Santoyo Castillo¹⁵³, A. Sapronov⁷⁷, J.G. Saraiva^{137a,137d}, O. Sasaki⁷⁹, K. Sato¹⁶⁷, E. Sauvan⁵,
 P. Savard^{165,ax}, N. Savic¹¹³, R. Sawada¹⁶¹, C. Sawyer¹⁴¹, L. Sawyer^{93,al}, C. Sbarra^{23b}, A. Sbrizzi^{23b,23a},
 T. Scanlon⁹², D.A. Scannicchio¹⁶⁹, J. Schaarschmidt¹⁴⁵, P. Schacht¹¹³, B.M. Schachtner¹¹²,
 D. Schaefer³⁶, L. Schaefer¹³⁴, J. Schaeffer⁹⁷, S. Schaepe³⁵, U. Schäfer⁹⁷, A.C. Schaffer¹²⁹, D. Schaile¹¹²,
 R.D. Schamberger¹⁵², N. Scharmberg⁹⁸, V.A. Schegelsky¹³⁵, D. Scheirich¹⁴⁰, F. Schenck¹⁹,
 M. Schernau¹⁶⁹, C. Schiavi^{53b,53a}, S. Schier¹⁴³, L.K. Schildgen²⁴, Z.M. Schillaci²⁶, E.J. Schioppa³⁵,
 M. Schioppa^{40b,40a}, K.E. Schleicher⁵⁰, S. Schlenker³⁵, K.R. Schmidt-Sommerfeld¹¹³, K. Schmieden³⁵,
 C. Schmitt⁹⁷, S. Schmitt⁴⁴, S. Schmitz⁹⁷, U. Schnoor⁵⁰, L. Schoeffel¹⁴², A. Schoening^{59b}, E. Schopf²⁴,
 M. Schott⁹⁷, J.F.P. Schouwenberg¹¹⁷, J. Schovancova³⁵, S. Schramm⁵², N. Schuh⁹⁷, A. Schulte⁹⁷,
 H-C. Schultz-Coulon^{59a}, M. Schumacher⁵⁰, B.A. Schumm¹⁴³, Ph. Schune¹⁴², A. Schwartzman¹⁵⁰,
 T.A. Schwarz¹⁰³, H. Schweiger⁹⁸, Ph. Schwemling¹⁴², R. Schwienhorst¹⁰⁴, A. Sciandra²⁴, G. Sciolla²⁶,
 M. Scornajenghi^{40b,40a}, F. Scuri^{69a}, F. Scutti¹⁰², L.M. Scyboz¹¹³, J. Searcy¹⁰³, C.D. Sebastiani^{70a,70b},
 P. Seema²⁴, S.C. Seidel¹¹⁶, A. Seiden¹⁴³, J.M. Seixas^{78b}, G. Sekhniaidze^{67a}, K. Sekhon¹⁰³, S.J. Sekula⁴¹,
 N. Semprini-Cesari^{23b,23a}, S. Senkin³⁷, C. Serfon¹³¹, L. Serin¹²⁹, L. Serkin^{64a,64b}, M. Sessa^{72a,72b},
 H. Severini¹²⁵, F. Sforza¹⁶⁸, A. Sfyrla⁵², E. Shabalina⁵¹, J.D. Shahinian¹⁴³, N.W. Shaikh^{43a,43b},
 L.Y. Shan^{15a}, R. Shang¹⁷¹, J.T. Shank²⁵, M. Shapiro¹⁸, A.S. Sharma¹, A. Sharma¹³², P.B. Shatalov¹⁰⁹,
 K. Shaw^{64a,64b}, S.M. Shaw⁹⁸, A. Shcherbakova¹³⁵, C.Y. Shehu¹⁵³, Y. Shen¹²⁵, N. Sherafati³³,
 A.D. Sherman²⁵, P. Sherwood⁹², L. Shi^{155,at}, S. Shimizu⁸⁰, C.O. Shimmin¹⁸¹, M. Shimojima¹¹⁴,

I.P.J. Shipsey¹³², S. Shirabe⁸⁵, M. Shiyakova⁷⁷, J. Shlomi¹⁷⁸, A. Shmeleva¹⁰⁸, D. Shoaleh Saadi¹⁰⁷,
 M.J. Shochet³⁶, S. Shojaii¹⁰², D.R. Shope¹²⁵, S. Shrestha¹²³, E. Shulga¹¹⁰, P. Sicho¹³⁸, A.M. Sickles¹⁷¹,
 P.E. Sidebo¹⁵¹, E. Sideras Haddad^{32c}, O. Sidiropoulou¹⁷⁵, A. Sidoti^{23b,23a}, F. Siegert⁴⁶, Dj. Sijacki¹⁶,
 J. Silva^{137a}, M. Silva Jr.¹⁷⁹, S.B. Silverstein^{43a}, L. Simic⁷⁷, S. Simion¹²⁹, E. Simioni⁹⁷, B. Simmons⁹²,
 M. Simon⁹⁷, R. Simoniello⁹⁷, P. Sinervo¹⁶⁵, N.B. Sinev¹²⁸, M. Sioli^{23b,23a}, G. Siragusa¹⁷⁵, I. Siral¹⁰³,
 S.Yu. Sivoklokov¹¹¹, J. Sjölin^{43a,43b}, M.B. Skinner⁸⁷, P. Skubic¹²⁵, M. Slater²¹, T. Slavicek¹³⁹,
 M. Slawinska⁸², K. Sliwa¹⁶⁸, R. Slovák¹⁴⁰, V. Smakhtin¹⁷⁸, B.H. Smart⁵, J. Smiesko^{28a}, N. Smirnov¹¹⁰,
 S.Yu. Smirnov¹¹⁰, Y. Smirnov¹¹⁰, L.N. Smirnova¹¹¹, O. Smirnova⁹⁴, J.W. Smith⁵¹, M.N.K. Smith³⁸,
 R.W. Smith³⁸, M. Smizanska⁸⁷, K. Smolek¹³⁹, A.A. Snesarev¹⁰⁸, I.M. Snyder¹²⁸, S. Snyder²⁹,
 R. Sobie^{174,ag}, F. Socher⁴⁶, A.M. Soffa¹⁶⁹, A. Soffer¹⁵⁹, A. Søgaard⁴⁸, D.A. Soh¹⁵⁵, G. Sokhrannyi⁸⁹,
 C.A. Solans Sanchez³⁵, M. Solar¹³⁹, E.Yu. Soldatov¹¹⁰, U. Soldevila¹⁷², A.A. Solodkov¹²¹,
 A. Soloshenko⁷⁷, O.V. Solovyanov¹²¹, V. Solovyev¹³⁵, P. Sommer¹⁴⁶, H. Son¹⁶⁸, W. Song¹⁴¹,
 A. Sopczak¹³⁹, F. Sopkova^{28b}, D. Sosa^{59b}, C.L. Sotiropoulou^{69a,69b}, S. Sottocornola^{68a,68b},
 R. Soualah^{64a,64c,j}, A.M. Soukharev^{120b,120a}, D. South⁴⁴, B.C. Sowden⁹¹, S. Spagnolo^{65a,65b},
 M. Spalla¹¹³, M. Spangenberg¹⁷⁶, F. Spanò⁹¹, D. Sperlich¹⁹, F. Spettel¹¹³, T.M. Spieker^{59a}, R. Spighi^{23b},
 G. Spigo³⁵, L.A. Spiller¹⁰², M. Spousta¹⁴⁰, A. Stabile^{66a,66b}, R. Stamen^{59a}, S. Stamm¹⁹, E. Stanecka⁸²,
 R.W. Stanek⁶, C. Stanescu^{72a}, M.M. Stanitzki⁴⁴, B. Stapf¹¹⁸, S. Stapnes¹³¹, E.A. Starchenko¹²¹,
 G.H. Stark³⁶, J. Stark⁵⁶, S.H Stark³⁹, P. Staroba¹³⁸, P. Starovoitov^{59a}, S. Stärz³⁵, R. Staszewski⁸²,
 M. Stegler⁴⁴, P. Steinberg²⁹, B. Stelzer¹⁴⁹, H.J. Stelzer³⁵, O. Stelzer-Chilton^{166a}, H. Stenzel⁵⁴,
 T.J. Stevenson⁹⁰, G.A. Stewart⁵⁵, M.C. Stockton¹²⁸, G. Stoica^{27b}, P. Stolte⁵¹, S. Stonjek¹¹³,
 A. Straessner⁴⁶, J. Strandberg¹⁵¹, S. Strandberg^{43a,43b}, M. Strauss¹²⁵, P. Strizenec^{28b}, R. Ströhmer¹⁷⁵,
 D.M. Strom¹²⁸, R. Stroynowski⁴¹, A. Strubig⁴⁸, S.A. Stucci²⁹, B. Stugu¹⁷, J. Stupak¹²⁵, N.A. Styles⁴⁴,
 D. Su¹⁵⁰, J. Su¹³⁶, S. Suchek^{59a}, Y. Sugaya¹³⁰, M. Suk¹³⁹, V.V. Sulin¹⁰⁸, D.M.S. Sultan⁵², S. Sultansoy^{4c},
 T. Sumida⁸³, S. Sun¹⁰³, X. Sun³, K. Suruliz¹⁵³, C.J.E. Suster¹⁵⁴, M.R. Sutton¹⁵³, S. Suzuki⁷⁹,
 M. Svatos¹³⁸, M. Swiatlowski³⁶, S.P. Swift², A. Sydorenko⁹⁷, I. Sykora^{28a}, T. Sykora¹⁴⁰, D. Ta⁹⁷,
 K. Tackmann^{44,ad}, J. Taenzer¹⁵⁹, A. Taffard¹⁶⁹, R. Tafirout^{166a}, E. Tahirovic⁹⁰, N. Taiblum¹⁵⁹, H. Takai²⁹,
 R. Takashima⁸⁴, E.H. Takasugi¹¹³, K. Takeda⁸⁰, T. Takeshita¹⁴⁷, Y. Takubo⁷⁹, M. Talby⁹⁹,
 A.A. Talyshев^{120b,120a}, J. Tanaka¹⁶¹, M. Tanaka¹⁶³, R. Tanaka¹²⁹, R. Tanioka⁸⁰, B.B. Tannenwald¹²³,
 S. Tapia Araya^{144b}, S. Tapprogge⁹⁷, A. Tarek Abouelfadl Mohamed¹³³, S. Tarem¹⁵⁸, G. Tarna^{27b,f},
 G.F. Tartarelli^{66a}, P. Tas¹⁴⁰, M. Tasevsky¹³⁸, T. Tashiro⁸³, E. Tassi^{40b,40a}, A. Tavares Delgado^{137a,137b},
 Y. Tayalati^{34e}, A.C. Taylor¹¹⁶, A.J. Taylor⁴⁸, G.N. Taylor¹⁰², P.T.E. Taylor¹⁰², W. Taylor^{166b}, A.S. Tee⁸⁷,
 P. Teixeira-Dias⁹¹, D. Temple¹⁴⁹, H. Ten Kate³⁵, P.K. Teng¹⁵⁵, J.J. Teoh¹³⁰, F. Tepel¹⁸⁰, S. Terada⁷⁹,
 K. Terashi¹⁶¹, J. Terron⁹⁶, S. Terzo¹⁴, M. Testa⁴⁹, R.J. Teuscher^{165,ag}, S.J. Thais¹⁸¹,
 T. Theveneaux-Pelzer⁴⁴, F. Thiele³⁹, J.P. Thomas²¹, A.S. Thompson⁵⁵, P.D. Thompson²¹,
 L.A. Thomsen¹⁸¹, E. Thomson¹³⁴, Y. Tian³⁸, R.E. Ticse Torres⁵¹, V.O. Tikhomirov^{108,ap},
 Yu.A. Tikhonov^{120b,120a}, S. Timoshenko¹¹⁰, P. Tipton¹⁸¹, S. Tisserant⁹⁹, K. Todome¹⁶³,
 S. Todorova-Nova⁵, S. Todt⁴⁶, J. Tojo⁸⁵, S. Tokár^{28a}, K. Tokushuku⁷⁹, E. Tolley¹²³, M. Tomoto¹¹⁵,
 L. Tompkins^{150,s}, K. Toms¹¹⁶, B. Tong⁵⁷, P. Tornambe⁵⁰, E. Torrence¹²⁸, H. Torres⁴⁶, E. Torró Pastor¹⁴⁵,
 C. Tosciri¹³², J. Toth^{99,af}, F. Touchard⁹⁹, D.R. Tovey¹⁴⁶, C.J. Treado¹²², T. Trefzger¹⁷⁵, F. Tresoldi¹⁵³,
 A. Tricoli²⁹, I.M. Trigger^{166a}, S. Trincaz-Duvold¹³³, M.F. Tripiana¹⁴, W. Trischuk¹⁶⁵, B. Trocmé⁵⁶,
 A. Trofymov⁴⁴, C. Troncon^{66a}, M. Trovatelli¹⁷⁴, F. Trovato¹⁵³, L. Truong^{32b}, M. Trzebinski⁸²,
 A. Trzupek⁸², F. Tsai⁴⁴, K.W. Tsang^{61a}, J.C-L. Tseng¹³², P.V. Tsiareshka¹⁰⁵, N. Tsirintanis⁹,
 S. Tsiskaridze¹⁴, V. Tsiskaridze¹⁵², E.G. Tskhadadze^{157a}, I.I. Tsukerman¹⁰⁹, V. Tsulaia¹⁸, S. Tsuno⁷⁹,
 D. Tsybychev¹⁵², Y. Tu^{61b}, A. Tudorache^{27b}, V. Tudorache^{27b}, T.T. Tulbure^{27a}, A.N. Tuna⁵⁷,
 S. Turchikhin⁷⁷, D. Turgeman¹⁷⁸, I. Turk Cakir^{4b,w}, R. Turra^{66a}, P.M. Tuts³⁸, G. Ucchielli^{23b,23a},
 I. Ueda⁷⁹, M. Ughetto^{43a,43b}, F. Ukegawa¹⁶⁷, G. Unal³⁵, A. Undrus²⁹, G. Unel¹⁶⁹, F.C. Ungaro¹⁰²,
 Y. Unno⁷⁹, K. Uno¹⁶¹, J. Urban^{28b}, P. Urquijo¹⁰², P. Urrejola⁹⁷, G. Usai⁸, J. Usui⁷⁹, L. Vacavant⁹⁹,

V. Vacek¹³⁹, B. Vachon¹⁰¹, K.O.H. Vadla¹³¹, A. Vaidya⁹², C. Valderanis¹¹², E. Valdes Santurio^{43a,43b}, M. Valente⁵², S. Valentineti^{23b,23a}, A. Valero¹⁷², L. Valéry⁴⁴, R.A. Vallance²¹, A. Vallier⁵, J.A. Valls Ferrer¹⁷², T.R. Van Daalen¹⁴, W. Van Den Wollenberg¹¹⁸, H. Van der Graaf¹¹⁸, P. Van Gemmeren⁶, J. Van Nieuwkoop¹⁴⁹, I. Van Vulpen¹¹⁸, M.C. van Woerden¹¹⁸, M. Vanadia^{71a,71b}, W. Vandelli³⁵, A. Vaniachine¹⁶⁴, P. Vankov¹¹⁸, R. Vari^{70a}, E.W. Varnes⁷, C. Varni^{53b,53a}, T. Varol⁴¹, D. Varouchas¹²⁹, A. Vartapetian⁸, K.E. Varvell¹⁵⁴, G.A. Vasquez^{144b}, J.G. Vasquez¹⁸¹, F. Vazeille³⁷, D. Vazquez Furelos¹⁴, T. Vazquez Schroeder¹⁰¹, J. Veatch⁵¹, V. Vecchio^{72a,72b}, L.M. Veloce¹⁶⁵, F. Veloso^{137a,137c}, S. Veneziano^{70a}, A. Ventura^{65a,65b}, M. Venturi¹⁷⁴, N. Venturi³⁵, V. Vercesi^{68a}, M. Verducci^{72a,72b}, W. Verkerke¹¹⁸, A.T. Vermeulen¹¹⁸, J.C. Vermeulen¹¹⁸, M.C. Vetterli^{149,ax}, N. Viaux Maira^{144b}, O. Viazlo⁹⁴, I. Vichou^{171,*}, T. Vickey¹⁴⁶, O.E. Vickey Boeriu¹⁴⁶, G.H.A. Viehhauser¹³², S. Viel¹⁸, L. Vigani¹³², M. Villa^{23b,23a}, M. Villaplana Perez^{66a,66b}, E. Vilucchi⁴⁹, M.G. Vincter³³, V.B. Vinogradov⁷⁷, A. Vishwakarma⁴⁴, C. Vittori^{23b,23a}, I. Vivarelli¹⁵³, S. Vlachos¹⁰, M. Vogel¹⁸⁰, P. Vokac¹³⁹, G. Volpi¹⁴, S.E. von Buddenbrock^{32c}, E. Von Toerne²⁴, V. Vorobel¹⁴⁰, K. Vorobej¹¹⁰, M. Vos¹⁷², J.H. Vossebeld⁸⁸, N. Vranjes¹⁶, M. Vranjes Milosavljevic¹⁶, V. Vrba¹³⁹, M. Vreeswijk¹¹⁸, T. Šfiligoj⁸⁹, R. Vuillermet³⁵, I. Vukotic³⁶, T. Ženiš^{28a}, L. Živković¹⁶, P. Wagner²⁴, W. Wagner¹⁸⁰, J. Wagner-Kuhr¹¹², H. Wahlberg⁸⁶, S. Wahrmund⁴⁶, K. Wakamiya⁸⁰, J. Walder⁸⁷, R. Walker¹¹², W. Walkowiak¹⁴⁸, V. Wallangen^{43a,43b}, A.M. Wang⁵⁷, C. Wang^{58b,f}, F. Wang¹⁷⁹, H. Wang¹⁸, H. Wang³, J. Wang¹⁵⁴, J. Wang^{59b}, P. Wang⁴¹, Q. Wang¹²⁵, R.-J. Wang¹³³, R. Wang^{58a}, R. Wang⁶, S.M. Wang¹⁵⁵, T. Wang³⁸, W. Wang^{155,q}, W.X. Wang^{58a,ah}, Y. Wang^{58a,am}, Z. Wang^{58c}, C. Wanotayaroj⁴⁴, A. Warburton¹⁰¹, C.P. Ward³¹, D.R. Wardrobe⁹², A. Washbrook⁴⁸, P.M. Watkins²¹, A.T. Watson²¹, M.F. Watson²¹, G. Watts¹⁴⁵, S. Watts⁹⁸, B.M. Waugh⁹², A.F. Webb¹¹, S. Webb⁹⁷, C. Weber¹⁸¹, M.S. Weber²⁰, S.A. Weber³³, S.M. Weber^{59a}, J.S. Webster⁶, A.R. Weidberg¹³², B. Weinert⁶³, J. Weingarten⁵¹, M. Weirich⁹⁷, C. Weiser⁵⁰, P.S. Wells³⁵, T. Wenaus²⁹, T. Wengler³⁵, S. Wenig³⁵, N. Wermes²⁴, M.D. Werner⁷⁶, P. Werner³⁵, M. Wessels^{59a}, T.D. Weston²⁰, K. Whalen¹²⁸, N.L. Whallon¹⁴⁵, A.M. Wharton⁸⁷, A.S. White¹⁰³, A. White⁸, M.J. White¹, R. White^{144b}, D. Whiteson¹⁶⁹, B.W. Whitmore⁸⁷, F.J. Wickens¹⁴¹, W. Wiedenmann¹⁷⁹, M. Wielers¹⁴¹, C. Wiglesworth³⁹, L.A.M. Wiik-Fuchs⁵⁰, A. Wildauer¹¹³, F. Wilk⁹⁸, H.G. Wilkens³⁵, H.H. Williams¹³⁴, S. Williams³¹, C. Willis¹⁰⁴, S. Willocq¹⁰⁰, J.A. Wilson²¹, I. Wingerter-Seez⁵, E. Winkels¹⁵³, F. Winklmeier¹²⁸, O.J. Winston¹⁵³, B.T. Winter²⁴, M. Wittgen¹⁵⁰, M. Wobisch⁹³, A. Wolf⁹⁷, T.M.H. Wolf¹¹⁸, R. Wolff⁹⁹, M.W. Wolter⁸², H. Wolters^{137a,137c}, V.W.S. Wong¹⁷³, N.L. Woods¹⁴³, S.D. Worm²¹, B.K. Wosiek⁸², K.W. Woźniak⁸², K. Wraight⁵⁵, M. Wu³⁶, S.L. Wu¹⁷⁹, X. Wu⁵², Y. Wu^{58a}, T.R. Wyatt⁹⁸, B.M. Wynne⁴⁸, S. Xella³⁹, Z. Xi¹⁰³, L. Xia^{15b}, D. Xu^{15a}, H. Xu^{58a,f}, L. Xu²⁹, T. Xu¹⁴², W. Xu¹⁰³, B. Yabsley¹⁵⁴, S. Yacoob^{32a}, K. Yajima¹³⁰, D.P. Yallup⁹², D. Yamaguchi¹⁶³, Y. Yamaguchi¹⁶³, A. Yamamoto⁷⁹, T. Yamanaka¹⁶¹, F. Yamane⁸⁰, M. Yamatani¹⁶¹, T. Yamazaki¹⁶¹, Y. Yamazaki⁸⁰, Z. Yan²⁵, H.J. Yang^{58c,58d}, H.T. Yang¹⁸, S. Yang⁷⁵, Y. Yang¹⁶¹, Y. Yang¹⁵⁵, Z. Yang¹⁷, W-M. Yao¹⁸, Y.C. Yap⁴⁴, Y. Yasu⁷⁹, E. Yatsenko⁵, K.H. Yau Wong²⁴, J. Ye⁴¹, S. Ye²⁹, I. Yeletskikh⁷⁷, E. Yigitbasi²⁵, E. Yildirim⁹⁷, K. Yorita¹⁷⁷, K. Yoshihara¹³⁴, C.J.S. Young³⁵, C. Young¹⁵⁰, J. Yu⁸, J. Yu⁷⁶, X. Yue^{59a}, S.P.Y. Yuen²⁴, I. Yusuff^{31,a}, B. Zabinski⁸², G. Zacharis¹⁰, R. Zaidan¹⁴, A.M. Zaitsev^{121,ao}, N. Zakharchuk⁴⁴, J. Zalieckas¹⁷, S. Zambito⁵⁷, D. Zanzi³⁵, C. Zeitnitz¹⁸⁰, G. Zemaityte¹³², J.C. Zeng¹⁷¹, Q. Zeng¹⁵⁰, O. Zenin¹²¹, D. Zerwas¹²⁹, M. Zgubic¹³², D.F. Zhang^{58b}, D. Zhang¹⁰³, F. Zhang¹⁷⁹, G. Zhang^{58a,ah}, H. Zhang^{15c}, J. Zhang⁶, L. Zhang⁵⁰, L. Zhang^{58a}, M. Zhang¹⁷¹, P. Zhang^{15c}, R. Zhang^{58a,f}, R. Zhang²⁴, X. Zhang^{58b}, Y. Zhang^{15d}, Z. Zhang¹²⁹, X. Zhao⁴¹, Y. Zhao^{58b,129,ak}, Z. Zhao^{58a}, A. Zhemchugov⁷⁷, B. Zhou¹⁰³, C. Zhou¹⁷⁹, L. Zhou⁴¹, M.S. Zhou^{15d}, M. Zhou¹⁵², N. Zhou^{58c}, Y. Zhou⁷, C.G. Zhu^{58b}, H.L. Zhu^{58a}, H. Zhu^{15a}, J. Zhu¹⁰³, Y. Zhu^{58a}, X. Zhuang^{15a}, K. Zhukov¹⁰⁸, V. Zhulanov^{120b,120a}, A. Zibell¹⁷⁵, D. Ziemińska⁶³, N.I. Zimine⁷⁷, S. Zimmermann⁵⁰, Z. Zinonos¹¹³, M. Zinser⁹⁷, M. Ziolkowski¹⁴⁸, G. Zobernig¹⁷⁹, A. Zoccoli^{23b,23a}, K. Zoch⁵¹, T.G. Zorbas¹⁴⁶, R. Zou³⁶, M. Zur Nedden¹⁹, L. Zwalinski³⁵.

- ¹Department of Physics, University of Adelaide, Adelaide; Australia.
- ²Physics Department, SUNY Albany, Albany NY; United States of America.
- ³Department of Physics, University of Alberta, Edmonton AB; Canada.
- ^{4(a)}Department of Physics, Ankara University, Ankara;^(b)Istanbul Aydin University, Istanbul;^(c)Division of Physics, TOBB University of Economics and Technology, Ankara; Turkey.
- ⁵LAPP, Université Grenoble Alpes, Université Savoie Mont Blanc, CNRS/IN2P3, Annecy; France.
- ⁶High Energy Physics Division, Argonne National Laboratory, Argonne IL; United States of America.
- ⁷Department of Physics, University of Arizona, Tucson AZ; United States of America.
- ⁸Department of Physics, University of Texas at Arlington, Arlington TX; United States of America.
- ⁹Physics Department, National and Kapodistrian University of Athens, Athens; Greece.
- ¹⁰Physics Department, National Technical University of Athens, Zografou; Greece.
- ¹¹Department of Physics, University of Texas at Austin, Austin TX; United States of America.
- ^{12(a)}Bahcesehir University, Faculty of Engineering and Natural Sciences, Istanbul;^(b)Istanbul Bilgi University, Faculty of Engineering and Natural Sciences, Istanbul;^(c)Department of Physics, Bogazici University, Istanbul;^(d)Department of Physics Engineering, Gaziantep University, Gaziantep; Turkey.
- ¹³Institute of Physics, Azerbaijan Academy of Sciences, Baku; Azerbaijan.
- ¹⁴Institut de Física d'Altes Energies (IFAE), Barcelona Institute of Science and Technology, Barcelona; Spain.
- ^{15(a)}Institute of High Energy Physics, Chinese Academy of Sciences, Beijing;^(b)Physics Department, Tsinghua University, Beijing;^(c)Department of Physics, Nanjing University, Nanjing;^(d)University of Chinese Academy of Science (UCAS), Beijing; China.
- ¹⁶Institute of Physics, University of Belgrade, Belgrade; Serbia.
- ¹⁷Department for Physics and Technology, University of Bergen, Bergen; Norway.
- ¹⁸Physics Division, Lawrence Berkeley National Laboratory and University of California, Berkeley CA; United States of America.
- ¹⁹Institut für Physik, Humboldt Universität zu Berlin, Berlin; Germany.
- ²⁰Albert Einstein Center for Fundamental Physics and Laboratory for High Energy Physics, University of Bern, Bern; Switzerland.
- ²¹School of Physics and Astronomy, University of Birmingham, Birmingham; United Kingdom.
- ²²Centro de Investigaciones, Universidad Antonio Nariño, Bogota; Colombia.
- ^{23(a)}Dipartimento di Fisica e Astronomia, Università di Bologna, Bologna;^(b)INFN Sezione di Bologna; Italy.
- ²⁴Physikalischs Institut, Universität Bonn, Bonn; Germany.
- ²⁵Department of Physics, Boston University, Boston MA; United States of America.
- ²⁶Department of Physics, Brandeis University, Waltham MA; United States of America.
- ^{27(a)}Transilvania University of Brasov, Brasov;^(b)Horia Hulubei National Institute of Physics and Nuclear Engineering, Bucharest;^(c)Department of Physics, Alexandru Ioan Cuza University of Iasi, Iasi;^(d)National Institute for Research and Development of Isotopic and Molecular Technologies, Physics Department, Cluj-Napoca;^(e)University Politehnica Bucharest, Bucharest;^(f)West University in Timisoara, Timisoara; Romania.
- ^{28(a)}Faculty of Mathematics, Physics and Informatics, Comenius University, Bratislava;^(b)Department of Subnuclear Physics, Institute of Experimental Physics of the Slovak Academy of Sciences, Kosice; Slovak Republic.
- ²⁹Physics Department, Brookhaven National Laboratory, Upton NY; United States of America.
- ³⁰Departamento de Física, Universidad de Buenos Aires, Buenos Aires; Argentina.
- ³¹Cavendish Laboratory, University of Cambridge, Cambridge; United Kingdom.
- ^{32(a)}Department of Physics, University of Cape Town, Cape Town;^(b)Department of Mechanical

Engineering Science, University of Johannesburg, Johannesburg;^(c)School of Physics, University of the Witwatersrand, Johannesburg; South Africa.

³³Department of Physics, Carleton University, Ottawa ON; Canada.

^{34(a)}Faculté des Sciences Ain Chock, Réseau Universitaire de Physique des Hautes Energies - Université Hassan II, Casablanca;^(b)Centre National de l'Energie des Sciences Techniques Nucleaires (CNESTEN), Rabat;^(c)Faculté des Sciences Semlalia, Université Cadi Ayyad, LPHEA-Marrakech;^(d)Faculté des Sciences, Université Mohamed Premier and LPTPM, Oujda;^(e)Faculté des sciences, Université Mohammed V, Rabat; Morocco.

³⁵CERN, Geneva; Switzerland.

³⁶Enrico Fermi Institute, University of Chicago, Chicago IL; United States of America.

³⁷LPC, Université Clermont Auvergne, CNRS/IN2P3, Clermont-Ferrand; France.

³⁸Nevis Laboratory, Columbia University, Irvington NY; United States of America.

³⁹Niels Bohr Institute, University of Copenhagen, Copenhagen; Denmark.

^{40(a)}Dipartimento di Fisica, Università della Calabria, Rende;^(b)INFN Gruppo Collegato di Cosenza, Laboratori Nazionali di Frascati; Italy.

⁴¹Physics Department, Southern Methodist University, Dallas TX; United States of America.

⁴²Physics Department, University of Texas at Dallas, Richardson TX; United States of America.

^{43(a)}Department of Physics, Stockholm University;^(b)Oskar Klein Centre, Stockholm; Sweden.

⁴⁴Deutsches Elektronen-Synchrotron DESY, Hamburg and Zeuthen; Germany.

⁴⁵Lehrstuhl für Experimentelle Physik IV, Technische Universität Dortmund, Dortmund; Germany.

⁴⁶Institut für Kern- und Teilchenphysik, Technische Universität Dresden, Dresden; Germany.

⁴⁷Department of Physics, Duke University, Durham NC; United States of America.

⁴⁸SUPA - School of Physics and Astronomy, University of Edinburgh, Edinburgh; United Kingdom.

⁴⁹INFN e Laboratori Nazionali di Frascati, Frascati; Italy.

⁵⁰Physikalisches Institut, Albert-Ludwigs-Universität Freiburg, Freiburg; Germany.

⁵¹II. Physikalisches Institut, Georg-August-Universität Göttingen, Göttingen; Germany.

⁵²Département de Physique Nucléaire et Corpusculaire, Université de Genève, Genève; Switzerland.

^{53(a)}Dipartimento di Fisica, Università di Genova, Genova;^(b)INFN Sezione di Genova; Italy.

⁵⁴II. Physikalisches Institut, Justus-Liebig-Universität Giessen, Giessen; Germany.

⁵⁵SUPA - School of Physics and Astronomy, University of Glasgow, Glasgow; United Kingdom.

⁵⁶LPSC, Université Grenoble Alpes, CNRS/IN2P3, Grenoble INP, Grenoble; France.

⁵⁷Laboratory for Particle Physics and Cosmology, Harvard University, Cambridge MA; United States of America.

^{58(a)}Department of Modern Physics and State Key Laboratory of Particle Detection and Electronics, University of Science and Technology of China, Hefei;^(b)Institute of Frontier and Interdisciplinary Science and Key Laboratory of Particle Physics and Particle Irradiation (MOE), Shandong University, Qingdao;^(c)School of Physics and Astronomy, Shanghai Jiao Tong University, KLPPAC-MoE, SKLPPC, Shanghai;^(d)Tsung-Dao Lee Institute, Shanghai; China.

^{59(a)}Kirchhoff-Institut für Physik, Ruprecht-Karls-Universität Heidelberg, Heidelberg;^(b)Physikalisches Institut, Ruprecht-Karls-Universität Heidelberg, Heidelberg; Germany.

⁶⁰Faculty of Applied Information Science, Hiroshima Institute of Technology, Hiroshima; Japan.

^{61(a)}Department of Physics, Chinese University of Hong Kong, Shatin, N.T., Hong Kong;^(b)Department of Physics, University of Hong Kong, Hong Kong;^(c)Department of Physics and Institute for Advanced Study, Hong Kong University of Science and Technology, Clear Water Bay, Kowloon, Hong Kong; China.

⁶²Department of Physics, National Tsing Hua University, Hsinchu; Taiwan.

⁶³Department of Physics, Indiana University, Bloomington IN; United States of America.

- ^{64(a)}INFN Gruppo Collegato di Udine, Sezione di Trieste, Udine; ^(b)ICTP, Trieste; ^(c)Dipartimento di Chimica, Fisica e Ambiente, Università di Udine, Udine; Italy.
^{65(a)}INFN Sezione di Lecce; ^(b)Dipartimento di Matematica e Fisica, Università del Salento, Lecce; Italy.
^{66(a)}INFN Sezione di Milano; ^(b)Dipartimento di Fisica, Università di Milano, Milano; Italy.
^{67(a)}INFN Sezione di Napoli; ^(b)Dipartimento di Fisica, Università di Napoli, Napoli; Italy.
^{68(a)}INFN Sezione di Pavia; ^(b)Dipartimento di Fisica, Università di Pavia, Pavia; Italy.
^{69(a)}INFN Sezione di Pisa; ^(b)Dipartimento di Fisica E. Fermi, Università di Pisa, Pisa; Italy.
^{70(a)}INFN Sezione di Roma; ^(b)Dipartimento di Fisica, Sapienza Università di Roma, Roma; Italy.
^{71(a)}INFN Sezione di Roma Tor Vergata; ^(b)Dipartimento di Fisica, Università di Roma Tor Vergata, Roma; Italy.
^{72(a)}INFN Sezione di Roma Tre; ^(b)Dipartimento di Matematica e Fisica, Università Roma Tre, Roma; Italy.
^{73(a)}INFN-TIFPA; ^(b)Università degli Studi di Trento, Trento; Italy.
⁷⁴Institut für Astro- und Teilchenphysik, Leopold-Franzens-Universität, Innsbruck; Austria.
⁷⁵University of Iowa, Iowa City IA; United States of America.
⁷⁶Department of Physics and Astronomy, Iowa State University, Ames IA; United States of America.
⁷⁷Joint Institute for Nuclear Research, Dubna; Russia.
^{78(a)}Departamento de Engenharia Elétrica, Universidade Federal de Juiz de Fora (UFJF), Juiz de Fora; ^(b)Universidade Federal do Rio De Janeiro COPPE/EE/IF, Rio de Janeiro; ^(c)Universidade Federal de São João del Rei (UFSJ), São João del Rei; ^(d)Instituto de Física, Universidade de São Paulo, São Paulo; Brazil.
⁷⁹KEK, High Energy Accelerator Research Organization, Tsukuba; Japan.
⁸⁰Graduate School of Science, Kobe University, Kobe; Japan.
^{81(a)}AGH University of Science and Technology, Faculty of Physics and Applied Computer Science, Krakow; ^(b)Marian Smoluchowski Institute of Physics, Jagiellonian University, Krakow; Poland.
⁸²Institute of Nuclear Physics Polish Academy of Sciences, Krakow; Poland.
⁸³Faculty of Science, Kyoto University, Kyoto; Japan.
⁸⁴Kyoto University of Education, Kyoto; Japan.
⁸⁵Research Center for Advanced Particle Physics and Department of Physics, Kyushu University, Fukuoka ; Japan.
⁸⁶Instituto de Física La Plata, Universidad Nacional de La Plata and CONICET, La Plata; Argentina.
⁸⁷Physics Department, Lancaster University, Lancaster; United Kingdom.
⁸⁸Oliver Lodge Laboratory, University of Liverpool, Liverpool; United Kingdom.
⁸⁹Department of Experimental Particle Physics, Jožef Stefan Institute and Department of Physics, University of Ljubljana, Ljubljana; Slovenia.
⁹⁰School of Physics and Astronomy, Queen Mary University of London, London; United Kingdom.
⁹¹Department of Physics, Royal Holloway University of London, Egham; United Kingdom.
⁹²Department of Physics and Astronomy, University College London, London; United Kingdom.
⁹³Louisiana Tech University, Ruston LA; United States of America.
⁹⁴Fysiska institutionen, Lunds universitet, Lund; Sweden.
⁹⁵Centre de Calcul de l'Institut National de Physique Nucléaire et de Physique des Particules (IN2P3), Villeurbanne; France.
⁹⁶Departamento de Física Teorica C-15 and CIAFF, Universidad Autónoma de Madrid, Madrid; Spain.
⁹⁷Institut für Physik, Universität Mainz, Mainz; Germany.
⁹⁸School of Physics and Astronomy, University of Manchester, Manchester; United Kingdom.
⁹⁹CPPM, Aix-Marseille Université, CNRS/IN2P3, Marseille; France.
¹⁰⁰Department of Physics, University of Massachusetts, Amherst MA; United States of America.

- ¹⁰¹Department of Physics, McGill University, Montreal QC; Canada.
- ¹⁰²School of Physics, University of Melbourne, Victoria; Australia.
- ¹⁰³Department of Physics, University of Michigan, Ann Arbor MI; United States of America.
- ¹⁰⁴Department of Physics and Astronomy, Michigan State University, East Lansing MI; United States of America.
- ¹⁰⁵B.I. Stepanov Institute of Physics, National Academy of Sciences of Belarus, Minsk; Belarus.
- ¹⁰⁶Research Institute for Nuclear Problems of Byelorussian State University, Minsk; Belarus.
- ¹⁰⁷Group of Particle Physics, University of Montreal, Montreal QC; Canada.
- ¹⁰⁸P.N. Lebedev Physical Institute of the Russian Academy of Sciences, Moscow; Russia.
- ¹⁰⁹Institute for Theoretical and Experimental Physics (ITEP), Moscow; Russia.
- ¹¹⁰National Research Nuclear University MEPhI, Moscow; Russia.
- ¹¹¹D.V. Skobeltsyn Institute of Nuclear Physics, M.V. Lomonosov Moscow State University, Moscow; Russia.
- ¹¹²Fakultät für Physik, Ludwig-Maximilians-Universität München, München; Germany.
- ¹¹³Max-Planck-Institut für Physik (Werner-Heisenberg-Institut), München; Germany.
- ¹¹⁴Nagasaki Institute of Applied Science, Nagasaki; Japan.
- ¹¹⁵Graduate School of Science and Kobayashi-Maskawa Institute, Nagoya University, Nagoya; Japan.
- ¹¹⁶Department of Physics and Astronomy, University of New Mexico, Albuquerque NM; United States of America.
- ¹¹⁷Institute for Mathematics, Astrophysics and Particle Physics, Radboud University Nijmegen/Nikhef, Nijmegen; Netherlands.
- ¹¹⁸Nikhef National Institute for Subatomic Physics and University of Amsterdam, Amsterdam; Netherlands.
- ¹¹⁹Department of Physics, Northern Illinois University, DeKalb IL; United States of America.
- ^{120(a)}Budker Institute of Nuclear Physics, SB RAS, Novosibirsk;^(b)Novosibirsk State University Novosibirsk; Russia.
- ¹²¹Institute for High Energy Physics of the National Research Centre Kurchatov Institute, Protvino; Russia.
- ¹²²Department of Physics, New York University, New York NY; United States of America.
- ¹²³Ohio State University, Columbus OH; United States of America.
- ¹²⁴Faculty of Science, Okayama University, Okayama; Japan.
- ¹²⁵Homer L. Dodge Department of Physics and Astronomy, University of Oklahoma, Norman OK; United States of America.
- ¹²⁶Department of Physics, Oklahoma State University, Stillwater OK; United States of America.
- ¹²⁷Palacký University, RCPTM, Joint Laboratory of Optics, Olomouc; Czech Republic.
- ¹²⁸Center for High Energy Physics, University of Oregon, Eugene OR; United States of America.
- ¹²⁹LAL, Université Paris-Sud, CNRS/IN2P3, Université Paris-Saclay, Orsay; France.
- ¹³⁰Graduate School of Science, Osaka University, Osaka; Japan.
- ¹³¹Department of Physics, University of Oslo, Oslo; Norway.
- ¹³²Department of Physics, Oxford University, Oxford; United Kingdom.
- ¹³³LPNHE, Sorbonne Université, Paris Diderot Sorbonne Paris Cité, CNRS/IN2P3, Paris; France.
- ¹³⁴Department of Physics, University of Pennsylvania, Philadelphia PA; United States of America.
- ¹³⁵Konstantinov Nuclear Physics Institute of National Research Centre "Kurchatov Institute", PNPI, St. Petersburg; Russia.
- ¹³⁶Department of Physics and Astronomy, University of Pittsburgh, Pittsburgh PA; United States of America.
- ^{137(a)}Laboratório de Instrumentação e Física Experimental de Partículas - LIP;^(b)Departamento de

Física, Faculdade de Ciências, Universidade de Lisboa, Lisboa;^(c)Departamento de Física, Universidade de Coimbra, Coimbra;^(d)Centro de Física Nuclear da Universidade de Lisboa, Lisboa;^(e)Departamento de Física, Universidade do Minho, Braga;^(f)Departamento de Física Teorica y del Cosmos, Universidad de Granada, Granada (Spain);^(g)Dep Física and CEFITEC of Faculdade de Ciências e Tecnologia, Universidade Nova de Lisboa, Caparica; Portugal.

¹³⁸Institute of Physics, Academy of Sciences of the Czech Republic, Prague; Czech Republic.

¹³⁹Czech Technical University in Prague, Prague; Czech Republic.

¹⁴⁰Charles University, Faculty of Mathematics and Physics, Prague; Czech Republic.

¹⁴¹Particle Physics Department, Rutherford Appleton Laboratory, Didcot; United Kingdom.

¹⁴²IRFU, CEA, Université Paris-Saclay, Gif-sur-Yvette; France.

¹⁴³Santa Cruz Institute for Particle Physics, University of California Santa Cruz, Santa Cruz CA; United States of America.

^{144(a)}Departamento de Física, Pontificia Universidad Católica de Chile, Santiago;^(b)Departamento de Física, Universidad Técnica Federico Santa María, Valparaíso; Chile.

¹⁴⁵Department of Physics, University of Washington, Seattle WA; United States of America.

¹⁴⁶Department of Physics and Astronomy, University of Sheffield, Sheffield; United Kingdom.

¹⁴⁷Department of Physics, Shinshu University, Nagano; Japan.

¹⁴⁸Department Physik, Universität Siegen, Siegen; Germany.

¹⁴⁹Department of Physics, Simon Fraser University, Burnaby BC; Canada.

¹⁵⁰SLAC National Accelerator Laboratory, Stanford CA; United States of America.

¹⁵¹Physics Department, Royal Institute of Technology, Stockholm; Sweden.

¹⁵²Departments of Physics and Astronomy, Stony Brook University, Stony Brook NY; United States of America.

¹⁵³Department of Physics and Astronomy, University of Sussex, Brighton; United Kingdom.

¹⁵⁴School of Physics, University of Sydney, Sydney; Australia.

¹⁵⁵Institute of Physics, Academia Sinica, Taipei; Taiwan.

¹⁵⁶Academia Sinica Grid Computing, Institute of Physics, Academia Sinica, Taipei; Taiwan.

^{157(a)}E. Andronikashvili Institute of Physics, Iv. Javakhishvili Tbilisi State University, Tbilisi;^(b)High Energy Physics Institute, Tbilisi State University, Tbilisi; Georgia.

¹⁵⁸Department of Physics, Technion, Israel Institute of Technology, Haifa; Israel.

¹⁵⁹Raymond and Beverly Sackler School of Physics and Astronomy, Tel Aviv University, Tel Aviv; Israel.

¹⁶⁰Department of Physics, Aristotle University of Thessaloniki, Thessaloniki; Greece.

¹⁶¹International Center for Elementary Particle Physics and Department of Physics, University of Tokyo, Tokyo; Japan.

¹⁶²Graduate School of Science and Technology, Tokyo Metropolitan University, Tokyo; Japan.

¹⁶³Department of Physics, Tokyo Institute of Technology, Tokyo; Japan.

¹⁶⁴Tomsk State University, Tomsk; Russia.

¹⁶⁵Department of Physics, University of Toronto, Toronto ON; Canada.

^{166(a)}TRIUMF, Vancouver BC;^(b)Department of Physics and Astronomy, York University, Toronto ON; Canada.

¹⁶⁷Division of Physics and Tomonaga Center for the History of the Universe, Faculty of Pure and Applied Sciences, University of Tsukuba, Tsukuba; Japan.

¹⁶⁸Department of Physics and Astronomy, Tufts University, Medford MA; United States of America.

¹⁶⁹Department of Physics and Astronomy, University of California Irvine, Irvine CA; United States of America.

¹⁷⁰Department of Physics and Astronomy, University of Uppsala, Uppsala; Sweden.

¹⁷¹Department of Physics, University of Illinois, Urbana IL; United States of America.

- ¹⁷²Instituto de Física Corpuscular (IFIC), Centro Mixto Universidad de Valencia - CSIC, Valencia; Spain.
- ¹⁷³Department of Physics, University of British Columbia, Vancouver BC; Canada.
- ¹⁷⁴Department of Physics and Astronomy, University of Victoria, Victoria BC; Canada.
- ¹⁷⁵Fakultät für Physik und Astronomie, Julius-Maximilians-Universität Würzburg, Würzburg; Germany.
- ¹⁷⁶Department of Physics, University of Warwick, Coventry; United Kingdom.
- ¹⁷⁷Waseda University, Tokyo; Japan.
- ¹⁷⁸Department of Particle Physics, Weizmann Institute of Science, Rehovot; Israel.
- ¹⁷⁹Department of Physics, University of Wisconsin, Madison WI; United States of America.
- ¹⁸⁰Fakultät für Mathematik und Naturwissenschaften, Fachgruppe Physik, Bergische Universität Wuppertal, Wuppertal; Germany.
- ¹⁸¹Department of Physics, Yale University, New Haven CT; United States of America.
- ¹⁸²Yerevan Physics Institute, Yerevan; Armenia.
- ^a Also at Department of Physics, University of Malaya, Kuala Lumpur; Malaysia.
- ^b Also at Borough of Manhattan Community College, City University of New York, NY; United States of America.
- ^c Also at California State University, East Bay; United States of America.
- ^d Also at Centre for High Performance Computing, CSIR Campus, Rosebank, Cape Town; South Africa.
- ^e Also at CERN, Geneva; Switzerland.
- ^f Also at CPPM, Aix-Marseille Université, CNRS/IN2P3, Marseille; France.
- ^g Also at Département de Physique Nucléaire et Corpusculaire, Université de Genève, Genève; Switzerland.
- ^h Also at Departament de Fisica de la Universitat Autònoma de Barcelona, Barcelona; Spain.
- ⁱ Also at Departamento de Física Teórica y del Cosmos, Universidad de Granada, Granada (Spain); Spain.
- ^j Also at Department of Applied Physics and Astronomy, University of Sharjah, Sharjah; United Arab Emirates.
- ^k Also at Department of Financial and Management Engineering, University of the Aegean, Chios; Greece.
- ^l Also at Department of Physics and Astronomy, University of Louisville, Louisville, KY; United States of America.
- ^m Also at Department of Physics and Astronomy, University of Sheffield, Sheffield; United Kingdom.
- ⁿ Also at Department of Physics, California State University, Fresno CA; United States of America.
- ^o Also at Department of Physics, California State University, Sacramento CA; United States of America.
- ^p Also at Department of Physics, King's College London, London; United Kingdom.
- ^q Also at Department of Physics, Nanjing University, Nanjing; China.
- ^r Also at Department of Physics, St. Petersburg State Polytechnical University, St. Petersburg; Russia.
- ^s Also at Department of Physics, Stanford University; United States of America.
- ^t Also at Department of Physics, University of Fribourg, Fribourg; Switzerland.
- ^u Also at Department of Physics, University of Michigan, Ann Arbor MI; United States of America.
- ^v Also at Dipartimento di Fisica E. Fermi, Università di Pisa, Pisa; Italy.
- ^w Also at Giresun University, Faculty of Engineering, Giresun; Turkey.
- ^x Also at Graduate School of Science, Osaka University, Osaka; Japan.
- ^y Also at Hellenic Open University, Patras; Greece.
- ^z Also at Horia Hulubei National Institute of Physics and Nuclear Engineering, Bucharest; Romania.
- ^{aa} Also at II. Physikalisches Institut, Georg-August-Universität Göttingen, Göttingen; Germany.
- ^{ab} Also at Institutio Catalana de Recerca i Estudis Avancats, ICREA, Barcelona; Spain.
- ^{ac} Also at Institut de Física d'Altes Energies (IFAE), Barcelona Institute of Science and Technology,

Barcelona; Spain.

ad Also at Institut für Experimentalphysik, Universität Hamburg, Hamburg; Germany.

ae Also at Institute for Mathematics, Astrophysics and Particle Physics, Radboud University Nijmegen/Nikhef, Nijmegen; Netherlands.

af Also at Institute for Particle and Nuclear Physics, Wigner Research Centre for Physics, Budapest; Hungary.

ag Also at Institute of Particle Physics (IPP); Canada.

ah Also at Institute of Physics, Academia Sinica, Taipei; Taiwan.

ai Also at Institute of Physics, Azerbaijan Academy of Sciences, Baku; Azerbaijan.

aj Also at Institute of Theoretical Physics, Ilia State University, Tbilisi; Georgia.

ak Also at LAL, Université Paris-Sud, CNRS/IN2P3, Université Paris-Saclay, Orsay; France.

al Also at Louisiana Tech University, Ruston LA; United States of America.

am Also at LPNHE, Sorbonne Université, Paris Diderot Sorbonne Paris Cité, CNRS/IN2P3, Paris; France.

an Also at Manhattan College, New York NY; United States of America.

ao Also at Moscow Institute of Physics and Technology State University, Dolgoprudny; Russia.

ap Also at National Research Nuclear University MEPhI, Moscow; Russia.

aq Also at Near East University, Nicosia, North Cyprus, Mersin; Turkey.

ar Also at Ochadai Academic Production, Ochanomizu University, Tokyo; Japan.

as Also at Physikalisch-es Institut, Albert-Ludwigs-Universität Freiburg, Freiburg; Germany.

at Also at School of Physics, Sun Yat-sen University, Guangzhou; China.

au Also at The City College of New York, New York NY; United States of America.

av Also at The Collaborative Innovation Center of Quantum Matter (CICQM), Beijing; China.

aw Also at Tomsk State University, Tomsk, and Moscow Institute of Physics and Technology State University, Dolgoprudny; Russia.

ax Also at TRIUMF, Vancouver BC; Canada.

ay Also at Universita di Napoli Parthenope, Napoli; Italy.

* Deceased